

# Reviews of Geophysics®














## REVIEW ARTICLE

10.1029/2020RG000730

## Climate Changes and Their Elevational Patterns in the Mountains of the World

### Key Points:

- Using station and gridded data sets, we compare global precipitation and temperature trends by elevation
- Local comparisons of paired stations and regional comparisons using gridded data often show faster mountain than lowland warming
- Precipitation differences between mountains and adjacent lowlands are reducing, often driven by stronger precipitation increase in lowlands

N. C. Pepin<sup>1</sup> , E. Arnone<sup>2,3</sup>, A. Gobiet<sup>4</sup>, K. Haslinger<sup>4</sup> , S. Kotlarski<sup>5</sup> , C. Notarnicola<sup>6</sup> , E. Palazzi<sup>2,3</sup> , P. Seibert<sup>7</sup>, S. Serafin<sup>8</sup> , W. Schönner<sup>9</sup> , S. Terzago<sup>3</sup> , J. M. Thornton<sup>10</sup> , M. Vuille<sup>11</sup> , and C. Adler<sup>10</sup> 

<sup>1</sup>School of the Environment, Geography and Geosciences, University of Portsmouth, Portsmouth, UK, <sup>2</sup>Department of Physics, University of Turin, Turin, Italy, <sup>3</sup>National Research Council of Italy, Institute of Atmospheric Sciences and Climate (CNR-ISAC), Turin, Italy, <sup>4</sup>Climate Research Department, Central Institute for Meteorology and Geodynamics (ZAMG), Vienna, Austria, <sup>5</sup>Federal Office of Meteorology and Climatology, MeteoSwiss, Zurich, Switzerland, <sup>6</sup>EURAC Research Institute for Earth Observation, Bolzano, Italy, <sup>7</sup>Institute of Meteorology and Climatology, University of Natural Resources and Life Sciences, Vienna, Austria, <sup>8</sup>Department of Meteorology and Geophysics, University of Vienna, Vienna, Austria, <sup>9</sup>Institute of Geography and Regional Science, University of Graz, Graz, Austria, <sup>10</sup>Mountain Research Initiative, c/o University of Bern, Bern, Switzerland, <sup>11</sup>Department of Atmospheric and Environmental Sciences, University at Albany, Albany, NY, USA

### Supporting Information:

Supporting Information may be found in the online version of this article.

### Correspondence to:

N. C. Pepin,  
[nicholas.pepin@port.ac.uk](mailto:nicholas.pepin@port.ac.uk)

### Citation:

Pepin, N. C., Arnone, E., Gobiet, A., Haslinger, K., Kotlarski, S., Notarnicola, C., et al. (2022). Climate changes and their elevational patterns in the mountains of the world. *Reviews of Geophysics*, 60, e2020RG000730. <https://doi.org/10.1029/2020RG000730>

Received 25 MAR 2021

Accepted 28 DEC 2021

### Author Contributions:

**Conceptualization:** N. C. Pepin, S. Kotlarski, E. Palazzi, P. Seibert, S. Serafin

**Data curation:** E. Arnone, S. Terzago

**Formal analysis:** N. C. Pepin, E. Arnone, E. Palazzi, S. Serafin, S. Terzago

**Funding acquisition:** C. Adler

**Methodology:** N. C. Pepin, E. Arnone, S. Kotlarski, E. Palazzi, P. Seibert, S. Serafin, S. Terzago

**Project Administration:** C. Adler

**Software:** E. Arnone, S. Terzago

**Visualization:** N. C. Pepin, S. Serafin, W. Schönner, J. M. Thornton

**Abstract** Quantifying rates of climate change in mountain regions is of considerable interest, not least because mountains are viewed as climate “hotspots” where change can anticipate or amplify what is occurring elsewhere. Accelerating mountain climate change has extensive environmental impacts, including depletion of snow/ice reserves, critical for the world's water supply. Whilst the concept of elevation-dependent warming (EDW), whereby warming rates are stratified by elevation, is widely accepted, no consistent EDW profile at the global scale has been identified. Past assessments have also neglected elevation-dependent changes in precipitation. In this comprehensive analysis, both in situ station temperature and precipitation data from mountain regions, and global gridded data sets (observations, reanalyses, and model hindcasts) are employed to examine the elevation dependency of temperature and precipitation changes since 1900. In situ observations in paired studies (using adjacent stations) show a tendency toward enhanced warming at higher elevations. However, when all mountain/lowland studies are pooled into two groups, no systematic difference in high versus low elevation group warming rates is found. Precipitation changes based on station data are inconsistent with no systematic contrast between mountain and lowland precipitation trends. Gridded data sets (CRU, GISTEMP, GPCC, ERA5, and CMIP5) show increased warming rates at higher elevations in some regions, but on a global scale there is no universal amplification of warming in mountains. Increases in mountain precipitation are weaker than for low elevations worldwide, meaning reduced elevation-dependency of precipitation, especially in midlatitudes. Agreement on elevation-dependent changes between gridded data sets is weak for temperature but stronger for precipitation.

**Plain Language Summary** Mountains cover a large part of the Earth's surface and harbor distinct ecosystems, hold most of snow and ice outside the polar regions, and provide water for billions of people. This research looks at recent climate changes in mountains and compares them with simultaneous changes in lowland regions using weather station data, large global data sets, and climate models. We examine changes since 1900, but also concentrate on the last 40 years since this is when many changes have started to accelerate. Nearly all regions of the globe are getting warmer. When we make local comparisons, mountain sites are usually warming faster than lower areas nearby. However, when we average data from all global mountains and compare them with those from all lowland areas, there is no significant difference. Rainfall/snowfall on the other hand is decreasing in some areas, and increasing in others. In nearly all cases the strongest increase is occurring in the lowland areas, with increases in the mountains being more subdued (if at all). One consequence of our findings is that stores of mountain snow and ice may decline even faster than previously assumed due to the combination of enhanced mountain warming and reduced elevation dependency of rainfall/snowfall.

© 2022. The Authors.

This is an open access article under the terms of the [Creative Commons Attribution License](https://creativecommons.org/licenses/by/4.0/), which permits use, distribution and reproduction in any medium, provided the original work is properly cited.

## 1. Introduction

Climate change is the most wide-ranging environmental issue facing mountain environments in the 21st century (Stocker et al., 2013). Mountains and high-elevation regions are particularly sensitive to future changes in climate,

**Writing – original draft:** N. C. Pepin, S. Kotlarski, C. Notarnicola, P. Seibert, S. Serafin

**Writing – review & editing:** N. C. Pepin, E. Arnone, A. Gobiet, K. Haslinger, S. Kotlarski, C. Notarnicola, E. Palazzi, P. Seibert, S. Serafin, W. Schöner, J. M. Thornton, M. Vuille

with numerous potential impacts ranging from decreasing biodiversity (La Sorte & Jetz, 2010), shrinking habitats for many species (Freeman et al., 2018; Parmesan, 2006), mismatches between ecosystem components due to variable range shifts (Chen et al., 2011), declining snowpacks (López-Moreno, 2005; Mote et al., 2005, 2018), and retreating glaciers (Huss & Hock, 2018; Huss et al., 2017; Kuhn, 1989; Marzeion et al., 2018; Oerlemans, 1994; Zemp et al., 2019). Mountains act as a major store of freshwater (Barnett et al., 2005; Viviroli et al., 2011), much of it currently in solid form (snow and ice). The diminishing cryosphere has many consequences, including the potential loss of water supply for billions of people in downstream regions worldwide (Bradley et al., 2006; Viviroli et al., 2020) and the shifting of snowmelt from spring/summer to earlier in the year (Musselman et al., 2017). In regions where annual mean temperatures are presently close to the melting point, small shifts in temperature often have large hydrological consequences (Haeberli & Weingartner, 2020).

Many studies have suggested that mountain warming rates (based on analyses of near-surface air temperatures) are elevation-dependent (Diaz & Bradley, 1997; Pepin et al., 2015; Qixiang et al., 2018; Rangwala & Miller, 2012; Vuille & Bradley, 2000). Elevation-dependent warming (EDW) does not always imply that warming is more rapid in mountains compared to lowlands, but rather that there is some systematic difference in warming rates with elevation. There is some evidence that temperature increases have been particularly rapid at the current boundary of the cryosphere (e.g., snowline region) due to the snow-albedo feedback (Pepin & Lundquist, 2008; Scherrer et al., 2012), and many model simulations project the acceleration of this effect (Kotlarski et al., 2012; Letcher & Minder, 2015; Rupp et al., 2017). Changes in rates of warming with elevation will also influence atmospheric static stability (Frierson, 2006) and thus patterns of precipitation.

Notwithstanding the important role of temperature changes, precipitation is also a critical control on mountain hydrological resources. Precipitation gradients with elevation can be extremely steep, with marked gradients within individual mountain regions being common. Changes in both orographic precipitation gradients (Luce et al., 2013) and its controlling processes (e.g., convection, windward/leeward blow over—Houze, 2012; Pavelsky et al., 2012) will therefore likely play an important role in any future local to regional-scale precipitation changes, but these phenomena remain poorly understood on a global scale. Neither observing nor simulating changes in mountain precipitation is straightforward. Due to the influence of orography, spatial climate variability in mountain settings is high (Daly, 2006). Local-scale variations in precipitation are strong which makes a dense network of observations necessary. Monitoring of in situ precipitation can be subject to large uncertainties due to gauge under-catch, especially for snowfall (Goodison et al., 1998; Kochendorfer et al., 2017) and when there are high wind speeds. A wealth of literature exists on mountain climate processes (see Barry, 2008; Whiteman, 2000), and on potential impacts of future climate change in mountains (e.g., Gobiet & Kotlarski, 2020; Gobiet et al., 2014; Kohler et al., 2010; Nogues-Bravo et al., 2008). However, although some local studies exist (Napoli et al., 2019; Pavelsky et al., 2012), making global comparisons of orographic precipitation gradients is extremely challenging and there is a general dearth of observations at high elevations.

The aims of this review are: (a) to examine the spatial and temporal patterns of recent changes in mountain climates around the globe with a focus on temperature and precipitation and their differences with elevation, (b) consolidate and summarize our current understanding of the drivers and processes that shape these changes, and (c) assess and summarize their respective environmental impacts. We take a global perspective, comparing and contrasting different mountain regions. We limit our discussion to bio-geophysical impacts, and although socio-economic impacts are increasingly important, these are beyond the scope of this current review.

Section 2 introduces important concepts of mountain climate and describes the basic controls of temperature and precipitation in such settings. Section 3 introduces the data sets used to examine global changes in temperature and precipitation with elevation. We perform a meta-analysis of studies reported in the IPCC Special Report on Oceans and Cryosphere (Hock et al., 2019; hereafter SROCC). We also examine past temperature/precipitation trends using gridded observational, reanalysis and modeled data sets (CRU, GISTEMP, GPCC, ERA5, and CMIP5 historical simulations). Section 4 concentrates on temperature, whilst Section 5 deals with precipitation. Limitations of our approach and opportunities for future work are discussed in Section 6. Consequences for the mountain cryosphere, hydrology and ecology are examined in Section 7, before we summarize results in Section 8.

## 2. Mountain Climates and the Effect of Elevation

### 2.1. Definitions Relevant to Climate Change and Its Elevation Component

Quantifying climate change in mountain areas is challenging, partly because mountains are not defined by climate. Many definitions of mountains exist, based on different criteria, including topographical parameters like elevation, relative relief and slope (Kapos et al., 2000; Meybeck et al., 2001; Sayre et al., 2014, 2018), hypsometric curves (Elsen & Tingley, 2015), geomorphological processes (Price et al., 2013), ecological zonation (Körner et al., 2011, 2017; Troll, 1973), or presence of snow and ice (Beniston et al., 2018). Depending on the choice of mountain delineation, 13%–30% of the land surface (excluding Antarctica) can be considered mountainous. Recently, mountain definitions have also been discussed in political or management contexts (Debarbieux & Rudaz, 2015; Price et al., 2019). Combined with choice of population data set, the number of people living in the world's mountains in 2015 ranged from 0.344 to 2.289 billion. While mountains can be defined by all these characteristics, they cannot simply be defined by climatological criteria such as mean temperature or growing-season length. In their comprehensive review of mapping mountain regions, Price et al. (2019) don't mention climate as a criterion. Because mountain climate is only a modification of the climate that would be present in the absence of orography, climates of different mountain ranges vary enormously. This wide variety of mountain climates potentially translates to a wide variety of responses to climate-change forcings. Nevertheless, within this variety, there are atmospheric processes common to mountain regions, possibly leading to the emergence of common change patterns.

Elevation is the dominant control of temperature and precipitation in mountains, and so any systematic change in this elevation component over time is of utmost importance. EDW has never been formally defined but Rangwala and Miller (2012) and Pepin et al. (2015) view it as any systematic change in warming rates with elevation, often (but not always) enhanced warming at high(er) elevations. EDW can be quantified either through systematic differences in high versus low elevation temperature trends, or through a trend in the temperature gradient derived over some arbitrary elevation interval. Because EDW is commonly evaluated on the basis of distributed temperature measurements at several surface stations, it comprises climatological variability in both the vertical and horizontal directions. However, vertical temperature gradients are usually a lot larger than the horizontal ones. It is therefore justified to use temperature differences between high- and low-elevation sites as proxies for the elevational trend. Instantaneous altitudinal temperature profiles are rarely linear or monotonically decreasing, but the climatologically averaged ones are usually well approximated by linear relationships. A difference in trends is not identical to a trend in the difference, but they are two sides of the same problem, and both approaches are commonly employed (see Section 2.4). Changes in temperature gradient and/or EDW are independent of the absolute sign of temperature changes at both high and low elevation.

We here extend this concept to EDPC (elevation-dependency of precipitation change) as evidenced by different trends in high versus low elevation precipitation, or a trend in orographic precipitation gradient (termed OPG in the literature: Lundquist et al., 2010; Scaff et al., 2017). The same concept can be extended to gradients in solid precipitation (Huning & Margulis, 2018). Similar to EDW, EDPC results from a combination of vertical and horizontal variability. In the vertical, changes of pressure and temperature during the orographically forced uplift of air masses favor moisture condensation and determine the hydrometeor type. In the horizontal, the combined effect of advection and hydrometeor fallout determines the areal distribution of precipitation. In contrast with temperature, in the case of precipitation the drivers of horizontal variability may offset the vertical ones. For instance, if an air mass is advected into a mountain range, most of the moisture condenses and precipitates on the outer boundary, leaving the interior relatively dry even if it is more elevated. For these reasons, the long-term altitudinal profile of precipitation is usually non-linear and so the concept of a single “gradient” to describe the elevation profile may be misleading. Notwithstanding this debate, we use the term “elevation-dependency of precipitation” to refer to the additional precipitation created by mountains, or the quantitative difference between lowland and mountain precipitation totals.

### 2.2. Atmospheric Processes Which Control Temperature and Precipitation Gradients in Mountain Regions

The rate of decrease of temperature with elevation in mountainous regions is determined by the superposition of the free-tropospheric temperature lapse rate with local effects, which are essentially controlled by the surface

energy balance. The various physical mechanisms that determine the evolution of local effects on a climatological scale (snow albedo feedback, atmospheric moisture, thermal emission, aerosols, and clouds) have been described extensively in previous reviews of EDW (Pepin et al., 2015; Rangwala & Miller, 2012) and our discussion here is brief. The first mechanism is snow albedo feedback, which enhances warming where the snowline is in retreat (Pepin & Lundquist, 2008). This effect can be amplified further where there is deposition of black carbon on snow/ice (Li et al., 2016). Increases in specific humidity have a larger effect on warming at high elevations where the atmosphere is initially drier (Rangwala et al., 2016). A fixed change in radiative forcing also has a larger effect on temperature at lower temperatures (higher elevations; Ohmura, 2012). Aerosol loadings typically decrease at higher elevations, reducing solar dimming and encouraging EDW (Zeng et al., 2015). The processes mentioned so far impact primarily surface energy balance. In what follows, we extend the discussion to dynamical processes connected with changes in prevailing atmospheric circulation at different scales. We first summarize the climatic controls of free-tropospheric lapse rates. Then, we move on to examining the potential impact of specific meteorological processes on the elevation profile of warming rates and on changes in the spatial variability of orographic precipitation.

At tropical and subtropical latitudes, mean tropospheric lapse rates are approximately saturated adiabatic (i.e., with temperature decreasing with height by  $\sim 6 \text{ K km}^{-1}$ , Stone & Carlson, 1979). At midlatitudes, baroclinic disturbances tend to make the lapse rate weaker than saturated adiabatic on average and proportional to meridional gradients in surface temperature and humidity (Juckes, 2000). Climate change projections concur in predicting increased static stability in a warmer climate, due both to adjustment toward a saturated adiabat with higher equivalent potential temperature, and (at midlatitudes) to increasing meridional gradients of equivalent potential temperature (Frierson, 2006). Larger static stability in a warmer climate implies relatively stronger free-air warming at higher elevations. Whether or not free-tropospheric lapse rate trends contribute to changes in surface climate depends on the strength of the coupling between the boundary layer and the free troposphere. Over mountainous regions, the vertical exchange depends on both dynamically driven and thermodynamically driven meteorological processes (Serafin et al., 2018), as detailed below.

On the timescales of midlatitude weather systems, the primary dynamical influence of mountains on the atmospheric flow is as a mechanical obstacle (R. B. Smith, 1979), which may lead to lee cyclogenesis (Buzzi & Tibaldi, 1978; Chung et al., 1976). Whether atmospheric flow is diverted around mountains or lifted over them depends on wind speed, static stability, and mountain height and form (Jackson et al., 2013). In midlatitudes, the flow over mountains can induce or modulate planetary waves of the jet stream, which characterize large-scale weather patterns downstream of the Rocky Mountains and the Tibetan Plateau in the Northern, and the Andes in the Southern, Hemisphere. A mesoscale orographic phenomenon on the upstream side is flow blocking (Pierrehumbert & Wyman, 1985), which may result in jets along barriers. Phenomena occurring on the downstream side include wakes on the scale of single mountain massifs (Rotunno et al., 1999), gap winds (Mayr et al., 2007), downslope windstorms affecting large portions of a mountain range, such as foehn (Elvidge & Renfrew, 2016; Richner & Hächler, 2013) and bora (Grisogono & Belušić, 2009), and mountain waves propagating into the free atmosphere (Durrán, 1990).

Mountains also induce a range of thermally driven, baroclinic meso- and micro-scale circulations (Vergeiner & Dreiseitl, 1987; Zardi & Whiteman, 2013). Their smallest-scale manifestations are slope winds (Defant, 1949), followed by valley breezes (Giovannini et al., 2017; Nickus & Vergeiner, 1984) and finally mountain-plain wind systems (Lugauer & Winkler, 2005). These circulations are usually favored by atmospheric stability below mountain crest height; they are therefore best developed in high mountains. The Kali Gandaki valley in the Himalayas is said to experience the strongest valley wind system on the globe (Egger et al., 2000). Thermally driven flows are caused by differential heating and cooling at elevated surfaces, and are connected with relatively weak horizontal pressure gradients; thus, they manifest primarily in situations with weak synoptic flows and have little influence under strong synoptic forcing. For this reason and being driven by net radiation, such breeze systems are most pronounced on fair-weather days. At night, radiative cooling and cold-air drainage favor cold air pools, forming preferably in basins (Clements et al., 2003; Dorninger et al., 2011; Lundquist et al., 2008); in the cold season, these often become persistent (Lareau et al., 2013).

While the dynamical and thermodynamical impacts of mountains on the atmosphere are often described separately, in reality they continuously interact with each other. For instance, low-level stable layers downstream of mountains (e.g., over a relatively cool sea surface) can generate waveguides, which promote the formation of

trapped lee waves (Scorer, 1949) and impede the vertical propagation of wave energy. Strong inversion layers, either surface-based or elevated, also prevent the large-scale flow from intruding deeply into valleys (Mayr & Armi, 2010; Strauss et al., 2016); but they can also be eroded by shear-driven turbulence if the large-scale flow is particularly vigorous (Lareau & Horel, 2015).

In an evolving climate, a changing interplay between dynamics and thermodynamics can result in significant climatic signals in temperature gradients. For instance, cold-air pooling contributes to stabilizing the valley atmosphere and to reversed temperature gradients with elevation; therefore, fewer such events due to more vigorous winds in a hypothetical global-warming scenario would lead to stronger relative warming at low elevations (Daly et al., 2010; Pike et al., 2013). Enhanced mesoscale advection toward major mountain ranges, partially thermally driven, can increase orographic cloudiness (e.g., Norris et al., 2020), thereby impacting the surface energy balance and thus snow-albedo and cloud-radiation feedbacks. Increased frequency of foehn events, and related leeside adiabatic compression of air masses, is suspected to be a major driver of enhanced low-level warming in the lee of the Antarctic peninsula, contributing to the accelerated melting of the Larsen C ice-shelf (Elvidge et al., 2020).

The impact of mountains on the airflow is also a major factor in controlling stable orographic precipitation (Smith, 1979; Roe, 2005). The extraction of precipitation from the incoming flow by mountains depends on dynamical, thermodynamic and microphysical factors (Houze, 2012). Specifically, for orographic precipitation to occur, orographic uplift should be sufficient to bring air parcels well beyond their lifting condensation level, and the time scale of rainfall formation should be shorter than that of cross-mountain advection. Flow patterns are rarely symmetric along a cross-mountain section (Seibert, 2012), and uplift on the windward side leads to increased precipitation.

Since the rate of condensation is roughly proportional to vertical uplift, precipitation rates often increase with elevation. However, precipitation-elevation relationships are very variable in space and depend on the scale considered (see Daly et al., 1994 and references therein). Monotonic precipitation-elevation relationships are not universal, the most significant exceptions being tropical mountains and very broad mountain barriers. In the Alps, for instance, most of the impinging moisture condenses and precipitates along the outer boundaries of the mountain range, leaving interior regions relatively dry, even if more elevated (Frei & Schär, 1998). Much of the Tibetan Plateau is dry for the same reason.

Stable precipitation can be displaced upstream of the mountains when strong orographic blocking occurs (Rotunno & Ferretti, 2001), or by advection of hydrometeors downstream with the winds (Smith & Barstad, 2004; Zängl et al., 2008). The airflow generally descends on the lee side, creating a relatively dry rainshadow region (Mass et al., 2015; Narkhedkar et al., 2015). In mountain ranges where the synoptic climatology features strong prevailing winds, systematic lee/windward contrasts in precipitation gradients with elevation emerge.

Orographic convection, which may occur in the warm season in areas of near-surface convergence, such as mountain tops at daytime or forelands at night (Banta, 1990; Kirshbaum et al., 2018), further complicates the picture. It imprints spatially variable diurnal patterns on the mean precipitation in mountain regions (Yaqub et al., 2011), and it generally enhances rainfall in the transition regions between mountains and their forelands, where convective ingredients are more likely to be optimally combined.

As is the case with temperature, the changing interaction between synoptic flow and orographically induced circulations can cause significant variations in the distribution of precipitation on climatological time scales. Idealized studies of the response of orographic precipitation to global warming suggest that its trend will be largely determined by the local interaction of the mean flow with the orography (Shi & Durran, 2014). Vertical velocity (dynamic factor) and the lapse rate of saturation specific humidity (thermodynamic factor) both play a role. In the case of orographic precipitation, the dynamic factor (enhanced windward ascent in a warmer climate) was shown to depend mostly on mid-tropospheric stability and low-level wind speed, and to determine both the spatially variable climate sensitivity of extreme orographic precipitation (Shi & Durran, 2015) and the lower climate sensitivity of extreme precipitation over mountains than over oceans or plains (Shi & Durran, 2016).



### 2.3. Challenges in Observing and Modeling Mountain Climates: Lessons From Past Studies

Since mountain climates are both diverse and complex, quantifying the relevant processes is challenging, and thus the quantification of past and future climate-change patterns as a function of elevation is subject to large uncertainty.

Due to the remote nature of mountain regions with frequent harsh weather conditions, observational networks are sparse or are not designed to measure elevation-dependencies in climate (Lawrimore et al., 2011; Oyler et al., 2015). The GHCNv4 data set, for instance, has more than 27,000 stations, but only 211 above 3,000 m (and none above 5,000 m: Menne et al., 2018). Both the orographic texture and the atmospheric response to dynamic and thermodynamic forcing induced by mountains contribute to the particularly strong spatial variability of weather and climate elements in mountains. Examples include cold air pools (which can cause extreme variations in minimum temperatures over distances as small as a few hundred meters; Pagès et al., 2017; Whiteman & Hoch, 2014), or the effects of aspect and topographic shading on radiation regimes (Dozier & Frew, 1990; Olson & Rupper, 2019). Point measurements from complex terrain usually have a peculiar representativeness (e.g., a mountain top station may broadly represent other mountain tops, but not nearby slopes or valleys), and thus high spatial density is mandatory if differential climate trends between mountains and adjacent plains are to be determined. Gridded analyses interpolating data from sparse networks, especially those with weak data coverage in complex orography, suffer from these problems, and require intelligent interpolation methods (Daly, 2006). A good example which illustrates some of the problems with using gridded analyses for trend estimation concerns the rugged terrain of the western US. In the 1980s, a network of high elevation SNOTEL sites was installed to measure high elevation precipitation. The post-1980 relative orographic enhancement field has been used as a static template of ratios to be applied to low elevation precipitation observations to estimate high elevation precipitation further back in time (Daly et al., 1994; Di Luzio et al., 2008). Thus, artificial stationarity is built into the trends of high elevation precipitation before 1980 (see also Vose et al., 2014 for a more recent example).

It is also challenging to detect elevation patterns in climate-change signals based on in situ stations (Pepin et al., 2015). Global, observation-based studies of mountain climate change have employed different methods to examine elevational gradients in change (Diaz & Bradley, 1997; Pepin & Lundquist, 2008; Qixiang et al., 2018; Zeng et al., 2015). Their outcomes depend heavily on how the comparisons were configured. For example, individual station trend comparisons may give contrasting results to trends aggregated for groups of stations by elevation band. Evidence exists that temperature trends on mountain summits show reduced regional variation and are more similar to changes in the free atmosphere than those in valleys, representing a broader signal in a “sea of noise” (Pepin & Lundquist, 2008). Suitable choices of lowland sites for comparisons to mountain sites are not trivial. In the case of a linear mountain range, lowlands lie on either side, often with highly contrasting climates, most starkly in the tropical Andes with desert versus rain forest. On the western and eastern slopes of the Andes, elevation gradients of temperature change have opposite signs, for example (Vuille et al., 2003, 2015). Urban and coastal effects and microclimates, particularly in deeply incised valley systems or plains abutting mountain ranges, will all influence “lowland” climate, and consequently any elevation gradient in warming obtained.

Climate model simulations are useful to investigate mechanisms responsible for mountain processes and their long-term changes, both in historical simulations and future projections. However, they are generally coarse in spatial resolution, hence they do not resolve, or resolve only partially, the scales of spatial variability of intra-mountain features and relevant meteorological processes. Numerical models rely on parameterizations of the effects of sub-grid processes, which are more complex and less well known over mountains (Chow et al., 2019) and thus represent a major source of uncertainty.

## 3. Methods

### 3.1. Meta-Analysis of Past Studies Using Station Observations

In contrast to other global studies which used historical time series of in situ stations directly (Diaz & Bradley, 1997; Pepin & Lundquist, 2008; Wang et al., 2016; Qixiang et al., 2018), here we use 70 published temperature trends (Table 1) and 34 precipitation trends (Table 2) in a meta-analysis of mean trend magnitudes.

**Table 1**  
*Seventy Observed Near-Surface Temperature Trends From Stations or Groups of Stations, Adapted From SROCC*

Region (mountain range)	Elevation band (High, Medium, or Low)	Trend/10yrs (°C/decade)	Study Period	Number of stations	Variable/Season	Reference (Lead Author)
Global	High/Low	+0.21/+0.04	1951-1989	250/993	Min/Annual	Diaz (1997)
Global	High	+0.12	1948-2002	1084	Mean/Annual	Pepin (2008)
Global	High/Low	+0.40/+0.32	1982-2010	640/2020	Mean/Annual	Zeng (2015)
Global	High/Low	+0.30/+0.24	1961-2010	910/1742	Mean/Annual	Wang (2016)
Global	High/Low	+0.43/+0.35	1961-2010	739/1262	Mean/Winter	Qixiang (2018)
N America Colorado/Pacific NW	High/Low	+0.75/+0.37	1979-2006	PRISM Gridded	Mean/Annual	Diaz (2007)
N America Appalachians	High/Low	+0.35/+0.31	1970-2005	1/1	Mean/Annual	Ohmura (2012)
N America W USA	High	+0.11	1991-2012	482	Mean/Annual	Oyler (2015)
N America USA	High	+0.14	1948-1998	552	Mean/Annual	Pepin (2005)
Europe Switzerland	High	+0.35	1959-2008	91	Mean/Annual	Ceppi (2012)
Europe Switzerland	High	+0.17	1959-2008	91	Mean/Autumn	Ceppi (2012)
Europe Switzerland	High	+0.48	1959-2008	91	Mean/Summer	Ceppi (2012)
Europe Switzerland	High	+0.13	1864-2016	19	Mean/Annual	Begert (2018)
Europe Switzerland	High/Medium/Low	+0.25/+0.31/+0.35	1981-2017	47/34/12	Mean/Annual	Rottler (2019)
Europe Switzerland	High	+0.51	1961-2011	6	Mean/April	Scherrer (2012)
Europe Switzerland	High	+0.43	1970-2011	1	Mean/Annual	Ohmura (2012)
Europe Switzerland	High	+0.3	1980-2011	1	Mean/Annual	Ohmura (2012)
Europe French Alps	High	+0.3	1960-2017	1	Mean/Winter	Lejeune (2019)
Europe French Alps	High	+0.14	1900-2004	1	Mean/Annual	Gilbert (2013)
Europe Italy	High/Low	+0.27/+0.49	1976-2010	12/12	Mean/Annual	Tudoroiu (2016)
Europe Italy	High	+0.15	1951-2012	24	Mean/Annual	Scorzini (2019)
Europe Pyrenees	High	+0.11	1910-2013	155	Max/Annual	Perez-Zanon (2017)
Europe Pyrenees	High	+0.57	1970-2013	155	Max/Annual	Perez-Zanon (2017)
Europe Pyrenees	High	+0.06	1910-2013	155	Min/Annual	Perez-Zanon (2017)
Europe Pyrenees	High	+0.23	1970-2013	155	Min/Annual	Perez-Zanon (2017)
Middle East	High	+0.14	1958-2000	Reanalysis NCEP/NCAR R1	Mean/Annual	Diaz (2003)
Middle East Palestine	High	+0.33	1970-2011	6	Mean/Annual	Hammad (2019)
S Andes	High	-0.05	1950-2010	75	Mean/Annual	Vuille (2015)

**Table 1**  
*Continued*

S Andes	High	+0.2	1980-2005	Gridded CRU TS3.21	Mean/Winter	Zazulie (2017)
S Andes	High	0	1980-2005	Gridded CRU TS3.21	Mean/Summer	Zazulie (2017)
Tropical Andes	High	+0.13	1950-2010	546	Mean/Annual	Vuille (2015)
Tropical Andes	High	-0.7	1985-2010	1	Mean/Annual	Ohmura (2012)
East Africa	High	+0.18	1958-2000	Reanalysis NCEP/NCA R 1	Mean/Annual	Diaz (2003)
South and East Africa	High	+0.14	1948-1998	41	Mean/Annual	Pepin (2005)
Himalaya	High	+0.1	1901-2014	122	Mean/Annual	Krishnan (2019)
Himalaya	High	+0.2	1951-2014	122	Mean/Annual	Krishnan (2019)
Himalaya	High	+0.48	1980-2010	1	Mean/Annual	Ohmura (2012)
Himalaya	High	+0.06	1958-2000	Reanalysis NCEP/NCA R 1	Mean/Annual	Diaz (2003)
Himalaya	High	+0.16	1901-2002	3	Mean/Annual	Bhutiyani (2007)
Himalaya	High	+0.57	1963-2009	3	Max/Annual	Nepal (2016)
Himalaya	High	+0.23	1975-2006	4	Mean/Winter	Dimri (2012)
Himalaya	High	+0.2	1975-2006	12	Mean/Winter	Dimri (2012)
Tibet	High	+0.02	1970-2005	1	Mean/Annual	Ohmura (2012)
Tibet	High	+0.4	1979-2011	83	Mean/Summer	Gao (2015)
Tibet	High	+0.54	1979-2011	83	Mean/Winter	Gao (2015)
<b>Tibet</b>	<b>High/Low</b>	<b>+0.69/+0.55</b>	<b>1981-2006</b>	<b>47/24</b>	<b>Mean/Annual</b>	<b>Qin (2009)</b>
Tibet	High	+0.53	1961-2006	116	Min/Annual	Liu (2009)
Tibet	High	+0.85	1961-2006	116	Min/Winter	Liu (2009)
Tibet	High	+0.16	1955-1996	97	Mean/Annual	Liu (2000)
Tibet	High	+0.32	1955-1996	97	Mean/Winter	Liu (2000)
<b>Tibet</b>	<b>High/Medium/Low</b>	<b>+0.25/+0.15 / +0.05</b>	<b>1961-1990</b>	<b>6/4/12</b>	<b>Mean/Annual</b>	<b>Liu (2000)</b>
Tibet	High	+0.28	1961-2007	72	Mean/Annual	Guo (2012)
Tibet	High	+0.4	1961-2004	71	Mean/Winter	You (2010)
Tibet	High	+0.2	1961-2004	71	Mean/Summer	You (2010)
<b>Tibet</b>	<b>High/Low</b>	<b>+0.36/+0.32</b>	<b>1961-2012</b>	<b>16/73</b>	<b>Mean/Annual</b>	<b>Yan (2014)</b>
Aust/NZ	High	+0.16	1948-1998	14	Mean/Annual	Pepin (2005)
Japan	High	+0.35	1985-2005	1	Mean/Annual	Ohmura (2012)

*Note.* The full list of the references is provided separately at the end of this article: direct paired comparisons (high vs. low elevation groups in the same region) are in bold. Elevation bands (high/medium/low) are relative and defined for this study. The total number of separate references is 57. Figures highlighted in yellow are modified from the original SROCC table (see notes in Text T3 in Supporting Information S1).

This list of studies was originally compiled for, and published as an annex to, Chapter 2 of the IPCC Special Report on Oceans and Cryosphere (<https://www.ipcc.ch/srocc/chapter/chapter-2/>; Tables SM2.2 and SM2.3 in Hock et al. (2019) for temperature and precipitation, respectively), and includes analyses between 1864–2017 (temperature) and 1866–2016 (precipitation) but with variable record lengths. In many of these studies, no explicit lowland versus mountain comparison is made, although in some cases paired comparisons between groups of mountain and lowland stations are performed. To be included in our analysis, the minimum information required for each study was: station (or station group mean) warming rate, time period start and end dates, the mountain region, and the number of stations used to derive the mean rate (which acts as a level of confidence for group values). Unfortunately, as precise elevation information was not always available, insisting on absolute elevation data for all stations would have severely limited the number of samples. The terms “mountain” and “lowland” sites are



**Table 2**

*Thirty-Four Observed Near-Surface Precipitation Trends From Stations or Groups of Stations, Adapted From SROCC*

Region (mountain range)	Percentage or absolute change (% or Abs)	Trend/10 years Abs (mm)	Study period	Number of stations	Variable/type	References
Alaska	%	+3.5	1949–2016	18	Annual total	Wendler et al. (2017)
USA	%	−1.1	1920–2014	102	Winter total	Mao et al. (2015)
Canada	%	+3.0	1948–2012	Gridded	Annual total	Vincent et al. (2015)
Alps	%	−1.8	1971–2008	Gridded	Winter total	Masson and Frei (2016)
Pyrenees	%	−0.6	1910–2013	24	Annual total	López-Moreno (2005)
Italy	%	−1.8	1951–2012	46	Annual total	Scorzini and Leopardi (2019)
Carpathians	%	+1.4	1960–2010	Gridded	Heavy precip	Spinoni et al. (2015)
Tian Shan	%	+4.3	1960–2014	Gridded	Winter total	Chen et al. (2016)
Karakorum	%	+1.7	1961–1999	17	Winter total	Archer and Fowler (2004)
Japan	%	+3.0	1898–2003	61	Heavy precip	Fujibe et al. (2005)
Kenya	%	−6.0	1979–2011	50	MAM total	Schmocker et al. (2016)
Kenya	%	+6.0	1979–2011	50	OND total	Schmocker et al. (2016)
Andes	%	−1.4	1981–2003	7	Annual total	Ruiz et al. (2008)
Alps	Abs	+0.3	1980–2010	43	Annual total	Kormann et al. (2015)
Scandinavia	Abs	+19.2	1909–2008	3	Annual ratio	Irannezhad et al. (2017)
Caucasus	Abs	−90.0	1936–2012	90	Annual total	Elizbarashvili et al. (2017)
Caucasus	Abs	+60.0	1936–2012	<90	Annual total	Elizbarashvili et al. (2017)
S Andes	Abs	−30.0	1979–2010	Gridded	Annual total	Rusticucci et al. (2014)
Karakorum	Abs	−14.6	1950–2009	Gridded	Winter total	Palazzi et al. (2013)
Himalaya	Abs	−36.5	1951–2007	Gridded	Summer total	Palazzi et al. (2013)
Himalaya	Abs	−76.7	1950–2009	Gridded	Summer total	Palazzi et al. (2013)
Himalaya	Abs	−137.2	1994–2012	7	Annual total	Salerno et al. (2015)
Himalaya	Abs	−92.8	1994–2012	7	Summer total	Salerno et al. (2015)
Tibet	Abs	+14.3	1960–2014	71	Annual total	Deng et al. (2017)
Altai	Abs	−1.4	1966–2015	9	Annual total	Zhang et al. (2018)
Altai	Abs	+9.0	1966–2015	8	Annual total	Zhang et al. (2018)
Hengduan	Abs	−11.4	1961–2011	90	Annual total	Xu et al. (2018)
Himalaya	Abs	+1.2	1960–2000	5	Heavy precip	Panday et al. (2015)
SW Australia	Abs	−7.5	1960–2012	Undefined	Annual total	Grose et al. (2015)
Iceland	Abs	Insig	1961–2000	40	Winter total	Crochet (2007)
Tropics	Abs	Insig	1982–2006	Gridded	Annual total	Krishnaswamy et al. (2014)
New Zealand	Abs	Insig	1900–2010	294	Annual total	Caloiero (2015)
NW India	Abs	Insig	1866–2006	10	Winter total	Bhutiyan et al. (2010)
NW India	Abs	−0.1	1866–2006	10	Summer SPI <sup>a</sup>	Bhutiyan et al. (2010)

*Note.* The full list of the references is provided separately at the end of this article. The original SROCC table was in many cases missing some information, meaning that the original publications had to be examined in detail to derive decadal (absolute or relative) changes. Note since some individual studies report more than one trend, the total number of references is less than 34.

<sup>a</sup>Standardized precipitation index.

relative and do not conform to a universal threshold elevation. Indeed, there is no single universally accepted definition of these terms. On the Tibetan Plateau, for example, “low elevation” stations (2,000–3,000 m) would still be higher than “mountain” sites in many other parts of the world. Thus, each study was included following its own internal classification.

Summary information from the 57 temperature studies included is listed in Table 1. Full references are given at the end of this article. The vast majority pertain to the midlatitudes of the northern hemisphere, namely Europe (9), North America (6), the Himalayas (7), and the Tibetan Plateau (17). The earliest was published in Diaz and Bradley (1997), and 35 (>60%) were published in the last decade (2010–2019). In 11 studies, explicit elevational comparisons, whereby trends at groups of high and low elevation sites were compared in the same mountain region, were built into the study. These are subsequently referred to as paired studies. In the other 46 cases, no explicit elevation comparison was made (unpaired). A subset of 5 studies had global scope (i.e., combined multiple mountain regions) and these are listed at the top of Table 1.

Precipitation trends (34) are comprised of both absolute (21) and relative (13) trends, and come from 27 different studies. Although most are based on annual values, some seasonal comparisons are included (Table 2).

We confined our analysis to published figures listed in the SROCC tables (reproduced in Tables 1 and 2). We checked these data for authenticity and did make one or two changes (highlighted - for further details see Supporting Information S1), but did not extract or estimate values from graphs in the original articles. Whilst temperature trends were uniformly expressed in °C/decade in the source material, precipitation trends were reported using a combination of absolute (e.g., in mm) and relative changes (as percentages relative to some baseline), and furthermore over different time periods. Decadal rates of change were therefore calculated by dividing total change by the length of period. Unfortunately, the two cannot easily be compared. Doing so would require information on mean annual precipitation, yet this information was generally not provided. Relative and absolute changes are therefore analyzed separately.

This literature-based approach is not comprehensive and is inherently somewhat subjective due to the different criteria applied by the various studies. The uneven distribution of observational studies (from Tables 1 and 2) across the globe is illustrated by Figure 1. We also directly compare observed temperature trends derived from our station-based analysis with the mean global observed temperature change over (a) land and sea combined according to HadCRUT4 (Morice et al., 2012), and (b) over the land surface only according to CRUTEM4 (Jones et al., 2012) for the equivalent time periods. We use the best estimate of annual temperature anomalies for both these data sets (see the original references for details).

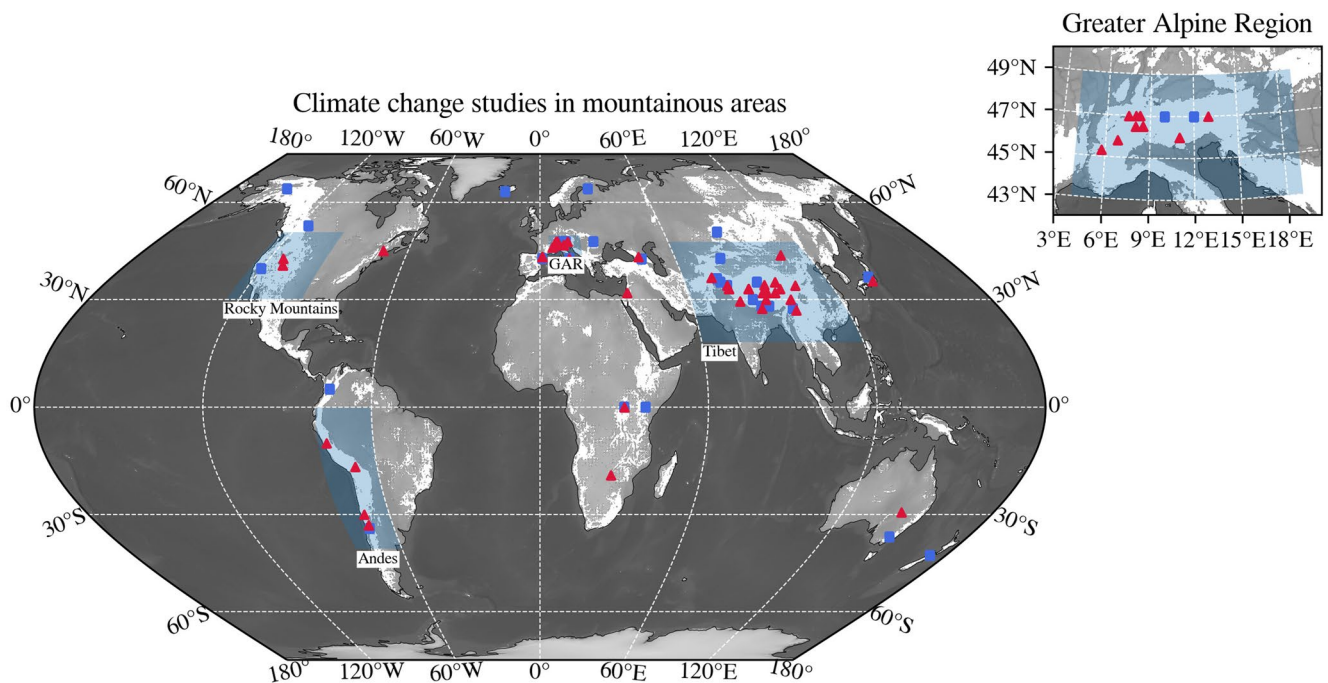


**Figure 1.** Map showing K1 mountain regions (in white). These are defined on a 1 km resolution using the criteria in Table 3. Representative locations of in situ station studies (Tables 1 and 2) are marked for precipitation (blue squares) and temperature (red triangles). A magnified map of the Greater Alpine Region is shown as an inset (top right). Key mountain regions considered in the study are highlighted with light blue shading.

**Table 3**  
*Characteristics of Gridded Data Sets Used in the Analysis*

Data set	Temperature metric	Precipitation metric	Spatial resolution (°)	Temporal resolution	Version (if applicable)	Source	Date of access	References
CRU	Near surface $T$ (K)	Total pr (mm/month)	$0.5^\circ \times 0.5^\circ$	Monthly	CRU TS4.0	<a href="http://badc.nerc.ac.uk/data/cru">http://badc.nerc.ac.uk/data/cru</a>	June 2019	Harris et al. (2020)
GISTEMP	T anomaly (K)	–	$2^\circ \times 2^\circ$	Monthly	v4	<a href="http://data.giss.nasa.gov/gistemp">http://data.giss.nasa.gov/gistemp</a>	August 2019	Lenssen et al. (2019) GISTEMP (2020)
GPCC	–	Total pr (mm/month)	$0.25^\circ \times 0.25^\circ$	Monthly	2018	<a href="http://gpcc.dwd.de">http://gpcc.dwd.de</a>	May 2018	Schneider et al. (2017, 2018)
ERA5	2 m T(K)	Total pr (mm/day)	$0.25^\circ \times 0.25^\circ$	Hourly	–	<a href="https://cds.climate.copernicus.eu/">https://cds.climate.copernicus.eu/</a>	September 2019	Hersbach et al. (2020)

*Note.* See Table S1 and Text T1 in Supporting Information S1 for a list of the CMIP5 models included in the ensemble. Detailed discussion of individual data sets is provided in Supporting Information S1 (Text T2).

### 3.2. Gridded Observations, Reanalyses, and CMIP5 Models

To provide a more spatially comprehensive and global assessment of mountain trends than station observations permit, we additionally calculated changes in mean annual temperature ( $^\circ\text{C}/\text{century}$ ) and precipitation ( $\text{mm}/\text{century}$ ) using gridded data sets that were produced by interpolating from observations (CRU, GISTEMP, and GPCC), a reanalysis data set (ERA5), and the ensemble mean of 32 historical simulations from CMIP5 global climate models. Further details of these data sets are provided in Table 3 and Table S1 in Supporting Information S1. We retained the gridded observational data sets at their original resolutions. Data from the individual climate models were first re-sampled to a common  $1^\circ \times 1^\circ$  reference grid and then averaged to obtain the multi-model ensemble mean (hereafter, CMIP5). A land-sea mask derived from GPCC ( $0.25^\circ \times 0.25^\circ$ ) was applied to all data sets after resampling it to its native grid. Grid cells with more than 50% land were considered as such, with the remainder excluded. The effects of the adopted land selection method were included as part of an uncertainty analysis (see Section 3.4).

### 3.3. Delineation of Mountain/Lowland Areas and Gridded Comparisons

To delineate mountain and lowland regions, we use the K1 layer (Kapos et al., 2000; a simple binary classification of mountain vs. non-mountain; also see Sayre et al., 2018). This enabled us to calculate global trends for mountain and non-mountain (lowland) areas separately. K1 relies solely on elevation to classify cells above 2,500 m as mountainous, but relative relief and slope gradient are also used below this threshold. According to K1, mountain areas occupy 35.9 million  $\text{km}^2$ , or 24.3% of the land surface. Figure 1 shows the resultant global distribution of mountain areas ( $0.25^\circ$  resolution). Our adopted K1 grid is GME 1.0 from <https://rmgsc.cr.usgs.gov/gme/>, derived from a global 250 m DEM (Kapos et al., 2000) and resampled to  $0.25^\circ$  (the highest resolution of our data sets, i.e., ERA5 and GPCC), considering as mountain all cells having >30% of mountain points in the original layer. Since the climate data sets have different grid resolutions (varying natively from  $0.25^\circ$  to  $2^\circ$ ), we then resampled K1 separately onto each via first order conservative remapping. Any grid cell having at least 50% of its area classed as mountainous in K1 is considered as such. In accordance with Sayre et al. (2018), Antarctica and Greenland were excluded from the analysis. Any regridding/interpolation was performed on the elevation grid and not on temperature and precipitation data sets.

We calculate mountain and adjacent lowland temperature/precipitation trends (and trends in the difference between them) over global  $30^\circ$  latitude bands (ignoring  $>60^\circ\text{S}$ ), as well as over the key mountain regions shown in Figure 1 (Rocky Mountains, Greater Alpine Region [GAR], Tibet, and Andes) considering the entire period 1900–2018 as well as sub-periods starting in 1940, 1960, and 1980. Trends were calculated using ordinary least squares regression on area-weighted annual averages over the target band or region, and the spatial variance of the trend within the region was retained as a measure of uncertainty. We evaluate trend significance by applying Mann-Kendall tests, both on individual trend lines and on the trend of the mountain-lowland difference. Note that ERA5 and CMIP5 were evaluated over the period of their data availability, that is, 1980–2018 for ERA5 and until 2005 for CMIP5.

The areas used to derive mountain/adjacent lowland regions are arbitrarily defined using the following boundaries: Rocky Mountains: 125°/95°W and 30°/50°N; GAR: 4°/19°W and 43°/49°N; Tibetan Plateau: 60°/120°E and 18°/47°N; and Andes: 80°/60°W and 40°/0°S (Figure 1). The four areas considered have similar (but not identical) mountain/lowland area ratios.

We also evaluated our results by resampling all data sets onto a common  $1^\circ \times 1^\circ$  grid. However, this involves considerable smoothing and the loss of topographic detail. We do not discuss these results here, but include the effects of resolution in the uncertainty analysis (Section 3.4).

### 3.4. Uncertainty and Quantification of Error

Several sources of uncertainty affect our study, ranging from measurement error at individual stations to the effects of interpolation processes. If temperature data can be generally considered stochastically with negligible error for individual measurements or systematic bias among stations, precipitation measuring errors are generally associated with a (sometimes considerable) degree of underestimation. This is due to factors such as evaporation, aerodynamic effects lifting rain droplets or snowflakes out of the gauge (“undercatch”), lack of heated pluviometers, and shear effects which cause flow acceleration around the gauge (Goodison et al., 1998; Kochendorfer et al., 2017). The error is typically largest in snowy regions during the cold season and largely depends on the meteorological conditions (especially wind), coupled with the instrumental design. Different biases between sites, station instrumentation, and through time (e.g., per event, winter vs. summer) make corrections difficult (Smith et al., 2020; Thornton, Brauchli, et al., 2021).

In the station meta-analysis, uncertainty can be measured in a qualitative manner using the number of stations used to calculate the mean warming rate (more stations implying a mean value which is closer to the actual mean over the region), but since we have no information on the standard deviation of group warming rate figures within individual studies, we cannot perform a traditional statistical error analysis. Trends derived from the published studies (Tables 1 and 2) were therefore considered stochastically and with no individual error.

Gridded observational data sets are similarly affected, with the addition of the likely unrepresentative sampling and interpolation errors due to the sparse and uneven distribution of stations. In mountain areas, weighting and interpolating station data across grid cells are further complicated by the representativity of the elevation of individual stations. It is not necessarily the case that the mean elevation of stations contributing to a given cell estimate is consistent with the mean average elevation of that cell. In addition, and more problematically, high elevation regions may be completely lacking stations, which causes mountain averages to be biased toward lower elevation values.

Gridded data sets adopt several strategies to overcome sparsely distributed input data, for example, applying weighting schemes such as the inverse of the distance between the stations and the grid point (thereby incorporating nearby stations only), their directional distribution, and the gradients of the data field in the vicinity of the grid point (e.g., GPCC). In regions and periods of reduced data coverage, data filling from climatological values can be adopted to avoid interpolation artifacts (e.g., GPCC), which may affect trend calculation. A further important factor in relation to uncertainty is the temporal variability of the number of stations included. There is an increase in the number of stations during the twentieth century, but some networks see a marked decrease in the 2010s (particularly GPCC and CRU; e.g., Jones et al., 2012).

Recently, climatological estimates of uncertainty were released for some of the gridded data sets. For example, the relative sampling error for monthly precipitation in GPCC is reported to be between 7% and 40% of the true area-mean if five rain-gauges are used, and between 5% and 20% if 10 rain-gauges are used. The uncertainty estimates for ERA5 are provided by a 10-member Ensemble Data Assimilations (EDA) system, which takes into account mostly random uncertainties in the observations, sea surface temperature and the physical parametrizations of the model, but it does not account for systematic model errors. The temporal evolution of the monthly and globally averaged ERA5 ensemble spread for surface temperature shows a gradual decrease in time from 1979 to 2018 from about 0.4 to 0.3 K (Hersbach et al., 2020). However, the ensemble spread should mainly be used to evaluate the uncertainty at a given time, rather than for long-term and/or large-scale averages. For CMIP5 models, the spread of the various models can be used as an estimate of the uncertainty of the ensemble mean. The spread depends, among others, on the considered variable, geographical area and season. For example, in their

paper analyzing precipitation in the western and eastern parts of the Himalayan chain, Palazzi et al. (2015) used the coefficient of variation (the percent ratio of the multi-model standard deviation to the multi-model mean) to provide a quantitative estimate of the variability of CMIP5 models with respect to their mean. That study showed that the largest inter-model spread is measured in the Hindu-Kush Karakoram in summer, with an average value of the coefficient of variation of  $\sim 50\%$  (meaning that the standard deviation of the models is on average about the 50% of the mean) in both the historical period (time average over the years 1901–2005) and in future decades.

Given these difficulties in correctly quantifying uncertainty affecting gridded data, we adopted a common strategy for all data sets. For the results presented in this paper, we evaluated the significance of the trends purely stochastically for temperature and precipitation time series and report results (with significance) following the methodologies introduced in Sections 3.2 and 3.3 (this is the reference analysis).

We also studied uncertainty in terms of sensitivity of these results (magnitude of trends and their significance) to various different analysis configurations: this included sensitivity to land/ocean masking method, mountain/lowland selection and regridding, data set spatial resolution (i.e., retaining native grids vs. standardizing the grid resolution to  $1^\circ$ ), and adopted region sizes. For example, an ensemble of 19 result sets was obtained for ERA5 temperature trends (during 1980–2018) in all regions and latitude bands, by varying the adopted analysis configuration. The ensemble shows consistent results for GAR, Rockies, Global and  $60^\circ\text{N}/90^\circ\text{N}$  in terms of trend differences (mean  $\pm 1\sigma = 0.72 \pm 0.17$ ,  $1.32 \pm 0.18$ ,  $0.52 \pm 0.51$ , and  $-1.34 \pm 0.36^\circ\text{C}/\text{century}$ , respectively), their significance (mean  $p$ -value  $\pm 1\sigma = 0.00 \pm 0.00$ ,  $0.05 \pm 0.03$ ,  $0.03 \pm 0.04$ , and  $0.01 \pm 0.02$ ) and the number of cases being significant (19/19, 10/19, 14/19, and 17/19, respectively), but somewhat less robustness for 30S/0 with a trend of  $0.38 \pm 0.30^\circ\text{C}/\text{century}$ , a  $p$ -value  $0.07 \pm 0.07$ , and significance in 9 of the 19 ensemble members. This uncertainty analysis shows that significant results from our reference analyses, as presented in this paper, tend to lie close to the mean of the ensemble, and that the choice of methodology adopted generally does not disproportionately influence the results (see the data availability statement for how to access the sensitivity analysis).

## 4. Results: Temperature Trends

### 4.1. Station Observations

Figure 2 shows the mean warming rate ( $^\circ\text{C}/\text{century}$ ) reported for each study against the mid-year of the respective observational record. There is a general tendency for trend magnitudes to be higher for the shorter records (which usually begin later), particularly in the Tibetan Plateau. The longest studies (with mid-points before 1970) have more stable temperature trends, below  $2^\circ\text{C}/\text{century}$ . Although this is partly a statistical artifact, it also suggests that mountain temperature trends may have accelerated in recent decades in comparison with earlier years. The Andes region shows weaker trends than many others, and includes one cooling site ( $-7^\circ\text{C}/\text{century}$ ).

Prior to 1980, differences between mountain trends and the global land and land/ocean trends were minimal. However, many of these studies are based on long records ( $>100$  years). Since 1980, however, mountain studies have, on average, reported higher trend values than the global mean (as given by both CRUTEM4 and HadCRUT4). Global mountain syntheses (defined as trends from the five studies with more than 500 stations distributed around the world, marked “global” in Table 1) are closer than individual mountain studies to CRUTEM4 and HadCRUT4 (for the same time point), but since 1970 have also tended to give marginally higher mean warming rates than the global average. Therefore, there appears to be some limited evidence for EDW with more pronounced warming at higher elevations, or at least enhanced mountain warming in comparison with the global land and land/ocean mean warming rates. Of the individual mountain studies ( $n = 61$ ), only 8 or 16 of the trends are weaker than the equivalent HadCRUT4 or CRUTEM4 trend over the same period, respectively.

As the above studies are taken from a variety of geographical regions, regional differences that are independent of elevation will be present. We therefore also compared trends from high/low elevation station groups within the same region. In 9 of 11 paired studies, the high-elevation stations exhibit a higher trend magnitude than the corresponding mid or low elevation stations (Figure 3). This indicates that within regions, more pronounced warming at high elevations often exists.

When a global comparison of mean temperature trends for all high-elevation/mountain regions versus all adjacent low elevation regions grouped together was performed (classifying unpaired studies in the high-elevation group),



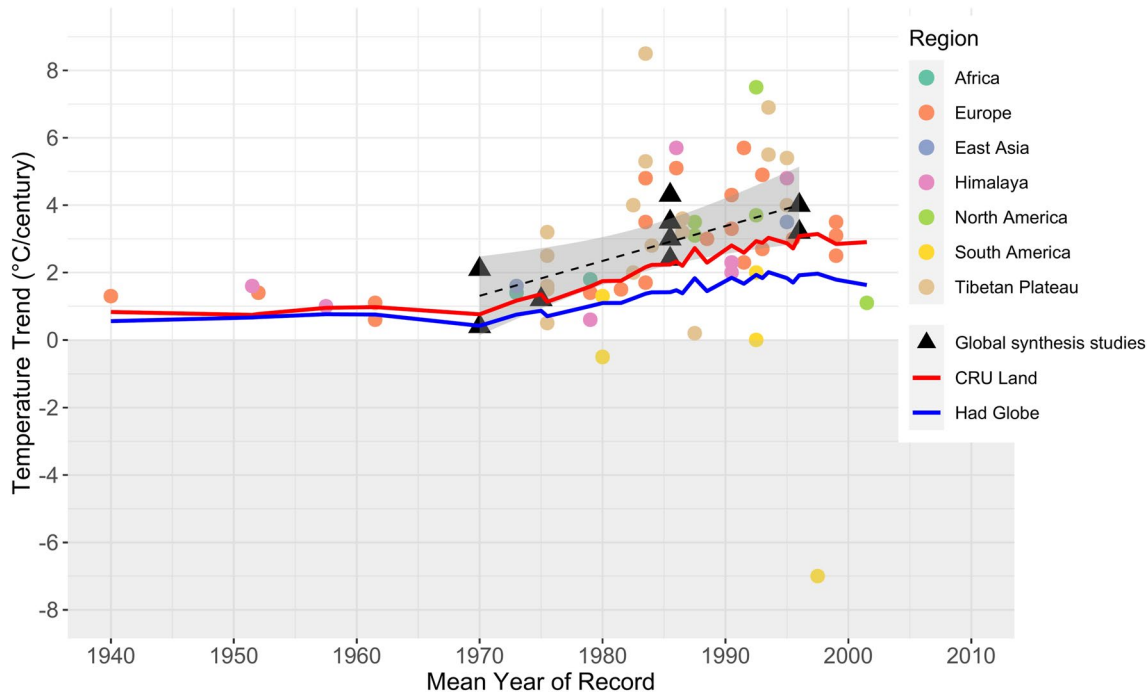


**Figure 2.** Mean warming rate versus observational record mid-point from all individual studies. Symbol colors indicate the region. Trends from the five global mountain syntheses (>500 stations) are represented by black triangles ( $n = 9$ ), and the global syntheses best-fit line by the dotted line (linear regression:  $r^2 = 0.70$ ,  $p < 0.01$ ). The HadCRUT4 (global land and sea combined) and CRUTEM4 (land surface only) trends for the same period as the mountain studies (variable in length) are represented by the two solid lines. The length of the running mean is indicative of the average length of record upon which the trends in the individual regions are based.

no significant difference in mean trend magnitude between the groups was detected. Median warming rates for the high group are  $+2.3^\circ\text{C}/\text{century}$  ( $n = 59$ ), compared with  $+3.2^\circ\text{C}/\text{century}$  ( $n = 11$ ) for the low group ( $p = 0.57$  based on two-tailed  $t$ -test; figure not shown). Although the high-elevation group is warming less rapidly on average, its variance is much higher. This is expected because the group is larger, but also because a random sample of  $n$  stations in mountain terrain would likely have more variable trends than the same sample in flatter regions due to the effects of complex topography. When the comparison is restricted to paired studies in the same geographical region (high- and low-elevation groups in close proximity), the pattern reverses and the mean/median high-elevation rate is  $+3.9^\circ\text{C}/+3.5^\circ\text{C}/\text{century}$ , compared with  $+3.1^\circ\text{C}/+3.2^\circ\text{C}/\text{century}$  for adjacent low elevation regions). Statistical significance for any consistent elevation difference is weak, however ( $p = 0.140$ : two tailed  $t$ -test). This finding implies that the uneven geographical distributions of mountain and lowland sites included in any “global scale” study may be at least partly responsible for the lack of consistent EDW pattern when all areas are assessed together. Given the appreciable difference it makes to results, consideration of the definition of the lowland area(s) with which mountain data are to be compared is an important area for further research.

## 4.2. Analyses of Gridded Data

### 4.2.1. Global

Table 4 shows temperature trends ( $^\circ\text{C}/\text{century}$ ) for four gridded data sets (CRU, GISTEMP, ERA5, and CMIP5) over four different periods for mountains (upper figure) and lowlands (lower figure). Changes in the mountain/lowland difference are indicated in the right of each cell. Enhanced mountain warming is represented by dark orange (significant) and light orange (insignificant) cells, and reduced warming by green (significant) and light blue (insignificant) cells.

In contrast to station observations, the pattern in the gridded data sets is somewhat less distinct, although on a global scale warming in mountains tends to be greater than the mean for their adjacent lowlands. This is particularly true for CRU over 1900–2018, and for CMIP5 over all periods. There is a slight tendency for positive EDW



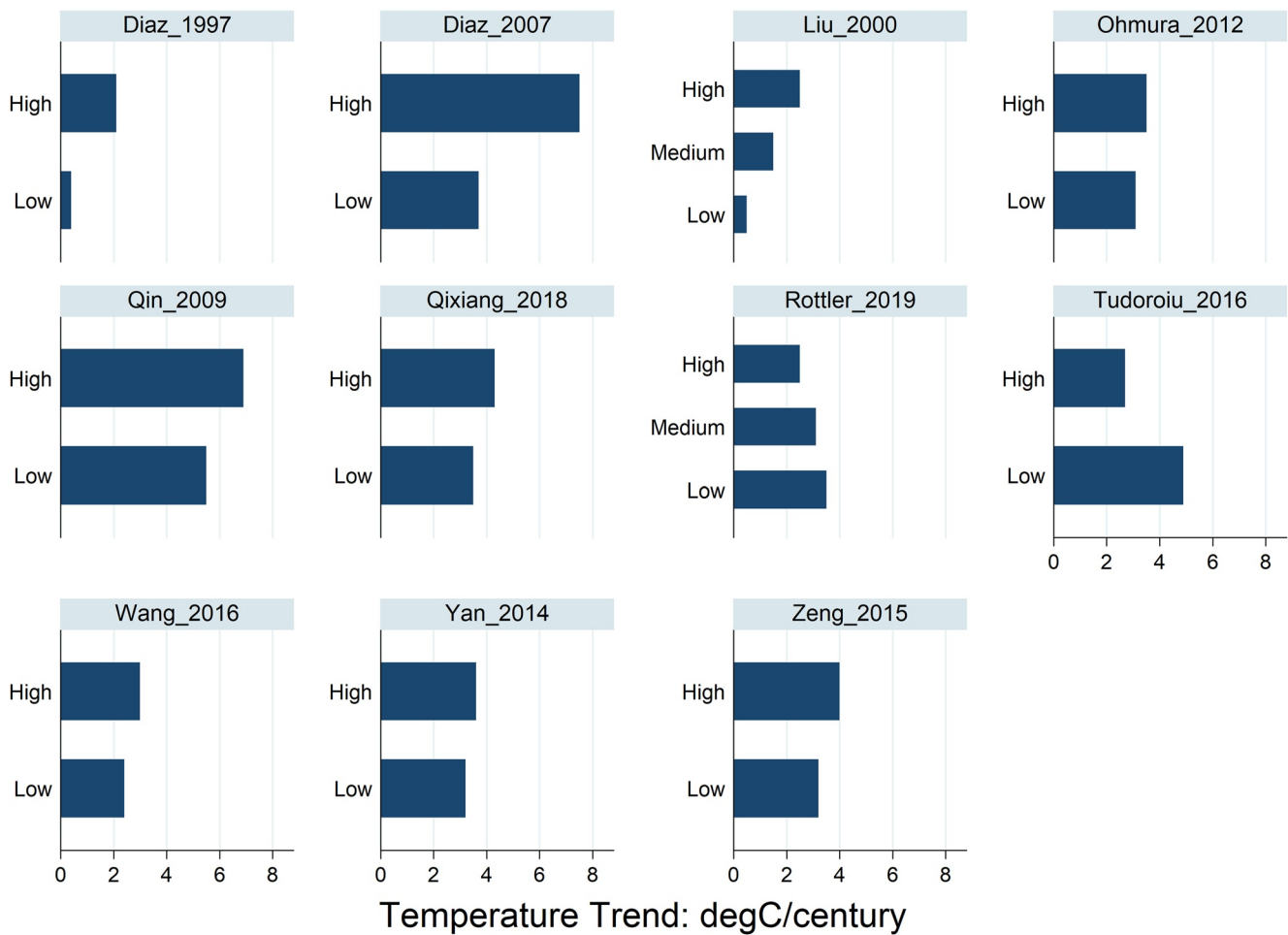


**Figure 3.** Mean warming rates for paired studies (i.e., comparing groups of adjacent high and low elevation stations in the same region). Traditional error bars and significance of differences in individual studies cannot be provided because information on trend variance between individual stations within each group is rarely available in the original references.

(enhanced mountain warming in comparison with lowlands) to be more frequent in 1980–2018. However, there are large inconsistencies and discrepancies between data sets. ERA5 shows positive EDW in all cases apart from high northern latitudes (data only exists since 1980), but GISTEMP and CRU are more ambivalent with many examples of negative EDW (reduced mountain warming in comparison with lowlands—green and blue shading). There is also a noticeable difference between hemispheres, with the southern hemisphere usually showing positive EDW (enhanced mountain warming) and the northern hemisphere sometimes the reverse. This contrast is particularly strong in the CMIP5 simulations.

#### 4.2.2. Regional

Individual mountain regions were also compared with their immediate surroundings (defined in Figure 1). In many cases, differences between mountain and surrounding lowland warming rates were significant (bold lines in Figure 4, and full figures in Table S2 in Supporting Information S1). Overall, enhanced mountain warming ( $p < 0.05$ ) is much more common (20 cases) than reduced warming (5 cases). Enhanced warming can be seen in many regions, especially in the GAR, and for CMIP5 hindcasts in general. Regions which show significantly weaker warming in comparison with lowland surroundings ( $p < 0.01$ ) include the Tibetan Plateau region for 1900–2018 and 1940–2018 (CRU) and 1940–2018 (GISTEMP), and the Andes for 1980–2018 (CRU). CRU tends to be an outlier in this regard. The Rocky Mountains as a whole show fewer significant differences with their surroundings.

**Table 4**

Temperature Trends (°C/100 years) for Mountain/Lowland/Elevation Difference by Latitudinal Band for Four Different Periods Using Four Different Global Gridded Data Sets

		1940-2018							
						1960-2018			
								1980-2018	
GLOBAL		1.02	0.06	1.50	0.00	2.37	0.09	2.75	0.14
		0.95		1.50		2.27		2.61	
NORTH	60-90	1.53	0.16	2.29	0.20	4.01	0.18	4.48	-0.23
		1.37		2.08		3.83		4.71	
	30-60	1.20	-0.07	1.76	-0.15	2.63	-0.06	3.14	0.03
		1.27		1.91		2.70		3.11	
	0-30	0.69	-0.04	1.06	-0.19	1.85	-0.10	2.25	0.07
		0.74		1.25		1.95		2.18	
SOUTH	0-30	0.64	0.03	0.91	-0.10	1.32	-0.11	1.29	-0.25
		0.62		1.01		1.43		1.53	
	30-60	0.69	-0.11	0.98	-0.24	1.34	-0.06	1.55	0.00
		0.80		1.22		1.40		1.55	
	60-90	INSUFFICIENT DATA							
		INSUFFICIENT DATA							

		1940-2018							
						1960-2018			
								1980-2018	
GLOBAL		1.13	-0.01	1.68	0.00	2.59	0.14	3.01	0.23
		1.13		1.68		2.45		2.78	
NORTH	60-90	1.50	-0.09	2.28	-0.05	3.89	-0.14	4.39	-0.68
		1.59		2.33		4.03		5.07	
	30-60	1.21	-0.01	1.89	-0.02	2.84	0.07	3.37	0.08
		1.22		1.90		2.77		3.29	
	0-30	0.83	-0.12	1.29	-0.20	2.09	-0.05	2.63	0.16
		0.95		1.48		2.14		2.47	
SOUTH	0-30	1.02	-0.09	1.22	-0.18	1.66	-0.16	1.65	0.00
		1.12		1.40		1.82		1.65	
	30-60	1.04	0.15	1.18	-0.09	1.54	0.01	1.52	-0.03
		0.89		1.27		1.53		1.55	
	60-90	INSUFFICIENT DATA							
		INSUFFICIENT DATA							

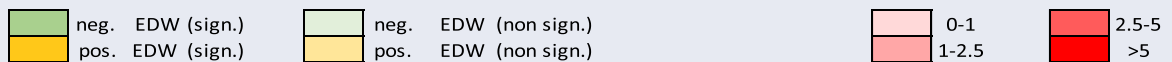
  

ERA5		1980-2018	
GLOBAL		3.32	0.27
		3.06	
NORTH	60-90	4.35	-1.21
		5.56	
	30-60	3.80	0.37
		3.43	
	0-30	2.89	0.09
		2.80	
SOUTH	0-30	2.25	0.36
		1.88	
	30-60	1.65	0.34
		1.31	
	60-90	INS. DATA	
		INS. DATA	

CMIP5		1900 - 2018							
						1960-2018			
								1980-2018	
GLOBAL		0.84	0.02	1.30	0.06	2.42	0.16	3.88	0.46
		0.83		1.24		2.26		3.42	
NORTH	60-90	1.39	-0.13	2.11	-0.18	3.50	-0.35	6.04	-0.26
		1.52		2.29		3.85		6.30	
	30-60	0.83	-0.01	1.36	-0.05	2.65	-0.08	4.42	0.01
		0.84		1.41		2.73		4.40	
	0-30	0.68	-0.03	1.01	-0.02	1.94	0.05	3.03	0.23
		0.71		1.03		1.89		2.80	
SOUTH	0-30	0.73	0.06	1.01	0.10	1.79	0.16	2.30	0.20
		0.66		0.91		1.64		2.10	
	30-60	0.64	0.08	0.85	0.10	1.37	0.16	1.56	0.11
		0.56		0.75		1.21		1.45	
	60-90	INSUFFICIENT DATA							
		INSUFFICIENT DATA							

Temperature trend (°C/century)



Note. Trend figures show mountain warming rate/lowland warming rate (left-hand side) and rate of change in the mountain/lowland difference (right-hand side). All absolute trends are positive (warming). Green = mountain warming significantly slower than lowlands; light blue = mountain warming slower (not significant); light orange = mountain warming faster (not significant); and dark orange = mountain warming significantly faster. Significance of trend in the difference is based on the Mann-Kendall test,  $p < 0.05$ .

A systematic examination of statistically significant trends in mountain/lowland temperature difference by season and by region is shown in Table 5 for two time periods (1900–2018 and 1980–2018). Clearly all mountain regions are different, but the Tibetan Plateau is most consistent in showing reduced warming with elevation, while the Andes, Rockies, and GAR often show enhanced warming, particularly in summer and over the longer time period (1900–2018). Trends over the most recent period (1980–2018) are somewhat more ambivalent, especially in the Andes. Overall it can be clearly seen that there is a predominance of positive trends for temperature (meaning enhanced warming at high elevation or positive EDW). Precipitation is discussed in Section 5.

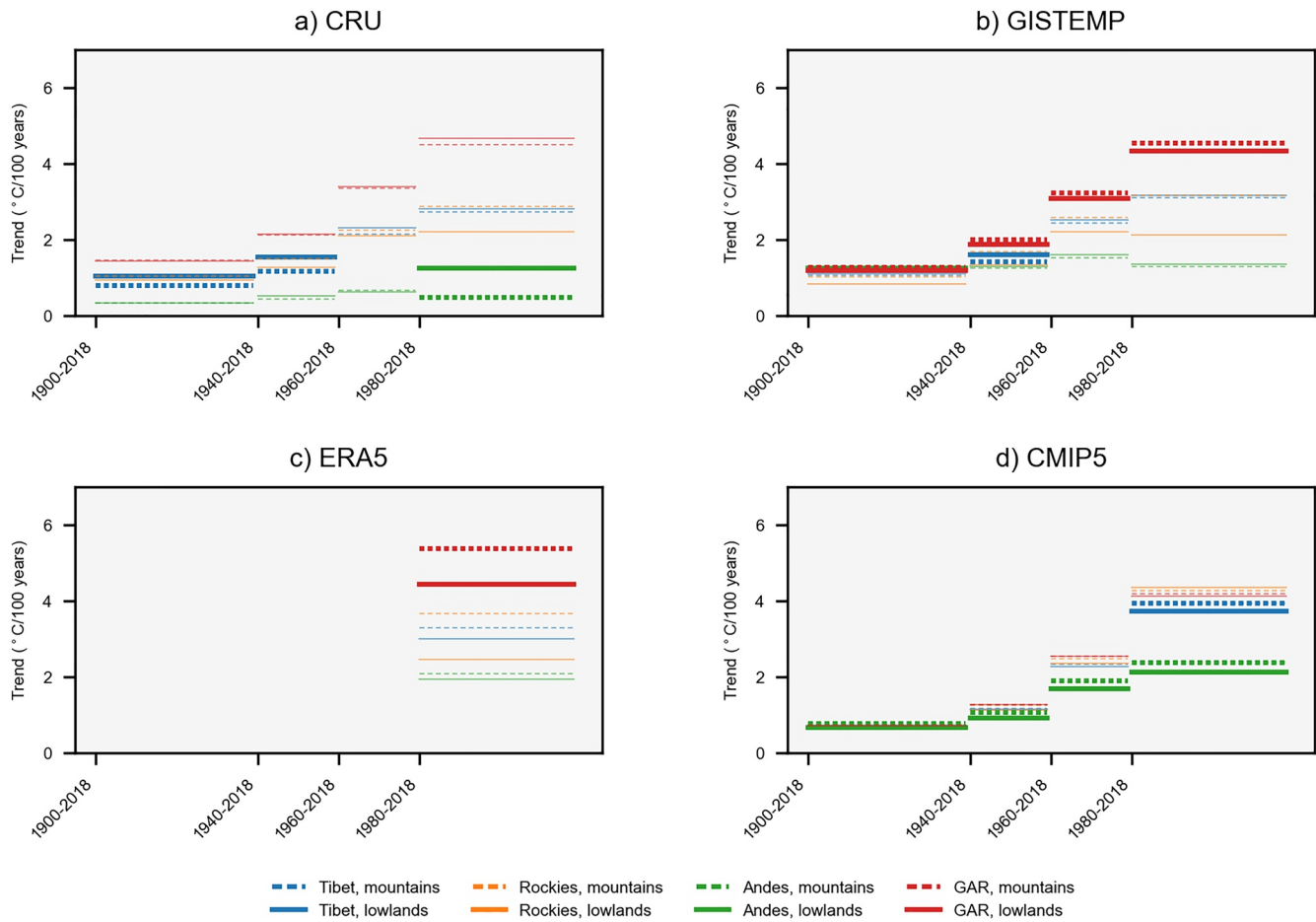


**Figure 4.** Temperature trends for four different mountain/lowland comparisons for (a) CRU, (b) GISTEMP, (c) ERA5, and (d) CMIP5 gridded data sets. Mountain/lowland rates are represented by dotted/solid lines, respectively. Significant differences ( $p < 0.01$ ) are represented by bold lines. Full trend comparison figures are listed in the Table S2 in Supporting Information S1. To improve clarity for the reader, the four periods are represented from left to right, and the lines do not overlap (they would otherwise extend to 2018 in all cases).

### 4.3. Discussion

#### 4.3.1. Global Synthesis

When all studies are combined, our meta-study shows no significant difference between high- and low-elevation temperature trends on a global scale. In this case, the pooled stations in each group come from a range of different global regions, and since no universal absolute elevation threshold was applied to distinguish these two groups, high and low elevation are purely relative terms. Thus, geographical differences may confound the straightforward quantification of EDW.

In contrast, most paired station comparisons (within the same region) indicate enhanced warming at higher elevations. However, this finding is based on a relatively small sample of localized studies. It is even possible, although unproven, that a reporting bias could exist, with enhanced mountain warming potentially being considered more worthy of reporting than the reverse finding. However, comparison between mountain warming and observed global temperature trends for combined land and sea (HadCRUT) and land only (CRUTEM4; Figure 2b) shows that in approximately 80% of cases, mountain temperature trends are stronger than the global mean trends calculated over the same time period. This again suggests, at least on a broad scale, that positive EDW appears to be the predominant overall situation.

When spatially continuous gridded data sets are used to compare mountain (K1) and lowland trends, a broadly similar picture emerges. Although more rapid mountain warming often exists in individual regions (Figure 4 and

Table 5

Trends in Mountain/Lowland Temperature and Precipitation Differences for Different Mountain Ranges in Different Seasons

		DJF	MAM	JJA	SON	YEAR	SUMMARY
Temperature Difference 1900-2018	Rockies			+GISTEMP	+GISTEMP		2+
	Andes	+CMIP5	+CMIP5	+CMIP5	+CMIP5	+CMIP5	5+
	GAR	-CMIP5	+CRU	+CRU/+GISTEMP			3+/1-
	Tibet	-CMIP5	-CRU/-GISTEMP	-CRU	-CRU/-GISTEMP	-CRU/-CMIP5	8-
	<b>Summary</b>	<b>1+/2-</b>	<b>2+/2-</b>	<b>4+/1-</b>	<b>2+/2-</b>	<b>1+/2-</b>	<b>10+/9-</b>
Temperature Difference 1980-2018	Rockies			+ERA5/+GISTEMP			2+
	Andes	+CMIP5	+CMIP5	-ERA5/-CRU	-CRU	-CRU/+CMIP5	3+/4-
	GAR	+ERA5	+ERA5			+ERA5	3+
	Tibet		-CRU/-GISTEMP				2-
	<b>Summary</b>	<b>2+/0-</b>	<b>2+/2-</b>	<b>2+/2-</b>	<b>0+/1-</b>	<b>2+/1-</b>	<b>8+/6-</b>
Precipitation Difference 1900-2018	Rockies		-CMIP5				1-
	Andes	-CRU	-CRU/-GPCC	-CMIP5	-CRU	-CRU	6-
	GAR		-CMIP5		-CMIP5	-CMIP5	3-
	Tibet	-CMIP5	+CRU	-CMIP5	-CMIP5	-CMIP5	1+/4-
	<b>Summary</b>	<b>0+/2-</b>	<b>1+/4-</b>	<b>0+/2-</b>	<b>0+/3-</b>	<b>0+/3-</b>	<b>1+/14-</b>
Precipitation Difference 1980-2018	Rockies			-ERA5			1-
	Andes			+ERA5	-ERA5		1+/1-
	GAR						0
	Tibet		+CMIP5		-ERA5	-ERA5	1+/2-
	<b>Summary</b>	<b>0+/0-</b>	<b>1+/0-</b>	<b>1+/1-</b>	<b>0+/2-</b>	<b>0+/1-</b>	<b>2+/4-</b>

Note. A negative trend (blue) means a decreasing difference (mountain warming less rapidly and more negative lapse rate for temperature, and mountain wetting less rapidly and reduced elevation-dependent precipitation). A positive trend (red) means an increasing difference (mountain warming more rapidly, and mountain wetting more rapidly with increased elevation-dependent precipitation).

Table S2 in Supporting Information S1), the evidence in broader latitudinal bands (Table 4) is more equivocal. When data from entire latitudinal bands are averaged, mountain trends are not consistently different from those of adjacent lowlands. Although warming trends have accelerated in many locations, this appears to be slightly more marked in many mountain regions, indicating a weak tendency for positive EDW to be more widespread than negative EDW, especially in the most recent period (from 1980 onwards). For example, for both ERA5 and CMIP5, five out of six comparisons shown suggest stronger mountain warming in the most recent period, although not always statistically significant (Table 4). These findings appear to be consistent with an increasingly clearer signal of positive EDW in the station analysis as time progresses (Figure 2b), and this has also been suggested in recent literature examining the temporal evolution of EDW on the Tibetan Plateau (Guo et al., 2021). Further work needs to break down sets of time series into sub-periods to examine the temporal evolution of trends.

### 4.3.2. Regional Contrasts and Differences

When individual mountain regions are examined in the gridded analysis, there is a much higher incidence of enhanced mountain warming in comparison with lowlands at the annual scale; four times that of the opposite pattern (Table S2 in Supporting Information S1). This agrees with the station analysis that suggests that positive EDW is more prevalent within mountain regions than when data from all mountain regions globally are pooled into a single group. Positive EDW signals in the GAR and the Rockies seem to be much more consistent between data sets and time periods than in the Tibetan Plateau region (which sometimes shows the reverse), which perhaps explains the high level of debate about the exact nature of EDW in the latter region (Gao et al., 2018; Guo et al., 2020; J. Qin et al., 2009; Li et al., 2020; You et al., 2008).

A simple lowland/mountain comparison using a binary mountain/non-mountain classification cannot quantify more complex EDW signals. In particular, any enhanced warming at moderate elevations might be overlooked by our methodology. Many studies within the Tibetan Plateau have suggested that more complex “banding” within EDW is present with enhanced warming up to and around the elevation of current snowline (~5,000 m a.s.l.; Gao et al., 2018; J. Qin et al., 2009; Pepin et al., 2019), but reduced warming above this. Moreover, because the altitudinal zonation of land-cover and snowlines vary across the globe (and indeed seasonally), potentially critical elevation bands could lie at different elevations in different locations. A more sophisticated analysis would therefore be required to analyze detailed vertical warming profiles. The K1 mountain classification distinguishes six separate elevation bands, so in theory such analyses would be possible. That said, using fixed elevation bands (e.g., absolute elevation thresholds) might conflate different signals in different regions, meaning a global analysis could hide complexities. Applying variable bands based on local climatology (e.g., mean annual temperatures) rather than elevation per se may overcome this issue to some extent.

Some regions show less warming than their surroundings over longer periods in CRU and GISTEMP (Table S2 in Supporting Information S1), including the Andes and Tibetan Plateau. Both these ranges are surrounded by very different lowland climates. For example, the western slopes of the Andes are primarily desert, while the eastern slopes fall into the humid Amazonian basin. Thus, the lowland mean is an average of several distinct climate zones. It is well known, for instance, that the western and eastern slopes of the Andes have demonstrated different patterns of temperature change in the recent past (Vuille et al., 2003). Changes in the Pacific Ocean low-level inversion and sea surface temperatures influence the vertical profile of EDW on the western slopes, but not in the east (Vuille et al., 2015). Lumping the whole “adjacent lowlands” together risks missing this detail. On the Tibetan Plateau, there are known differences in EDW between the continental regime to the north, and the wetter humid regime to the south and east (Li et al., 2020; You et al., 2008), with different controls on lapse rates in the south-western plateau and Himalaya (Kattel et al., 2015) versus inland China (Li et al., 2012, 2013). It is therefore possible that EDW profiles on opposing slopes of the same mountain range may be physically decoupled, and could therefore cancel out or reinforce each other in our broad analyses. Further work must be conducted to subdivide the surroundings to examine different slope aspects separately.

The brief seasonal analysis (Table 5) again shows a predominance of enhanced mountain warming overall, but also especially in boreal summer (1900–2018). However, in other seasons the opposite is sometimes apparent. Summer mountain climate is often dominated by isolated convective events and strong thermal circulations, whilst any free-air effect is often less prominent because prevailing winds are often at their weakest. Further investigations into seasonal contrasts in changing elevational temperature differences may elucidate how such mechanisms are responding to climate forcing. Since many broader impacts are seasonal in nature, it is critical to understand how seasonal contrasts in EDW may arise, and perhaps persist, in future.

#### 4.3.2.1. Caveats

It should be a simple task to assess whether high and low elevation temperature trends are different using station data. However, choice of methodology is a complex decision. The majority of past studies which have paired high and low elevation station groups in the same region have demonstrated evidence of positive EDW (enhanced mountain warming). When a more extensive approach is given, categorizing all stations in discrete elevation bands (in our case solely high vs. low) and then comparing mean (or median) trends for different bands, results are more equivocal. Other decisions include whether to contrast station groupings (as we have done in this review) or to plot a regression line between individual trend magnitudes (for many stations) and elevation. There is no agreed “right” and “wrong” methodology, even though such choices influence the findings.

Individual gridded data sets do not consistently agree in their broad global temperature change patterns. CRU and GISTEMP, for example, show opposing global patterns in the mountain/lowland temperature difference over the 1900–2018 period. These gridded data sets are interpolated from irregularly spaced point data, and use of different stations and/or different interpolation techniques is likely responsible for some of the differences between them. For future region-specific mountain versus lowland comparisons, it might prove fruitful to include regional/national scale grids, which often have a denser underlying station network. Regarding reanalysis products, although ERA5 was considered the best of several alternatives at replicating observed trends in air temperatures at high elevation in the Alps, some errors were still considerable, particularly in winter (Scherrer, 2020).

That CMIP5 model simulations are more likely to show positive EDW in historical runs than the observed data sets (at least in the southern hemisphere and on a global scale) is a surprising finding and requires further research. It may be that this signal is externally forced. Internal variability on the other hand, which is reflected in observational data sets but not in a CMIP5 ensemble mean, might control EDW signals in many mountain regions. In the tropical Andes, for example, the observed EDW profile reversed sign between an earlier (1961–1990) and a later period (1981–2010), in response to a phase shift of the Pacific Decadal Oscillation (PDO; Vuille et al., 2015). Since CMIP5 models represent coupled simulations, their phasing of internal variability driven by El-Niño Southern Oscillation or PDO may not align with reality, and once CMIP5 models are averaged into a multi-model mean, the internal variability cancels out. This might result in a stronger, externally forced EDW signal in CMIP models compared to observations. It is imperative that differences between various temperature data sets (station observations, both point and interpolated, reanalyses and model runs) be better understood if we are to have confidence in assessment of past trends and future EDW predictions (Kotlarski et al., 2015; Palazzi et al., 2017; Rangwala et al., 2016).

## 5. Precipitation

### 5.1. Evidence From Station Observations

Observed precipitation trends are quoted in either absolute (e.g., mm/decade) or percentage terms. It is difficult to compare the two because of challenges in converting one to the other. Therefore, studies providing information on absolute and relative (%) precipitation change remained separated (Table 2). No clear patterns arise from the meta-analysis of trend magnitudes (standardized per decade) with respect to time (Figure 5). Roughly an equal number of studies suggest climatic wetting and drying. No significant relationship between the mean of the period and the rate of wetting/drying is apparent, and no consistent increase in the trend magnitude over time emerges, in contrast to temperature. Trends appear to be slightly less variable when the mean year of record is earlier (left of graph) but this is partly a statistical artifact, the length of period being longer for earlier studies.

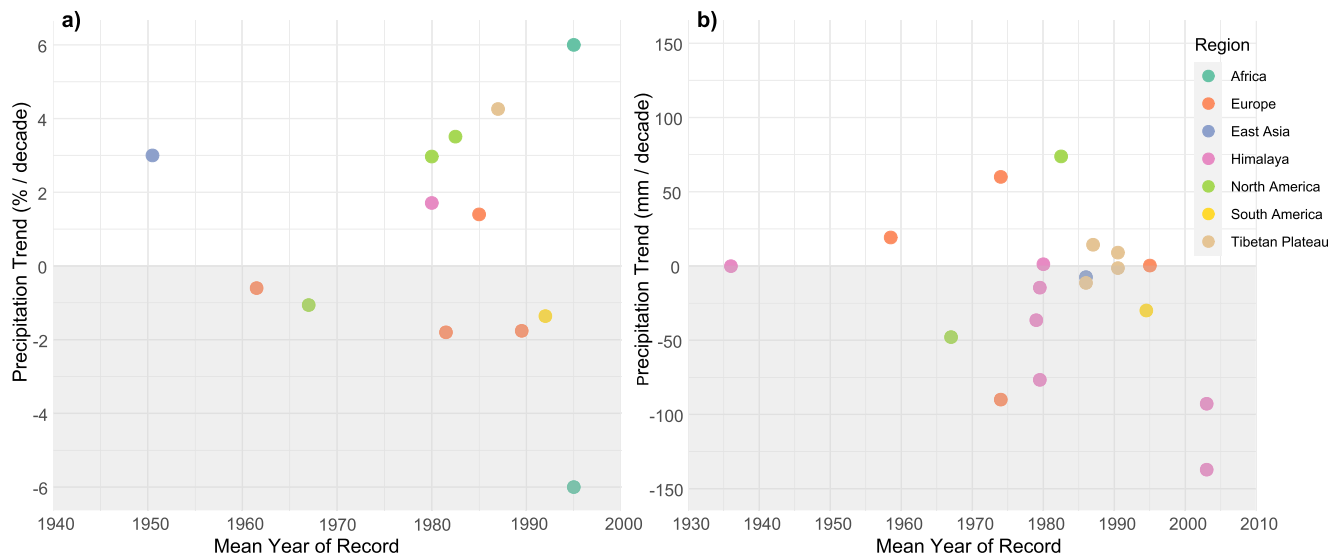


**Figure 5.** (a) Relative, and (b) absolute changes in mountain precipitation (in situ station studies from SROCC) plotted against the mean year of the respective record. The respective scales are not strictly comparable in terms of vertical stretching as the conversion from absolute to relative change (and vice versa) is dependent upon mean annual precipitation, which varies from place to place.



Depending on the period considered, there may be inter-decadal oscillations in trend magnitudes, although the high noise levels and measurement uncertainties make them difficult to quantify globally.

**5.2. Analyses of Gridded Data**

**5.2.1. Global**

The global gridded precipitation data sets show more consistent patterns in differences between mountain and lowlands (Table 6) than the station analysis. CRU and GPCC show broadly similar patterns, with a predominance toward increased drying/decreased wetting in mountain regions in comparison with adjacent lowlands, that is,

**Table 6**  
Precipitation Trends (mm/Year/Century) for Mountain/Lowland Areas (Left-Hand Side) and Orographic Effect (Right-Hand Side) by Latitudinal Band Over Four Different Periods Extracted From Four Different Global Gridded Data Sets

		CRU		1900 - 2018							
				1940-2018				1960-2018			
						1980-2018					
NORTH	GLOBAL	14	-8	8	-11	1	-21	31	-47		
		22		19		22		78			
	60-90	33	-5	25	-11	24	-15	67	8		
		37		36		39		59			
30-60		19	-15	12	-30	4	-37	5	-44		
		33		42		42		49			
0-30		-5	3	1	24	20	11	104	-41		
		-3		-22		9		145			
SOUTH	0-30	19	-11	7	-21	-30	-38	30	-44		
		30		28		8		74			
	30-60	-5	-48	-61	-79	-105	-95	-190	-111		
		43		18		-9		-79			
60-90	INSUFFICIENT DATA										

		GPCC		1900 - 2018							
				1940-2018				1960-2018			
						1980-2018					
NORTH	GLOBAL	5	-7	9	-9	6	-15	23	-58		
		11		18		21		81			
	60-90	21	-13	40	-21	26	-8	54	-19		
		34		61		34		73			
30-60		16	-15	25	-22	13	-25	29	-13		
		31		48		38		42			
0-30		-16	-2	-23	5	3	-1	41	-84		
		-15		-28		3		124			
SOUTH	0-30	-1	-4	-3	-13	-12	-20	-16	-108		
		3		10		8		92			
	30-60	-31	-62	-56	-104	-68	-128	84	-105		
		31		48		60		21			
60-90	INSUFFICIENT DATA										

		ERAS	
		1980-2018	
GLOBAL		-96	-108
		12	
NORTH	60-90	77	25
		53	
	30-60	-103	-58
		-45	
0-30		-142	-166
		24	
SOUTH	0-30	-123	-192
		68	
	30-60	-159	-31
		-128	
60-90	INS. DATA		

		CMIP5		1900 - 2018							
				1940-2018				1960-2018			
						1980-2018					
NORTH	GLOBAL	-4	-5	-1	-7	26	-6	70	4		
		1		6		32		66			
	60-90	25	3	43	5	79	8	137	38		
		22		37		71		99			
30-60		0	-4	4	-6	22	-9	63	2		
		4		10		31		61			
0-30		-30	-17	-23	-18	22	-8	112	-6		
		-13		-5		30		118			
SOUTH	0-30	-2	-5	-16	-15	11	-9	-1	-6		
		2		-1		20		5			
	30-60	-15	-16	-9	-18	-8	-21	-17	-29		
		1		9		12		12			
60-90	v										

Precipitation trend (mm/year/century)

increased orographic gradient (sign.)   
  increased orographic gradient (non sign.)   
  positive   
  negative  
 decreased orographic gradient (sign.)   
  decreased orographic gradient (non sign.)

Note. Orange = increased orographic effect (significant); pink = increased orographic effect (not significant); dark blue = decreased orographic effect (significant); light blue = decreased orographic effect (not significant). Significance of trend in the difference is based on the Mann-Kendall test,  $p < 0.05$ .

a decrease in elevation-dependency of precipitation. The latitudinal band 0°–30°N (tropical highlands) in CRU, where the elevation dependence has strengthened in some time periods (although not significantly), is an exception. In more than half of the cases (15/13 of 24 comparisons for CRU and GPCC, respectively), a long-term precipitation increase has occurred in both lowlands and mountains, but this has been stronger in the lowlands (thus reducing elevation-dependence of precipitation). In both CRU and GPCC there is also little difference between periods, although from 1980 onwards the strengthening of the orographic effect in the tropics disappears and elevation-dependence of precipitation is reduced globally. ERA5 also shows consistent weakening of the orographic effect, as does CMIP5 in most locations, although this is offset in CMIP5 by significant steepened orographic effects in high northern latitudes (above 60°N) in all periods, which becomes even more distinct in the most recent period. Being inconsistent with the other global changes, this is something of an outlier.

### 5.2.2. Regional

Comparisons of regional mountain precipitation changes in Figure 6 shows that trends vary by region, but that relatively few are significant. Globally, decreasing elevation-dependence of precipitation (relative lowland wetting) dominates (Table S3 in Supporting Information S1). All but one of the 16 significant regional trends in mountain/lowland precipitation difference are negative (weakening orographic effect). Absolute precipitation trends tend to become more variable over 1980–2018. Significant contrasts between regions are apparent, but this also depends on the data set. Tibet shows a decreasing orographic effect (ERA5) driven by strong mountain drying. The Rockies also show a significant decreasing orographic effect over 1940–2018 and 1960–2018 (CMIP5),

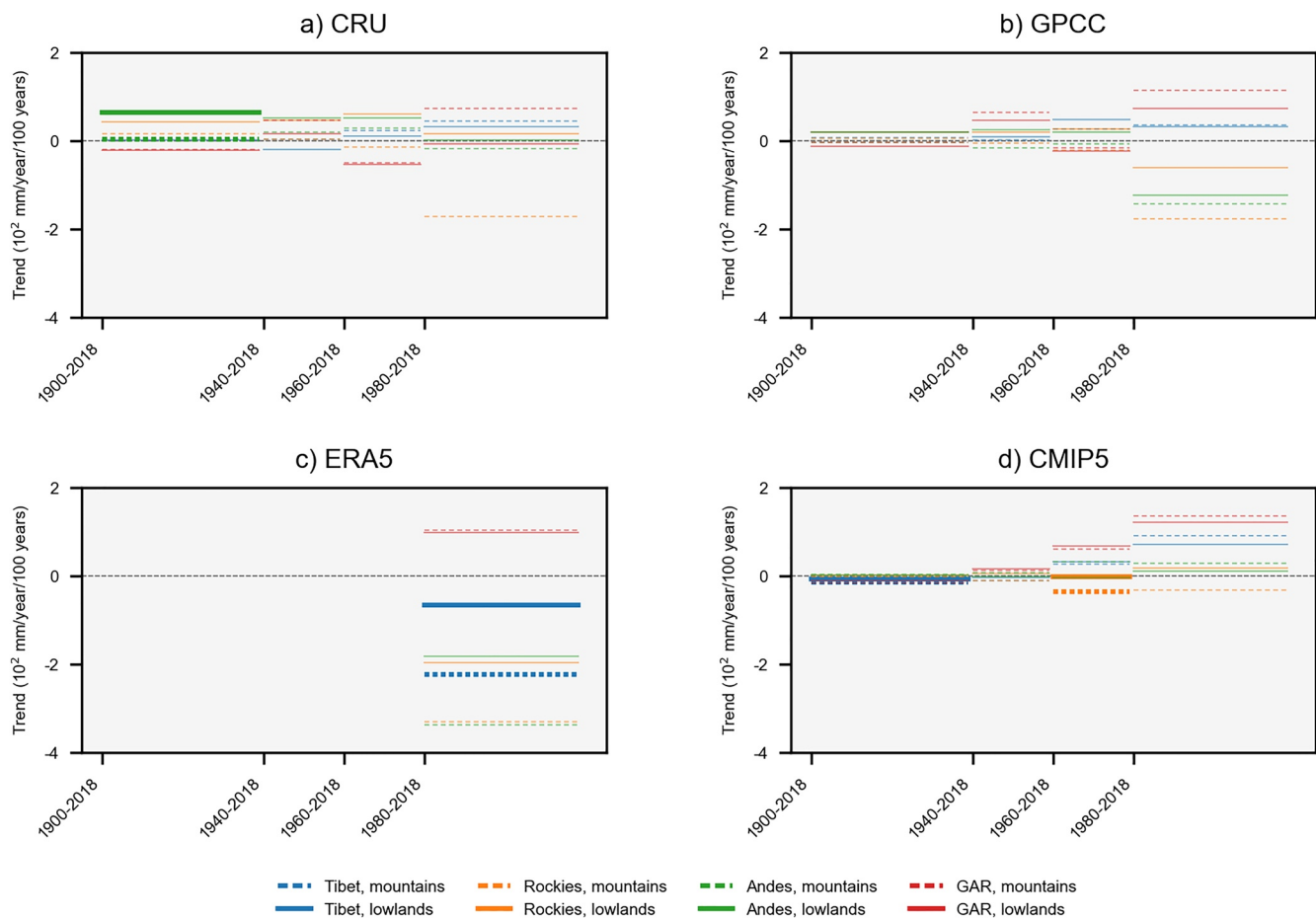


**Figure 6.** Precipitation trends for four different mountain/lowland comparisons for (a) CRU, (b) GISTEMP, (c) ERA5, and (d) CMIP5 gridded data sets. Mountain/lowland rates are represented by dotted/solid lines respectively. Significant differences ( $p < 0.01$ ) are represented by bold lines. Full trend comparison data are listed in Table S3 in Supporting Information S1. For clarity, the four periods are represented from left to right, and the lines do not overlap (they would otherwise extend to 2018 in all cases).

as do the Andes over 1900–2018 (CRU). The only increasing difference is reported in the Andes for 1960–2018 (CMIP5), but absolute changes are small.

Unlike for temperature, there was generally no systematic contrast in trends by season (Table 5). The observed weakening of elevation-dependency of precipitation was consistent in all seasons (i.e., all seasons contribute equally to the annual trend), particularly over the longer period of 1900–2018. The Andes and Tibet tend to show more significant changes overall than the Rockies and GAR. In the most recent period (1980–2018) the weakening is somewhat less distinct, but still the dominant pattern.

### 5.3. Discussion

#### 5.3.1. Global Synthesis

Based on station data published in IPCC SROCC, it is uncertain whether elevation-dependency of precipitation is changing. The small sample size, wide variety of mountain regions sampled, and the difficulties associated with easily comparing absolute and relative changes are all contributory factors which obscure the results. The measurement of high-elevation precipitation is particularly difficult, especially when the proportion of snowfall is high and conditions are windy. Due to the resultant gauge undercatch (Goodison et al., 1998; Kochendorfer et al., 2017), mountain precipitation measurements are often unreliable and systematically biased toward underestimation (Whiteman, 2000), and this bias probably increases with elevation. Moreover, the number of long-term high-elevation stations is severely limited, and comprehensive studies of mountain precipitation are rare. Controversially, our ability to model mountain precipitation may now exceed our ability to measure it (Lundquist et al., 2019).

The use of gridded observational and modeled data sets provides a slightly more comprehensive picture, reducing some of the noise arising from irregular station distribution and facilitating analyses of regional trends. Perhaps surprisingly, due to the general dominance of decreasing orographic effects, there was much more agreement between data sets than was the case for temperature trends. Occurrences of increasing orographic effects (only 11 in Table 6) appear to be limited to tropical latitudes (CRU) or above 60°N (CMIP5). It is not unexpected that trends in mountain/lowland precipitation differences would show different behavior according to latitude, since it is established that the instantaneous gradients themselves are very different in tropical and extra-tropical locations (Barry, 2008). In the mid and high latitudes, precipitation tends to increase with elevation up to the highest summits, and orographic enhancement is largely controlled by the strength of the upslope flow. The strong westerly jet flow in the midlatitudes causes both more rainfall to fall on exposed upper slopes, and generates a strong lee sheltering effect (notwithstanding some “blow over” precipitation which falls beyond the crest).

The observed weakening orographic precipitation effect in these latitudes would be consistent with a weaker and/or more variable midlatitude jet, which would also weaken windward/leeward slope precipitation contrasts in midlatitude mountains. There is indeed some evidence for a weakening midlatitude jet stream, perhaps related to more amplified long-wave patterns due to Arctic Amplification (Barnes & Screen, 2015; Francis & Vavrus, 2015). Observed decreases in windward slope rainfall in maritime mountains, such as the Washington Cascades, are proposed to result from slowing westerlies which would also fit in with this hypothesis (Luce et al., 2013). Many recent regional climate model (RCM) simulations have also alluded to a decrease in winter rainfall in midlatitudes on the upper windward slopes of many mountain ranges (Grose et al., 2019; Salathé et al., 2010). In relatively dry inland locations and on lee-slopes such as the Sierra Nevada, the convective component of rainfall is often more dominant, and thus lee slope precipitation would decrease less than that on windward slopes under such circumstances. Overall, on an annual basis, a weakened westerly circulation would be one possible cause of the apparent observed decreased elevation-dependency of precipitation in midlatitude mountains.

In contrast, Grose et al. (2019) suggested that convective precipitation has increased—particularly in summer in continental regions such as the Alps—as a result of enhanced thermal circulations coupled with a moister and warmer atmosphere. This finding is supported by other studies both in the Alps (Giorgi et al., 2016) and elsewhere (Chernokulsky et al., 2019). You et al. (2014) have reported a widespread stilling of wind speeds on the Tibetan Plateau, which would also increase local thermal circulations and convective precipitation at the expense of mechanically induced orographic enhancement of precipitation in the prevailing westerly airflow. On the other hand, the western US has seen a tendency toward longer dry intervals between summer rainfall events (Holden

et al., 2018), and there may be dynamic (circulation) influences controlling this. From the theories discussed above, one might expect seasonal contrasts in the changing orographic effect to be apparent in our data (a strong winter weakening and perhaps even a summer strengthening). However, based on a seasonal breakdown examining individual mountain regions (Table 5), no such pattern was discerned.

According to model hindcasts (CMIP5), polar latitudes of the northern hemisphere are an exception to the general decreasing orographic effect (mountain/lowland differences appear to be increasing here). However, this pattern is not observed in either GPCC or CRU, and is only weak in ERA5. The steepening could be due to a simulated northerly movement of the westerly storm track, so while in midlatitudes the orographic effect has weakened in the simulation, the reverse could be true north of 60°N. Further research is required to substantiate this.

The climatology in the tropics is somewhat different, with annual precipitation amounts usually decreasing with elevation (Anders & Nesbitt, 2015), sometimes peaking at intermediate elevations and creating distinct cloud forests in certain locations (Appelhans et al., 2016; Hemp, 2006). Upper level winds are often weak, and the vertical atmospheric profile of stability plays a large role in tropical rainfall through convection. The increasing orographic effects sometimes observed in tropical highlands may relate to an increased stability in the tropical atmosphere as a result of greenhouse warming being focused at higher elevations in the free troposphere (i.e., around 400 hPa; Collins et al., 2013). Further work is again required to understand such changing free atmospheric profiles and how they may influence cloud forest location, for example (Helmer et al., 2019).

### 5.3.2. Regional Contrasts and Differences

In accordance with the global picture, most significant changes in the elevation-dependency of precipitation within individual regions (Table S3 in Supporting Information S1) are negative (weakening). However, there are differences between data sets and regions. For example, there is a disagreement between past model simulations (CMIP5) and observations (CRU, GPCC) in terms of the sign of changing elevation-dependency of precipitation in the Andes. The same mismatch applies, to a lesser extent, in the GAR. Some of these disagreements may result from fundamental differences between observed data and results obtained from coupled models. CMIP5 models cannot simulate observed internal variability, related to the phasing of SSTs, and once they are averaged into an ensemble mean, any signal related to internal variability is lost. Since SSTs in the tropical Pacific are fundamentally important to understand precipitation trends in the Andes (Vuille et al., 2003), model-simulated trends may differ from trends derived from observations on timescales where internal variability matters (interannual to multidecadal).

### 5.3.3. Caveats

Both high-elevation observations and model simulations of precipitation are notoriously unreliable because of lack of representative high-elevation precipitation data, undercatch being a serious issue in windy locations and/or where a large proportion of the annual total is in the form of snow. Most global data sets (e.g., GPCC) are not corrected for this. There are additional limitations inherent in the use of global data sets such as ERA5 and CMIP5 to uncover trends in precipitation, particularly in mountain regions. Reanalyses (e.g., ERA5) use whatever stations are available and so stations come and go as time progresses which may influence trends in an unpredictable way (Henn et al., 2018). Model simulations using GCMs have coarse resolution (see broader discussion in Section 6) and regional examples using RCMs have shown sometimes contrasting results to global-scale analyses (Giorgi et al., 2016; Wrzesien et al., 2019).

Processes operating on scales finer than the model's spatial resolution must be incorporated via parameterizations (Lal et al., 2000), which are often tuned to generate a present climate that is as close as possible to available observations (Mauritsen et al., 2012). Cloud microphysics, the planetary boundary layer, and convection are among the parameterized processes; the choice of the particular convective scheme has traditionally represented a key source of uncertainty in GCM-simulated precipitation (Arakawa & Kitoh, 2004). In addition, the coarse model resolution, in both vertical and horizontal directions, limits the capability of models to realistically reproduce the orography and to adequately represent regional forcings and orographic uplift. Recent implementation of non-hydrostatic equations for the atmosphere in high-resolution regional models has allowed handling of scales down to 1–3 km. This regional approach, which was applied in the past mainly on synoptic timescales, is now available for climate simulation, also in small ensembles of RCMs such as in the CORDEX-FPS experiment (Coppola et al., 2020). RCMs and especially their upcoming convection-permitting setups can be expected to

improve further in the near future (e.g., Lundquist et al., 2019; Lind et al., 2020; Schär et al., 2020). However, since different RCMs are required for different regions, optimizing data sets for each region could lead to a rash of different (local) data sets/simulations, which arguably are then more difficult to compare.

As well as limitations in the data sets, there are analytical decisions which constrain our findings. Including mountains and adjacent lowlands as two distinct, pooled categories means that differences within regions such as between windward and leeward slopes, or on different aspects, are lost in the global and regional results. It is therefore recommended that future analyses are undertaken, subdividing mountain ranges into windward and leeward components, or by more detailed elevation bands. This would require a modification of the mountain classification scheme, and may even require a temporally variable classification of windward/leeward to account for circulation changes. More detailed seasonal analyses for specific regions may also help improve our understanding of the driving mechanisms. This is because the dominant precipitation forcing changes with season (as well as being location-dependent). Many midlatitude locations dominated by convective precipitation in spring and summer could theoretically exhibit contrasting changes in the elevation-dependency of precipitation during this period compared with autumn and winter, when rainfall is frontal-dominated. Further research is required to examine such processes in more detail, but is beyond the scope of this paper.

## 6. Broader Limitations and Proposals for Future Work

Several broader limitations associated with our approach must be considered. The station analysis has a subjective element, particularly when examining paired comparisons, as there is no universally accepted definition of high- or low-elevation. Global studies tend to use 500 m asl as a lower threshold to limit high elevation sites (Pepin & Lundquist, 2008; Wang et al., 2016; Qixiang et al., 2018), but in areas like the Tibetan Plateau the threshold could reasonably be 2,000 m or higher. Many features used to define high mountain regions, such as the treeline or snowline, are indeed not fixed at an absolute elevation, but change with latitude and continentality, so future work needs to design classifications which take this into account. Only having access to overall trends at each station, we could not examine changes in trends at individual sites over time. In the gridded analysis, we used one binary mountain classification (K1) as the high elevation “group,” and even though future work could examine the elevational profile across the six classes of the K1 classification (or other subdivisions, for example according to climate zones), absolute elevation zones do not always correspond with common patterns of ecological zonation or “real-world” features. Future work should therefore examine how changing the absolute elevation threshold may influence results, or consider applying a different threshold dependent on latitude and larger scale climate. The gridded analysis also has spatial limitations. Antarctica/Greenland have been excluded and some mountain areas which straddle mid and low latitudes (e.g., the Andes) with contrasting synoptic regimes were considered as one region here for sake of convenience. Surrounding lowland regions are defined based on land area only and oceanic areas have been ignored (which cover about 70% of the Earth's surface). This is common practice, as oceans are expected to show much more stable climate regimes. Adding oceans to the lowland counterpart would probably lead to enhanced mountain warming by default (since temperature trends over the ocean tend to be weaker than over land) and therefore such an analysis could be misleading. This may even be the case to a lesser extent when including coastal regions which are more climatically stable than areas inland.

Uncertainty in trend estimates for individual station studies can be approximated statistically by the number of stations which contribute to the individual results in the meta-analysis (see Tables 1 and 2 or SM2.2/SM2.3 in Hock et al., 2019). Trend estimates which are based on a large number of stations (e.g., Zeng et al., 2015: >2,000 stations) are more robust than those based on one station (see examples from Ohmura, 2012). They will also tend to be less extreme since locally more extreme trends will be smoothed over. Precipitation trends were originally reported either as percentage or absolute terms. In order to combine them (or convert one to the other), reliable (local) measures of mean annual precipitation would be required. Since trend estimates are usually based on a mean derived from many stations, the mean precipitation for the region (at the very least) would be necessary to do this. Ideally the mean precipitation value for each station needs to be used to convert the trend at each station separately from absolute to relative (or vice versa) and then the mean regional trend should be calculated, rather than just converting the regionwide trend using a mean regional precipitation figure.

Because of the limitations with station analysis (a result of the variety of approaches in the literature), using common gridded data sets may seem more attractive. However, these also suffer from uncertainties and important



limitations. Some of the factors which lead to errors (grid resolution, lack of coverage, and land-sea mask) have been discussed in Section 3.4 and further work is using an ensemble approach to quantify how such factors influence uncertainty in extracted trends. In mountain regions, gridded values are estimated from the limited data available via interpolation. Metadata often emphasizes low-elevation locations, due to site accessibility and maintenance limitations at high elevation sites. Information on the stations which feed into the gridded data sets, including how the number and elevation distribution vary over time, is not always easily available, and raster data sets can convey a false sense of accuracy in the high mountains that does not match station density (which often decreases at high elevations). The number of stations included may vary significantly in time, and in most cases has increased since early 1900 but shows a significant drop over the last 10–20 years of the data set due to delays in station data reporting (e.g., GPCC and CRU). Reanalysis data sets are less exposed to shortages of stations at high elevation since they assimilate satellite observations too (since 1979).

In this study, we retained the data sets' original resolutions to avoid smoothing and losing further topographic detail. However, even a gridded resolution of  $0.25^\circ$  (GPCC and ERA5) likely underestimates the highest elevations (and deep valleys) due to topographic smoothing. In the Alps ( $\sim 45^\circ\text{N}$ ) this resolution represents around 20 km which is commonly the distance between adjacent ridges or valleys. Underestimation is particularly important for sharp or isolated peaks. In the tropics  $1^\circ$  of longitude is over 100 km, and even spatially extensive peaks such as Kilimanjaro (5,895 m; 20 km by 40 km) may be severely underestimated. At  $0.25^\circ$  (ERA5/GPCC) its summit "elevation" is 2,996 m, and at  $2^\circ$  (GISTEMP) only 1,258 m (figures derived from NOAA high resolution DEM). If high elevations are smoothed low, and high elevations are actually warming more rapidly, this might lead to underestimation of trend magnitudes overall. There may also be additional errors in elevation measurements within gridded data sets themselves, irrespective of resolution. Problems of horizontal resolution are also highly relevant for model data sets, which in addition may be affected by limitations in simulating mountain-specific processes (Baldwin et al., 2021).

The K1 definition offers a method to map mountain regions, but adjacent lowlands are less easy to define. How far away from the mountain region should the lowlands extend? Should there be separate comparisons on windward or leeward sides? This is particularly relevant where strong circulations from west to east operate which creates contrasting climate regimes upstream and downstream of the mountains, as in many maritime ranges of midlatitudes. Changes on either side of the same mountain range may show opposite trends as observed in the Sierra Nevada (Lundquist & Cayan, 2007) and the Pacific North-West (Luce et al., 2013). In the tropics or in areas where convective precipitation is dominant, there may be particular slope aspects which show contrasting trends to other slopes. The simple comparison of the mountain range with adjacent lowlands on all sides thus may miss important detail, and further work needs to subdivide mountain/lowland comparisons into smaller areas with more uniform synoptic activity. Many additional sensitivity analyses could be useful to examine changing trend profiles, including windward versus leeward slope contrasts, microscale aspect and topographical differences, and the effect of grid resolution and data quality/abundance on the results. Some of these have been included in the ensemble approach discussed in Section 3.4, but others fall beyond the scope of this paper.

Spatial variability or inconsistency in the elevational contrasts of temperature/precipitation trends across different mountainous regions, or within different latitudinal bands, suggests that the physical drivers of warming and moistening may have different relative importance in different regions. For instance, the snow-albedo feedback may be a major driver of EDW in the Alps or Himalayas, but may be much less important in tropical mountains with limited snow and ice cover. Therefore, a regional differentiation of the most relevant processes is a key for understanding different regional patterns of elevation-dependent climate change. In addition, the local impacts of changes in global circulation, and how they may affect elevation-dependent climate change in specific areas, need to be better understood.

Systematic changes in temperature and precipitation gradients with elevation may be related to one another. The temperature lapse rate is the main factor of atmospheric stability, modified by moisture influences. When atmospheric stratification is becoming more unstable (increasing vertical temperature gradient), stronger convective precipitation can be expected. On the other hand, in orographic precipitation events due to flow blocking and dynamic lifting, the dependence on the temperature lapse rate is more complex. In these conditions, latent heat release due to the condensation of hydrometeors considerably weakens the lapse rate. Thus, the relationship between gradients of temperature and precipitation on an instantaneous (meteorological) timescale is not trivial, and



may vary depending on the dominant precipitation-forming processes. Further work should examine the observed relationships between the two gradients, for different locations and seasons.

## 7. Impacts and Implications of Changing Elevation-Dependent Climate Gradients

The combined influence of temperature and precipitation changes with elevation is highly relevant for cryospheric features as they ultimately control the amount of solid precipitation (snowfall) and influence snow/ice ablation, as well as impacting on hydrological systems more generally and mountain ecology. Below, focusing on mountain cryosphere, hydrology and ecology, we discuss potential broader changes which may result due to a change in elevation profiles of temperature and precipitation. Although the concentration here is on temperature and precipitation changes, additional atmospheric variables such as wind speed and direction, humidity, cloud cover, and energy budget components (radiation) may also be strongly affected. Such changes are often controlled to a lesser extent by simple thermodynamic considerations (discussed in Section 2), but rather often involve important contributions from circulation variability and, hence, chaotic internal climate variability (Shepherd, 2014).

### 7.1. Mountain Cryosphere

In recent decades, cryosphere changes in mountain areas (snow, glaciers, and permafrost) have been quantified through observations from surface stations, remotely sensed data, and model simulations (Beniston et al., 2018; Hammond et al., 2018; Huss et al., 2017; Mote et al., 2018; Notarnicola, 2020). Regarding snow cover, a complex heterogeneous picture emerges, where snow variability depends on elevation, season, location, and is driven by an interplay of meteorological variables with orography, although air temperature and precipitation are dominant controls (Mote et al., 2018; Notarnicola, 2020).

Due to the complex interaction between temperature and precipitation influences, the reaction of surface snowpack to climate change and variability is, in principle, dependent on elevation, but the profile of change varies across the globe. The critical variable is often mean temperature rather than elevation per se. Numerous studies have shown quite predictable sensitivity of snowpack to temperature across wide areas (Luce, Lopez-Burgos, & Holden, 2014; Cooper et al., 2016). At temperatures  $< -5^{\circ}\text{C}$  sensitivity is typically low (Ikeda et al., 2021; Lute & Luce, 2017). At temperatures just below/above the freezing level, increased precipitation will increase/reduce snowpack, and sensitivity is much higher. EDW with enhanced high elevation warming favors increased sensitivity over a wider elevation range, since the freezing level height rises disproportionately over high mountains (Diaz et al., 2003). Following the general elevation dependency of the available snowpack (larger snow accumulations at higher elevations) the quantitative impacts of EDW on snowmelt rates can also be expected to increase disproportionately overall. Weakening orographic precipitation gradients may also reduce snowfall (and hence snowpack), but only at the very highest elevations which would otherwise remain cold enough to benefit from solid precipitation. The separation of the influences of changing elevation gradients from absolute temperature/precipitation changes at a given elevation requires dedicated analyses employing models of snowpack and is beyond the scope of the present work, but observed snowpack trends can already provide some indications.

A reliable and robust trend detection of snowpack is often hampered by the fact that low and mid-elevation snowpacks (in zones where rain and snow are equally prevalent) often exhibit high temporal variability (Lievens et al., 2019). Records from the European Alps present strong negative trends for snow cover duration and depth below 2,000 m, and weaker trends are detected above this (Beniston et al., 2018; Matiu et al., 2021; Olefs et al., 2020). In contrast, Klein et al. (2016) showed declines at both lower and higher elevations in the Swiss Alps. Snow has also generally declined in High Mountain Asia (e.g., from 1997 to 2009; Smith & Bookhagen, 2018), but the pattern on the Tibetan Plateau is complex. Decreasing snow cover duration has been reported below 3,500 m (2000–2015), but there are increases in the south-western and central plateau (Wang et al., 2017). Such trends are supported by long snow depth time-series, which reveal a slight decrease from 1997 to 2012 (Shen et al., 2015), following a longer-term increase between 1951 and 1997 (Qin et al., 2006; Qian et al., 2011). Guo et al. (2021) show that declines in plateau snow cover were strongest at lower elevations ( $\sim 2,000$ – $3,000$  m) between 1973 and 2002, but at higher elevations ( $\sim 4,000$ – $5,000$  m) between 1989 and 2018, so the elevation profile of snow trends has shifted and even reversed over time. Some contrasting trends are identified in Fennoscandian mountain areas, where the higher/colder regions often show positive trends of maximum snow depth and maximum SWE, which in some cases have recently become negative (Beniston

et al., 2018). Other European mountain regions in Spain, Romania, Croatia, and Bulgaria, show a reduction in the main snowpack parameters. In the Andes, the most rapid decline in snowpack persistence is located at mid–high elevations (between 3,000 and 5,000 m), but there is a strong dependence on latitude and contrasting patterns on eastern/western slopes (Saavedra et al., 2018), which are exacerbated by the fact that at low latitudes no seasonal snow pack exists, as snow tends to melt within a few days outside of glaciated areas (Vuille et al., 2018). Notarnicola (2020) analyzed trends in several snow parameters (snow cover, snow cover duration, snow onset and melt) over the last two decades at global scale using MODIS products. At moderate elevations between 1,000 and 4,000 m, mixed snow trends are found, while at elevations >4,000 m, only negative changes (decreasing snow depth) were detected. This is surprising since we would expect some increases in the highest (coldest) areas with generally rising (or consistent) precipitation sums. Decreasing orographic precipitation may be partly responsible for the declines in these cases. Areas of the western USA, South America, and Australia are suffering from extensive declines in many snow parameters, while colder areas in northeastern Russia, northern Europe, and some parts of central Asia show some positive trends (Beniston et al., 2018; Hammond et al., 2018; Huss et al., 2017; Mote et al., 2018). Although historical trends have often been relatively small, larger trends are often projected for the foreseeable future, as temperatures continue to rise. A final factor is heavy pollution, present in East Asia, the United States, and Europe, which can lead to aerosol deposition, decreased albedo, and ultimately enhanced snow melt (Barnett et al., 2005; Mote et al., 2018; Saavedra et al., 2018). However, evidence of the impact of black carbon from anthropogenic and biomass burning on snow melt in High Mountain Asia and South America is limited (Li et al., 2016; Magalhães et al., 2019; Molina et al., 2015; Zhang et al., 2018).

In addition to the snowpack decrease in many mountain regions is the observed rapid decline of the area and mass of global mountain glaciers (Hock et al., 2019; Zemp et al., 2015, 2019). In the European Alps, an estimated 50% of 1,850 glacier area was lost by 2,000 (Paul et al., 2020; Zemp et al., 2006). Excluding contributions from the glaciers and ice sheets of Greenland and Antarctica, the total contribution of the world's glaciers to sea level rise during the period 1961–2016 amounts to  $0.4 \pm 0.3 \text{ mm yr}^{-1}$ . Presently, this flux is equivalent to the sea level contribution of the Greenland Ice Sheet (Zemp et al., 2019). Atmospheric warming is very likely the primary driver for this global glacier recession (Hock et al., 2019). Moreover, in many regions, because large glaciers have response times of several decades, current glacier mass is in disequilibrium with climate. Accordingly, even if the climate was to stabilize rapidly, further glacier area and mass losses >30% are inevitable (Marzeion et al., 2018; Mernild et al., 2013). Despite the projected widespread glacier loss (Frans et al., 2018; McCabe & Fountain, 1995), to our knowledge no global meta-analysis has been undertaken on the explicit influence of EDW and changing orographic precipitation gradients on glacier hypsometry and projected future decline. Glaciers flow downhill and therefore cross several elevation zones making this question more complex than it might otherwise be.

Compared to surface snow cover and glaciers, the temporal evolution of mountain permafrost is considerably less understood, partly because it cannot be directly monitored/observed remotely (Gruber et al., 2017). We do not even have a good idea of its elevation distribution. Based on modeling studies, around 27%–29% of permafrost is thought to be located in mountain areas, covering an area 14–21 times larger than that of glaciers in these regions (Hock et al., 2019). While identifying mountain permafrost requires specific methods due to its high local heterogeneity and its existence in different landforms (rock walls, unconsolidated sediments), the basic relationships with climate are the same as in polar regions. Permafrost in the European Alps, Canada, Scandinavia, and Tibetan Plateau has shown degradation. Although this is primarily related to increasing temperatures, one cannot simply translate profiles of atmospheric warming to elevation profiles of permafrost change. Besides air temperature, snow cover can also exert a major influence on ground temperatures and, hence, on permafrost. Permafrost cooling periods can be related to years with low-snow conditions while summer heat waves can be related to an increase of the active-layer thickness such as in the European Alps (Etzelmüller et al., 2020; PERMOS, 2016). Moreover, in some regions, near-surface air temperature is warming less than ground surface temperature, probably again a consequence of reduced snow cover duration (Etzelmüller et al., 2020). The joint and partly counteracting influences of temperature and snow cover changes on permafrost bodies, combined with the complex spatial distribution of permafrost (only partly controlled by elevation), makes it hard to assess patterns of permafrost sensitivity to changing gradients of meteorological forcing. Still, contemporaneous temperature increases, relative precipitation declines (at high elevations) and snow cover decreases will very likely lead to accentuated permafrost decline in high mountain regions in coming decades (Lu et al., 2017).

## 7.2. Mountain Hydrology and Ecology

Mountains act as “water towers,” storing freshwater over a range of timescales (Barnett et al., 2005; Immerzeel et al., 2020; Sturm et al., 2017; Viviroli et al., 2011), mostly in solid form (i.e., snow and ice). Accordingly, the diminishing cryosphere described above and its reaction to changing elevational gradients of atmospheric forcing have a range of hydrological consequences, including threats to water supply in mountains and downstream regions (Bradley et al., 2006; Haerberli & Weingartner, 2020; Viviroli et al., 2020), and the shift of snowmelt from late spring/summer to earlier in the year (Jenicek et al., 2018; Musselman et al., 2017; Parajka et al., 2016). As these hydrological changes highly depend on the presence of seasonal snow or perennial ice cover, elevational gradients of changes in climatic forcing play a key role. Within a given mountain range catchments at higher elevation are typically subject to a higher degree of snow and ice coverage and, hence, will respond differently compared to lower elevation catchments. However, it is difficult to make generalizations about the response of flow regimes in mountain catchments to changing elevational gradients, since discharge at a given point depends on the integrated effect of changes at a range of elevations above that point, and to an extent this should smooth out any contrasts, assuming the relevant elevation range is wide. Changes in the seasonal distribution of precipitation and the decrease of water volume stored as snow will also cause discharge regimes to shift seasonally (Godsey et al., 2014; Jenicek et al., 2016). While global analyses mostly provide no coherent picture on such changes (although regional evidence exists, e.g., Bard et al., 2015), future climate change projections indicate shifts of the snowmelt streamflow peak to earlier in spring, coupled with the transition to pluvially dominated regimes as the freezing level rises (e.g., Arnell & Gosling, 2013; Horton et al., 2006; Schnorbus et al., 2014).

Considering extreme hydrometeorological conditions like droughts, there may be elevation dependence in potential response. Examples from the midlatitudes show a mixed picture but overall indicate an increasing importance of precipitation and evapotranspiration anomalies below roughly 2,000 m a.s.l., shifting toward snow accumulation processes at higher elevations (Bales et al., 2018; Floriancic et al., 2020; Gilbert & Maxwell, 2018). However, analysis on the 2003 Alpine drought event highlighted the importance of enhanced evapotranspiration fluxes in forested areas above 1,000 m a.s.l. which significantly reduced lower valley and foreland runoff (Mastrotheodoros et al., 2020). Via impacts on mountain groundwater recharge and storage, earlier snowmelt peaks might also enhance the likelihood and/or severity of late summer and autumn low flows and hydrological droughts (van Huijgevoort et al., 2014). However, analysis in the western US has identified the relative importance of declines in orographic precipitation (compared to reductions in snowpack storage driven by warming) in accounting for extreme low flow events in summer (Kormos et al., 2016). Heavily glacierized river catchments where glacial melt water represents a substantial contribution to total runoff will initially generate increased runoff up to a point of peak water, beyond which a critical glacier extent is surpassed and runoff decreases (Huss & Hock, 2018). This threshold has already been breached in some catchments. To what extent these changes are indeed influenced by elevational gradients of changes in the respective climatic forcing remains largely unknown but can be expected to depend on the region. Further research is required to provide a more comprehensive picture.

Partly connected to hydrological changes, mountain ecological systems have also been affected by mountain climate change. These impacts are often related to upward moving temperature isotherms and a general decrease of the land area that is subject to low mean annual temperatures. The concept of climate velocity or the “distance species have to move to maintain constant temperatures” is dependent on the current climate spatial gradient (or temperature lapse rate in mountains) and the rate of warming (Burrows et al., 2014; Loarie et al., 2009). In a mountain context, the velocity is often expressed as rates of uphill movement of isotherms rather than horizontal distance, and many studies compare rates of observed uphill movement with theoretical climate velocity to see whether species are “tracking” climate forcing (Corlett & Westcott, 2013; Dial et al., 2016). This of course assumes a constant lapse rate, and EDW—as demonstrated in this review—breaks this assumption meaning that different isotherms could move different distances concurrently, which in turn implies the compression or expansion of isotherm spacing on a given mountain slope. Enhanced warming at higher elevations implies habitats between isotherms will expand since higher elevation isotherms will move uphill more rapidly than lower ones. This in turn implies a larger land area between two given isotherms, and potentially a larger elevation range may be available for a particular temperature-sensitive species, which could be beneficial. However, there are additional complexities. Many climatic refugia are associated with local

reversal of regional lapse rates (e.g., cold air ponding, Dobrowski, 2011; Curtis et al., 2014) and are therefore decoupled from the broader climate velocity in the region. Although it is suspected that processes such as cold air drainage may become less frequent in a warmer world (Daly et al., 2010), there is no systematic analysis of how this could influence species migration and range shifts in mountains. Other habitats such as mountain streams may be largely decoupled from air temperature changes. There is evidence that so far mountain snowpack has acted as a buffer to moderate temperature changes in high elevation streams, an important habitat for trout in the western US, for example (Luce, Staab, et al., 2014; Isaak et al., 2016). Temperature increases may also impact mountain ecology through secondary effects such as upslope advances of forest fire lines (Alizadeh et al., 2021).

## 8. Conclusions and Outlook

In this paper, we sought (a) to examine the spatial and temporal patterns of recent changes in mountain climates around the globe with a focus on temperature and precipitation and how changes vary by elevation, (b) consolidate and summarize our current understanding of the drivers and processes that shape such changes, and (c) begin to consider the consequences of uneven elevational temperature and precipitation change for broader changes in mountain systems such as the cryosphere and ecosystems. As the main findings show, a more nuanced understanding of the governing processes that underpin these spatially distributed patterns and changes are not only relevant for key resource planning purposes, but also for the fit-for-purpose monitoring efforts that are needed within observational networks (Shahgedanova et al., 2021; Thornton, Palazzi, et al., 2021) and to substantiate the calls for actions around predictions (Adler et al., 2020).

### 8.1. Summary of Main Findings

Our main findings are as follows:

#### 8.1.1. Temperature: Station Analysis

In the majority of paired station studies within regions, high elevation warming is more rapid than at lower elevations. However, a global meta-analysis including all mountain regions does not show a significant elevation difference in warming rates.

#### 8.1.2. Gridded Data Sets

Global analyses for mountain temperature trends based on CRU, GISTEMP, ERA5, and CMIP5 in comparison with adjacent lowlands in the same latitude band do not show consistent differences by elevation. In the most recent period (1980–2018), there is a slight tendency toward more pronounced warming in mountains.

Regions show contrasting mountain/lowland differences, with the Rocky Mountains and GAR showing enhanced warming in comparison with adjacent lowlands for most data sets. The Andes show opposing trends for gridded observations (weaker warming) and model simulations (stronger warming) but there may be good reasons for this difference. The Tibetan Plateau shows weaker warming in many cases.

#### 8.1.3. Precipitation: Station Analysis

Station precipitation trends are inconsistent and are affected by higher uncertainties. They do not show systematic changes with elevation.

#### 8.1.4. Gridded Data Sets

Precipitation changes in gridded data sets tend to show reductions in the elevation dependency of precipitation, particularly in midlatitudes. This is often due to wetting in the lowlands but weaker wetting or even drying at high elevations.

More agreement between data sets is found concerning trends in the elevation-dependency of precipitation than for changes in temperature gradients.

## 8.2. Final Remarks

This extensive global analysis of changes in vertical gradients of temperature and precipitation in mountain areas has shown broad agreement between results from station data and gridded data sets. For temperature, paired station analyses tend to demonstrate enhanced warming in mountain regions, but a global analysis did not find clear difference between warming rates at high and low elevations. Gridded data sets corroborate this finding. Even though there are many regions with significant individual contrasts, however, there is no unequivocal single result on a global scale when all mountains are amalgamated. For precipitation, the station analysis did not produce clear trends, but gridded data sets suggest a weakening of orographic enhancement in a warmer world with more rapid wetting in lowland regions. This is consistent with a range of other regional modeling and observational analyses of past climates.

Overall, given the underlying data, we have more confidence in our conclusions regarding temperature than precipitation. Mountain precipitation remains extremely difficult to measure and model, with large and likely elevation-dependent biases that could overshadow elevation-dependent trends, and may be temporally non-stationary (e.g., if rain/snow ratios or instrumentation change). To our best understanding, precipitation undercatch corrections are not applied to most of the data sets employed here. Going forward, it may prove fruitful to develop global assessments by aggregating the results of regional scale-analyses that involve denser in situ and higher resolution gridded data. Assessing the extent to which elevation-dependent signals detected in globally consistent (but coarse) gridded data sets are also present in regional products, could help build confidence, or alternatively identify areas for improvement, in global data sets.

The consequences of our findings are important, not least for the status of water reserves in mountain regions. Should past trends continue, locally enhanced warming in some mountain regions may further deplete snow and ice reserves, while a weakened orographic precipitation effect could limit any counter-benefit from increased rainfall which instead may be focused at lower elevations. Our findings therefore stress the importance of understanding elevation-dependent climate change as systematic (yet spatially variable) changes in climate trends with elevation. Our work identifies, for the first time, preliminary evidence of the potential weakening elevation-dependency of precipitation. As the planet warms, precipitation increase in mountainous regions may not occur as rapidly as in lowland regions. Thus, enhanced warming (EDW) combined with a weakening orographic effect may aggravate negative consequences for the world's snow and ice reserves at high elevation.

## Data Availability Statement

The station metadata (Tables SM2.2 and SM2.3) are available in the IPCC Special Report on Ocean and Cryosphere in a Changing Climate (SROCC) at [https://www.ipcc.ch/site/assets/uploads/sites/3/2019/11/SROCC\\_Ch02-SM\\_FINAL.pdf](https://www.ipcc.ch/site/assets/uploads/sites/3/2019/11/SROCC_Ch02-SM_FINAL.pdf). The gridded data sets are available as follows: CRU (<http://badc.nerc.ac.uk/data/cru/>), GISTEMP (<http://data.giss.nasa.gov/gistemp/>), GPCC ([https://opendata.dwd.de/climate\\_environment/GPCC/html/fulldata-monthly\\_v2018\\_doi\\_download.html](https://opendata.dwd.de/climate_environment/GPCC/html/fulldata-monthly_v2018_doi_download.html)), ERA5 (<https://cds.climate.copernicus.eu/#!/search?text=ERA5&type=dataset>), and CMIP5 model simulations are downloaded from <https://esgf-node.llnl.gov/projects/cmip5/>. K1 mountain classification is available at <https://rmgsc.cr.usgs.gov/gme/>. Note that the version used in this study has since been updated. Data sets created in this research and the sensitivity analysis (discussed in Section 3.4) are available at <http://wilma.to.isac.cnr.it/arnone/Pepin2021RG/>.

## References

- Adler, C., Pomeroy, J., & Nitu, R. (2020). High mountain summit: Outcomes and outlook. *World Meteorological Organization Bulletin*, 69, 34–37.
- Alizadeh, M. R., Abatzoglou, J. T., Luce, C. H., Adamowski, J. F., Farid, A., & Sadegh, M. (2021). Warming enabled upslope advance in western US forest fires. *Proceedings of the National Academy of Sciences*, 118(22), e2009717118. <https://doi.org/10.1073/pnas.2009717118>
- Anders, A. M., & Nesbitt, S. W. (2015). Altitudinal precipitation gradients in the tropics from tropical rainfall measuring mission (TRMM) precipitation radar. *Journal of Hydrometeorology*, 16(1), 441–448. <https://doi.org/10.1175/JHM-D-14-0178.1>
- Appelhans, T., Mwangomo, E., Otte, I., Detsch, F., Nauss, T., & Hemp, A. (2016). Eco-meteorological characteristics of the southern slopes of Kilimanjaro, Tanzania. *International Journal of Climatology*, 36(9), 3245–3258. <https://doi.org/10.1002/joc.4552>
- Arakawa, O., & Kitoh, A. (2004). Comparison of local precipitation-SST relationship between the observation and a reanalysis dataset. *Geophysical Research Letters*, 31(12). <https://doi.org/10.1029/2004GL020283>
- Arnell, N. W., & Gosling, S. N. (2013). The impacts of climate change on river flow regimes at the global scale. *Journal of Hydrology*, 486, 351–364. <https://doi.org/10.1016/j.jhydrol.2013.02.010>

### Acknowledgments

The authors thank the Mountain Research Initiative (MRI) for sponsoring a workshop and splinter meeting with members of the MRI Elevation Dependent Climate Change Working Group at EGU in 2019 at which the idea for this review was conceived. The MRI supported the workshop conducted at the margins of the EGU through coordination, facilitation and funding provided to the MRI by the Swiss Academy of Sciences (Project No. FNW0004\_004-2019-00). The authors acknowledge the World Climate Research Programme's Working Group on Coupled Modelling, which is responsible for CMIP, and also thank the climate modeling groups (listed in Table S1 in Supporting Information S1) for producing and making available their model output. For CMIP, the U.S. Department of Energy's Program for climate model diagnosis and intercomparison provides coordinating support and led development of software infrastructure in partnership with the Global Organization for Earth System Science Portals.



- Baldwin, J. W., Atwood, A. R., Vecchi, G. A., & Battisti, D. S. (2021). Outsize influence of Central American orography on global climate. *AGU Advances*, 2(2). <https://doi.org/10.1029/2020AV000343>
- Bales, R. C., Goulden, M. L., Hunsaker, C. T., Conklin, M. H., Hartsough, P. C., O'Geen, A. T., et al. (2018). Mechanisms controlling the impact of multi-year drought on mountain hydrology. *Scientific Reports*, 8(1). <https://doi.org/10.1038/s41598-017-19007-0>
- Banta, R. M. (1990). The role of mountain flows in making clouds. In *Atmospheric processes over complex terrain* (pp. 229–283). American Meteorological Society. [https://doi.org/10.1007/978-1-935704-25-6\\_9](https://doi.org/10.1007/978-1-935704-25-6_9)
- Bard, A., Renard, B., Lang, M., Giuntoli, I., Korck, J., Koboltschnig, G., et al. (2015). Trends in the hydrologic regime of Alpine rivers. *Journal of Hydrology*, 529, 1823–1837. <https://doi.org/10.1016/j.jhydrol.2015.07.052>
- Barnes, E. A., & Screen, J. A. (2015). The impact of Arctic warming on the midlatitude jet-stream: Can it? Has it? Will it? *Wiley Interdisciplinary Reviews: Climate Change*, 6(3), 277–286. <https://doi.org/10.1002/wcc.337>
- Barnett, T. P., Adam, J. C., & Lettenmaier, D. P. (2005). Potential impacts of a warming climate on water availability in snow-dominated regions. *Nature*, 438(7066), 303–309. <https://doi.org/10.1038/nature04141>
- Barry, R. G. (2008). *Mountain weather and climate* (3rd ed.). Cambridge University Press. <https://doi.org/10.1017/CBO9780511754573>
- Beniston, M., Farinotti, D., Stoffel, M., Andreassen, L. M., Coppola, E., Eckert, N., et al. (2018). The European mountain cryosphere: A review of its current state, trends, and future challenges. *The Cryosphere*, 12(2), 759–794. <https://doi.org/10.5194/tc-12-759-2018>
- Bradley, R. S., Vuille, M., Diaz, H. F., & Vergara, W. (2006). Threats to water supplies in the Tropical Andes. *Science*, 312(5781), 1755–1756. <https://doi.org/10.1126/science.1128087>
- Burrows, M. T., Schoeman, D. S., Richardson, A. J., Molinos, J. G., Hoffmann, A., Buckley, L. B., et al. (2014). Geographical limits to species-range shifts are suggested by climate velocity. *Nature*, 507(7493), 492–495. <https://doi.org/10.1038/nature12976>
- Buzzi, A., & Tibaldi, S. (1978). Cyclogenesis in the lee of the Alps: A case study. *Quarterly Journal of the Royal Meteorological Society*, 104(440), 271–287. <https://doi.org/10.1002/qj.49710444004>
- Chen, I.-C., Hill, J. K., Ohlemuller, R., Roy, D. B., & Thomas, C. D. (2011). Rapid range shifts of species associated with high levels of climate warming. *Science*, 333(6045), 1024–1026. <https://doi.org/10.1126/science.1206432>
- Chernokulsky, A., Kozlov, F., Zolina, O., Bulygina, O., Mokhov, I. I., & Semenov, V. A. (2019). Observed changes in convective and stratiform precipitation in Northern Eurasia over the last five decades. *Environmental Research Letters*, 14(4), 45001. <https://doi.org/10.1088/1748-9326/aafb82>
- Chow, F., Schär, C., Ban, N., Lundquist, K., Schlemmer, L., & Shi, X. (2019). Crossing multiple gray zones in the transition from mesoscale to microscale simulation over complex terrain. *Atmosphere*, 10(5), 274. <https://doi.org/10.3390/atmos10050274>
- Chung, Y.-S., Hage, K. D., & Reinelt, E. R. (1976). On Lee cyclogenesis and airflow in the Canadian Rocky Mountains and the east Asian Mountains. *Monthly Weather Review*, 104(7), 879–891. [https://doi.org/10.1175/1520-0493\(1976\)104<0879:OLCAA1>2.0.CO;2](https://doi.org/10.1175/1520-0493(1976)104<0879:OLCAA1>2.0.CO;2)
- Clements, C. B., Whiteman, C. D., & Horel, J. D. (2003). Cold-air-pool structure and evolution in a mountain basin: Peter Sinks, Utah. *Journal of Applied Meteorology*, 42(6), 752–768. [https://doi.org/10.1175/1520-0450\(2003\)042<0752:CSAIEA>2.0.CO;2](https://doi.org/10.1175/1520-0450(2003)042<0752:CSAIEA>2.0.CO;2)
- Collins, M., Knutti, R., Arblaster, J., Dufresne, J.-L., Fichefet, T., Friedlingstein, P., et al. (2013). Long-term climate change: Projections, commitments and irreversibility. In T. F. Stocker, D. Qin, G.-K. Plattner, M. M. B. Tignor, S. K. Allen, J. Boschung, et al. (Eds.), *Climate change 2013 – The physical science basis* (pp. 1029–1136). Cambridge University Press.
- Cooper, M. G., Nolin, A. W., & Saafeq, M. (2016). Testing the recent snow drought as an analog for climate warming sensitivity of Cascades snowpacks. *Environmental Research Letters*, 11(8). <https://doi.org/10.1088/1748-9326/11/8/084009>
- Coppola, E., Sobolowski, S., Pichelli, E., Raffaele, F., Ahrens, B., Anders, I., et al. (2020). A first-of-its-kind multi-model convection permitting ensemble for investigating convective phenomena over Europe and the Mediterranean. *Climate Dynamics*, 55(1–2), 3–34. <https://doi.org/10.1007/s00382-018-4521-8>
- Corlett, R. T., & Westcott, D. A. (2013). Will plant movements keep up with climate change? *Trends in Ecology & Evolution*, 28(8), 482–488. <https://doi.org/10.1016/j.tree.2013.04.003>
- Curtis, J. A., Flint, L. E., Flint, A. L., Lundquist, J. D., Hudgens, B., Boydston, E. E., & Young, J. K. (2014). Incorporating cold-air pooling into downscaled climate models increases potential refugia for snow-dependent species within the Sierra Nevada Ecoregion, CA. *PLoS One*, 9(9), e106984. <https://doi.org/10.1371/journal.pone.0106984>
- Daly, C. (2006). Guidelines for assessing the suitability of spatial climate data sets. *International Journal of Climatology*, 26(6), 707–721. <https://doi.org/10.1002/joc.1322>
- Daly, C., Conklin, D. R., & Unsworth, M. H. (2010). Local atmospheric decoupling in complex topography alters climate change impacts. *International Journal of Climatology*, 30(12), 1857–1864. <https://doi.org/10.1002/joc.2007>
- Daly, C., Neilson, R. P., & Phillips, D. L. (1994). A statistical-topographic model for mapping climatological precipitation over mountainous Terrain. *Journal of Applied Meteorology*, 33(2), 140–158. [https://doi.org/10.1175/1520-0450\(1994\)033<0140:ASTMFM>2.0.CO;2](https://doi.org/10.1175/1520-0450(1994)033<0140:ASTMFM>2.0.CO;2)
- Debarbieux, B., & Rudaz, G. (2015). *The mountain: A political history from the enlightenment to the present*. University of Chicago Press.
- Defant, F. (1949). Zur Theorie der Hangwinde, nebst Bemerkungen zur Theorie der Berg- und Talwinde. *Archiv Für Meteorologie, Geophysik Und Bioklimatologie Serie A*, 1(3–4), 421–450. <https://doi.org/10.1007/BF02247634>
- Di Luzio, M., Johnson, G. L., Daly, C., Eischeid, J. K., & Arnold, J. G. (2008). Constructing retrospective gridded daily precipitation and temperature datasets for the conterminous United States. *Journal of Applied Meteorology and Climatology*, 47(2), 475–497. <https://doi.org/10.1175/2007JAMC1356.1>
- Dial, R. J., Scott Smeltz, T., Sullivan, P. F., Rinas, C. L., Timm, K., Geck, J. E., et al. (2016). Shrubline but not treeline advance matches climate velocity in montane ecosystems of south-central Alaska. *Global Change Biology*, 22(5), 1841–1856. <https://doi.org/10.1111/gcb.13207>
- Diaz, H. F., & Bradley, R. S. (1997). Temperature variations during the last century at high elevation sites. *Climatic Change*, 36(3–4), 253–279. <https://doi.org/10.1023/a:1005335731187>
- Diaz, H. F., Eischeid, J. K., Duncan, C., & Bradley, R. S. (2003). Variability of freezing levels, melting season indicators, and snow cover for selected high-elevation and continental regions in the last 50 years. *Climatic Change*, 33–52. [https://doi.org/10.1007/978-94-015-1252-7\\_3](https://doi.org/10.1007/978-94-015-1252-7_3)
- Dobrowski, S. Z. (2011). A climatic basis for microrefugia: The influence of terrain on climate. *Global Change Biology*, 17(2), 1022–1035. <https://doi.org/10.1111/j.1365-2486.2010.02263.x>
- Dorning, M., Whiteman, C. D., Bica, B., Eisenbach, S., Pospichal, B., & Steinacker, R. (2011). Meteorological events affecting cold-air pools in a small basin. *Journal of Applied Meteorology and Climatology*, 50(11), 2223–2234. <https://doi.org/10.1175/2011JAMC2681.1>
- Dozier, J., & Frew, J. (1990). Rapid calculation of terrain parameters for radiation modeling from digital elevation data. *IEEE Transactions on Geoscience and Remote Sensing*, 28(5), 963–969. <https://doi.org/10.1109/36.58986>
- Durran, D. R. (1990). Mountain waves and downslope winds. In *Atmospheric processes over complex terrain* (pp. 59–81). American Meteorological Society. [https://doi.org/10.1007/978-1-935704-25-6\\_4](https://doi.org/10.1007/978-1-935704-25-6_4)



- Egger, J., Bajrachaya, S., Egger, U., Heinrich, R., Reuder, J., Shayka, P., et al. (2000). Diurnal winds in the Himalayan Kali Gandaki Valley. Part I: Observations. *Monthly Weather Review*, 128(4), 1106–1122. [https://doi.org/10.1175/1520-0493\(2000\)128<1106:DWITHK>2.0.CO;2](https://doi.org/10.1175/1520-0493(2000)128<1106:DWITHK>2.0.CO;2)
- Elsen, P. R., & Tingley, M. W. (2015). Global mountain topography and the fate of montane species under climate change. *Nature Climate Change*, 5(8), 772–776. <https://doi.org/10.1038/nclimate2656>
- Elvidge, A. D., Kuipers Munneke, P., King, J. C., Renfrew, I. A., & Gilbert, E. (2020). Atmospheric drivers of melt on Larsen C Ice Shelf: Surface energy budget regimes and the impact of foehn. *Journal of Geophysical Research: Atmospheres*, 125(17). <https://doi.org/10.1029/2020JD032463>
- Elvidge, A. D., & Renfrew, I. A. (2016). The causes of foehn warming in the lee of mountains. *Bulletin of the American Meteorological Society*, 97(3), 455–466. <https://doi.org/10.1175/BAMS-D-14-00194.1>
- Etzelmüller, B., Guglielmin, M., Hauck, C., Hilbich, C., Hoelzle, M., Isaksen, K., et al. (2020). Twenty years of European mountain permafrost dynamics—the PACE legacy. *Environmental Research Letters*, 15(10). <https://doi.org/10.1088/1748-9326/abae9d>
- Floriancic, M. G., Berghuijs, W. R., Jonas, T., Kirchner, J. W., & Molnar, P. (2020). Effects of climate anomalies on warm-season low flows in Switzerland. *Hydrology and Earth System Sciences*, 24(11), 5423–5438. <https://doi.org/10.5194/hess-24-5423-2020>
- Francis, J. A., & Vavrus, S. J. (2015). Evidence for a wavier jet stream in response to rapid Arctic warming. *Environmental Research Letters*, 10(1), 14005. <https://doi.org/10.1088/1748-9326/10/1/014005>
- Frans, C., Istanbuluoglu, E., Lettenmaier, D. P., Fountain, A. G., & Riedel, J. (2018). Glacier recession and the response of summer streamflow in the Pacific Northwest United States, 1960–2009. *Water Resources Research*, 54(9), 6202–6225. <https://doi.org/10.1029/2017WR021764>
- Freeman, B. G., Scholer, M. N., Ruiz-Gutierrez, V., & Fitzpatrick, J. W. (2018). Climate change causes upslope shifts and mountaintop extirpations in a tropical bird community. *Proceedings of the National Academy of Sciences*, 115(47), 11982–11987. <https://doi.org/10.1073/pnas.1804224115>
- Frei, C., & Schär, C. (1998). A precipitation climatology of the Alps from high-resolution rain-gauge observations. *International Journal of Climatology*, 18(8), 873–900. [https://doi.org/10.1002/\(SICI\)1097-0088\(19980630\)18:8<873::AID-JOC255>3.0.CO;2-9](https://doi.org/10.1002/(SICI)1097-0088(19980630)18:8<873::AID-JOC255>3.0.CO;2-9)
- Frierson, D. M. W. (2006). Robust increases in midlatitude static stability in simulations of global warming. *Geophysical Research Letters*, 33(24), L24816. <https://doi.org/10.1029/2006GL027504>
- Gao, Y., Chen, F., Lettenmaier, D. P., Xu, J., Xiao, L., & Li, X. (2018). Does elevation-dependent warming hold true above 5000 m elevation? Lessons from the Tibetan Plateau. *Npj Climate and Atmospheric Science*, 1(1), 19. <https://doi.org/10.1038/s41612-018-0030-z>
- Gilbert, J. M., & Maxwell, R. M. (2018). Contrasting warming and drought in snowmelt-dominated agricultural basins: Revealing the role of elevation gradients in regional response to temperature change. *Environmental Research Letters*, 13(7), 074023. <https://doi.org/10.1088/1748-9326/aacb38>
- Giorgi, F., Torma, C., Coppola, E., Ban, N., Schär, C., & Somot, S. (2016). Enhanced summer convective rainfall at Alpine high elevations in response to climate warming. *Nature Geoscience*, 9(8), 584–589. <https://doi.org/10.1038/ngeo2761>
- Giovannini, L., Laiti, L., Serafin, S., & Zardi, D. (2017). The thermally driven diurnal wind system of the Adige Valley in the Italian Alps. *Quarterly Journal of the Royal Meteorological Society*, 143(707), 2389–2402. <https://doi.org/10.1002/qj.3092>
- GISTEMP Team. (2020). *GISS surface temperature analysis (GISTEMP), version 4*. NASA Goddard Institute for Space Studies. Retrieved from <https://data.giss.nasa.gov/gistemp/>
- Gobiet, A., & Kotlarski, S. (2020). Future climate change in the European Alps. In A. Gobiet & S. Kotlarski (Eds.), *Oxford research encyclopedia of climate science*. Oxford University Press. <https://doi.org/10.1093/acrefore/9780190228620.013.767>
- Gobiet, A., Kotlarski, S., Beniston, M., Heinrich, G., Rajczak, J., & Stoffel, M. (2014). 21st century climate change in the European Alps—A review. *The Science of the Total Environment*, 493, 1138–1151. <https://doi.org/10.1016/j.scitotenv.2013.07.050>
- Godsey, S. E., Kirchner, J. W., & Tague, C. L. (2014). Effects of changes in winter snowpacks on summer low flows: Case studies in the Sierra Nevada, California, USA: Winter snowpacks and summer low flows. *Hydrological Processes*, 28(19), 5048–5064. <https://doi.org/10.1002/hyp.9943>
- Goodison, B. E., Louie, P. Y. T., & Yang, D. (1998). *WMO solid precipitation measurement intercomparison final report* (WMO Instruments and Observing Methods Report No. 67). Retrieved from <https://www.wmo.int/pages/prog/www/reports/WMOtd872.pdf>
- Grisogono, B., & Belušić, D. (2009). A review of recent advances in understanding the meso- and microscale properties of the severe Bora wind. *Tellus, Series A: Dynamic Meteorology and Oceanography*, 61 A(1), 1–16. <https://doi.org/10.1111/j.1600-0870.2008.00369.x>
- Grose, M. R., Syktus, J., Thatcher, M., Evans, J. P., Ji, F., Rafter, T., & Remenyi, T. (2019). The role of topography on projected rainfall change in mid-latitude mountain regions. *Climate Dynamics*, 53(5–6), 3675–3690. <https://doi.org/10.1007/s00382-019-04736-x>
- Gruber, S., Fleiner, R., Guegan, E., Panday, P., Schmid, M.-O., Stumm, D., et al. (2017). Review article: Inferring permafrost and permafrost thaw in the mountains of the Hindu Kush Himalaya region. *The Cryosphere*, 11(1), 81–99. <https://doi.org/10.5194/tc-11-81-2017>
- Guo, D., Pepin, N., Yang, K., Sun, J., & Li, D. (2021). Local changes in snow depth dominate the evolving pattern of elevation-dependent warming on the Tibetan Plateau. *Science Bulletin*, 66(11), 1146–1150. <https://doi.org/10.1016/j.scib.2021.02.013>
- Guo, D., Sun, J., Yang, K., Pepin, N., Xu, Y., Xu, Z., & Wang, H. (2020). Satellite data reveal southwestern Tibetan Plateau cooling since 2001 due to snow-albedo feedback. *International Journal of Climatology*, 40(3), 1644–1655. <https://doi.org/10.1002/joc.6292>
- Haerberli, W., & Weingartner, R. (2020). In full transition: Key impacts of vanishing mountain ice on water-security at local to global scales. *Water Security*, 11, 100074. <https://doi.org/10.1016/j.wasec.2020.100074>
- Hammond, J. C., Saavedra, F. A., & Kampf, S. K. (2018). Global snow zone maps and trends in snow persistence 2001–2016. *International Journal of Climatology*, 38(12), 4369–4383. <https://doi.org/10.1002/joc.5674>
- Harris, I., Osborn, T. J., Jones, P., & Lister, D. (2020). Version 4 of the CRU TS monthly high-resolution gridded multivariate climate dataset. *Scientific Data*, 7(1), 109. <https://doi.org/10.1038/s41597-020-0453-3>
- Helmer, E. H., Gerson, E. A., Baggett, L. S., Bird, B. J., Ruzycski, T. S., & Voggesser, S. M. (2019). Neotropical cloud forests and páramo to contract and dry from declines in cloud immersion and frost. *PLoS One*, 14(4), e0213155. <https://doi.org/10.1371/journal.pone.0213155>
- Hemp, A. (2006). Continuum or zonation? Altitudinal gradients in the forest vegetation of Mt. Kilimanjaro. *Plant Ecology*, 184(1), 27–42. <https://doi.org/10.1007/s11258-005-9049-4>
- Henn, B., Newman, A. J., Livneh, B., Daly, C., & Lundquist, J. D. (2018). An assessment of differences in gridded precipitation datasets in complex terrain. *Journal of Hydrology*, 556, 1205–1219. <https://doi.org/10.1016/j.jhydrol.2017.03.008>
- Hersbach, H., Bell, B., Berrisford, P., Hirahara, S., Horányi, A., Muñoz-Sabater, J., et al. (2020). The ERA5 global reanalysis. *Quarterly Journal of the Royal Meteorological Society*, 146(730), 1999–2049. <https://doi.org/10.1002/qj.3803>
- Hock, R., Rasul, G., Adler, C., Cáceres, B., Gruber, S., Hirabayashi, Y., et al. (2019). High mountain areas. Chapter 2. In H.-O. Pörtner, D. C. Roberts, V. Masson-Delmotte, P. Zhai, M. Tignor, E. Poloczanska, et al. (Eds.), *IPCC special report on the ocean and cryosphere in a changing climate* (pp. 131–202).

- Holden, Z. A., Swanson, A., Luce, C. H., Jolly, W. M., Maneta, M., Oyler, J. W., et al. (2018). Decreasing fire season precipitation increased recent western US forest wildfire activity. *Proceedings of the National Academy of Sciences*, *115*(36), E8349–E8357. <https://doi.org/10.1073/pnas.1802316115>
- Horton, P., Schaeffli, B., Mezghani, A., Hingray, B., & Musy, A. (2006). Assessment of climate-change impacts on alpine discharge regimes with climate model uncertainty. *Hydrological Processes*, *20*(10), 2091–2109. <https://doi.org/10.1002/hyp.6197>
- Houze, R. A. (2012). Orographic effects on precipitating clouds. *Reviews of Geophysics*, *50*(1), RG1001. <https://doi.org/10.1029/2011RG000365>
- Huning, L. S., & Margulis, S. A. (2018). Investigating the variability of high-elevation seasonal orographic snowfall enhancement and its drivers across Sierra Nevada, California. *Journal of Hydrometeorology*, *19*(1), 47–67. <https://doi.org/10.1175/JHM-D-16-0254.1>
- Huss, M., Bookhagen, B., Huggel, C., Jacobsen, D., Bradley, R. S., Clague, J. J., et al. (2017). Toward mountains without permanent snow and ice. *Earth's Future*, *5*(5), 418–435. <https://doi.org/10.1002/2016EF000514>
- Huss, M., & Hock, R. (2018). Global-scale hydrological response to future glacier mass loss. *Nature Climate Change*, *8*(2), 135–140. <https://doi.org/10.1038/s41558-017-0049-x>
- Ikedda, K., Rasmussen, R., Liu, C., Newman, A., Chen, F., Barlage, M., et al. (2021). Snowfall and snowpack in the Western U.S. as captured by convection permitting climate simulations: Current climate and pseudo global warming future climate. *Climate Dynamics*. <https://doi.org/10.1007/s00382-021-05805-w>
- Immerzeel, W. W., Lutz, A. F., Andrade, M., Bahl, A., Biemans, H., Bolch, T., et al. (2020). Importance and vulnerability of the world's water towers. *Nature*, *577*(7790), 364–369. <https://doi.org/10.1038/s41586-019-1822-y>
- Isaak, D. J., Young, M. K., Luce, C. H., Hostetler, S. W., Wenger, S. J., Peterson, E. E., et al. (2016). Slow climate velocities of mountain streams portend their role as refugia for cold-water biodiversity. *Proceedings of the National Academy of Sciences of the United States of America*, *113*(16), 4374–4379. <https://doi.org/10.1073/pnas.1522429113>
- Jackson, P. L., Mayr, G., & Vosper, S. (2013). Dynamically-driven winds. In F. K. Chow, S. F. J. De Wekker, & B. Snyder (Eds.), *Mountain weather research and forecasting* (pp. 121–218). Springer. [https://doi.org/10.1007/978-94-007-4098-3\\_3](https://doi.org/10.1007/978-94-007-4098-3_3)
- Jenicek, M., Seibert, J., & Staudinger, M. (2018). Modeling of future changes in seasonal snowpack and impacts on summer low flows in Alpine catchments. *Water Resources Research*, *54*(1), 538–556. <https://doi.org/10.1002/2017WR021648>
- Jenicek, M., Seibert, J., Zappa, M., Staudinger, M., & Jonas, T. (2016). Importance of maximum snow accumulation for summer low flows in humid catchments. *Hydrology and Earth System Sciences*, *20*(2), 859–874. <https://doi.org/10.5194/hess-20-859-2016>
- Jones, P. D., Lister, D. H., Osborn, T. J., Harpham, C., Salmon, M., & Morice, C. P. (2012). Hemispheric and large-scale land-surface air temperature variations: An extensive revision and an update to 2010. *Journal of Geophysical Research: Atmospheres*, *117*(D5). <https://doi.org/10.1029/2011JD017139>
- Juckes, M. N. (2000). The static stability of the midlatitude troposphere: The relevance of moisture. *Journal of the Atmospheric Sciences*, *57*(18), 3050–3057. [https://doi.org/10.1175/1520-0469\(2000\)057<3050:tsotom>2.0.co;2](https://doi.org/10.1175/1520-0469(2000)057<3050:tsotom>2.0.co;2)
- Kapos, V., Rhind, J., Edwards, M., Price, M. F., & Ravilious, C. (2000). Developing a map of the world's mountain forests. In *Forests in sustainable mountain development: A state of knowledge report for 2000. Task force on forests in sustainable mountain development* (pp. 4–19). <https://doi.org/10.1079/9780851994468.0004>
- Kattel, D. B., Yao, T., Yang, W., Gao, Y., & Tian, L. (2015). Comparison of temperature lapse rates from the northern to the southern slopes of the Himalayas. *International Journal of Climatology*, *35*(15), 4431–4443. <https://doi.org/10.1002/joc.4297>
- Kirshbaum, D., Adler, B., Kalthoff, N., Barthlott, C., & Serafin, S. (2018). Moist orographic convection: Physical mechanisms and Links to surface-exchange processes. *Atmosphere*, *9*(3), 80. <https://doi.org/10.3390/atmos9030080>
- Klein, G., Vitasse, Y., Rixen, C., Marty, C., & Rebetez, M. (2016). Shorter snow cover duration since 1970 in the Swiss Alps due to earlier snow-melt more than to later snow onset. *Climatic Change*, *139*(3–4), 637–649. <https://doi.org/10.1007/s10584-016-1806-y>
- Kochendorfer, J., Rasmussen, R., Wolff, M., Baker, B., Hall, M. E., Meyers, T., et al. (2017). The quantification and correction of wind-induced precipitation measurement errors. *Hydrology and Earth System Sciences*, *21*(4), 1973–1989. <https://doi.org/10.5194/hess-21-1973-2017>
- Kohler, T., Giger, M., Hurni, H., Ott, C., Wiesmann, U., Wymann von Dach, S., & Maselli, D. (2010). Mountains and climate change: A global concern. *Mountain Research and Development*, *30*(1), 53–55. <https://doi.org/10.1659/MRD-JOURNAL-D-09-00086.1>
- Kormos, P. R., Luce, C. H., Wenger, S. J., & Berghuijs, W. R. (2016). Trends and sensitivities of low streamflow extremes to discharge timing and magnitude in Pacific Northwest mountain streams. *Water Resources Research*, *52*(7), 4990–5007. <https://doi.org/10.1002/2015WR018125>
- Körner, C., Jetz, W., Paulsen, J., Payne, D., Rudmann-Maurer, K., & Spehn, M. E. (2017). A global inventory of mountains for bio-geographical applications. *Alpine Botany*, *127*(1), 1–15. <https://doi.org/10.1007/s00035-016-0182-6>
- Körner, C., Paulsen, J., & Spehn, E. M. (2011). A definition of mountains and their bioclimatic belts for global comparisons of biodiversity data. *Alpine Botany*, *121*(2), 73. <https://doi.org/10.1007/s00035-011-0094-4>
- Kotlarski, S., Bosshard, T., Lüthi, D., Pall, P., & Schär, C. (2012). Elevation gradients of European climate change in the regional climate model COSMO-CLM. *Climatic Change*, *112*(2), 189–215. <https://doi.org/10.1007/s10584-011-0195-5>
- Kotlarski, S., Lüthi, D., & Schär, C. (2015). The elevation dependency of 21st century European climate change: An RCM ensemble perspective. *International Journal of Climatology*, *35*(13), 3902–3920. <https://doi.org/10.1002/joc.4254>
- Kuhn, M. (1989). The response of the equilibrium line altitude to climate fluctuations: Theory and observations. In J. Oerlemans (Ed.), *Glacier fluctuations and climatic change* (pp. 407–417). Springer. [https://doi.org/10.1007/978-94-015-7823-3\\_26](https://doi.org/10.1007/978-94-015-7823-3_26)
- La Sorte, F. A., & Jetz, W. (2010). Projected range contractions of montane biodiversity under global warming. *Proceedings of the Royal Society B: Biological Sciences*, *277*(1699), 3401–3410. <https://doi.org/10.1098/rspb.2010.0612>
- Lal, M., Meehl, G. A., & Arblaster, J. M. (2000). Simulation of Indian summer monsoon rainfall and its intraseasonal variability in the NCAR climate system model. *Regional Environmental Change*, *1*(3–4), 163–179. <https://doi.org/10.1007/s101130000017>
- Lareau, N. P., Crosman, E., Whiteman, C. D., Horel, J. D., Hoch, S. W., Brown, W. O. J., & Horst, T. W. (2013). The persistent cold-air pool study. *Bulletin of the American Meteorological Society*, *94*(1). <https://doi.org/10.1175/BAMS-D-11-00255.1>
- Lareau, N. P., & Horel, J. D. (2015). Turbulent erosion of persistent cold-air pools: Numerical simulations. *Journal of the Atmospheric Sciences*, *72*(4), 1409–1427. <https://doi.org/10.1175/JAS-D-14-0173.1>
- Lawrimore, J. H., Menne, M. J., Gleason, B. E., Williams, C. N., Wuertz, D. B., Vose, R. S., & Rennie, J. (2011). An overview of the Global Historical Climatology Network monthly mean temperature data set, version 3. *Journal of Geophysical Research*, *116*(D19), D19121. <https://doi.org/10.1029/2011JD016187>
- Lenssen, N. J. L., Schmidt, G. A., Hansen, J. E., Menne, M. J., Persin, A., Ruedy, R., & Zyss, D. (2019). Improvements in the GISTEMP uncertainty model. *Journal of Geophysical Research: Atmospheres*, *124*(12), 6307–6326. <https://doi.org/10.1029/2018JD029522>
- Letcher, T. W., & Minder, J. R. (2015). Characterization of the simulated regional snow Albedo feedback using a regional climate model over complex Terrain. *Journal of Climate*, *28*(19), 7576–7595. <https://doi.org/10.1175/JCLI-D-15-0166.1>

- Li, B., Chen, Y., Li, W., Chen, Z., Zhang, B., & Guo, B. (2013). Spatial and temporal variations of temperature and precipitation in the arid region of northwest China from 1960–2010. *Fresenius Environmental Bulletin*, 22(2), 362–371.
- Li, B., Chen, Y., & Shi, X. (2012). Why does the temperature rise faster in the arid region of northwest China? *Journal of Geophysical Research*, 117(D16). <https://doi.org/10.1029/2012JD017953>
- Li, B., Chen, Y., & Shi, X. (2020). Does elevation dependent warming exist in high mountain Asia? *Environmental Research Letters*, 15(2), 24012. <https://doi.org/10.1088/1748-9326/ab6d7f>
- Li, C., Bosch, C., Kang, S., Andersson, A., Chen, P., Zhang, Q., et al. (2016). Sources of black carbon to the Himalayan–Tibetan Plateau glaciers. *Nature Communications*, 7(1), 12574. <https://doi.org/10.1038/ncomms12574>
- Lievens, H., Demuzere, M., Marshall, H.-P., Reichle, R. H., Brucker, L., Brangers, I., et al. (2019). Snow depth variability in the Northern Hemisphere mountains observed from space. *Nature Communications*, 10(1), 4629. <https://doi.org/10.1038/s41467-019-12566-y>
- Lind, P., Belušić, D., Christensen, O. B., Dobler, A., Kjellström, E., Landgren, O., et al. (2020). Benefits and added value of convection-permitting climate modeling over Fenno-Scandinavia. *Climate Dynamics*, 55(7), 1893–1912. <https://doi.org/10.1007/s00382-020-05359-3>
- Loarie, S. R., Duffy, P. B., Hamilton, H., Asner, G. P., Field, C. B., & Ackerly, D. D. (2009). The velocity of climate change. *Nature*, 462(7276), 1052–1055. <https://doi.org/10.1038/nature08649>
- López-Moreno, J. I. (2005). Recent variations of snowpack depth in the Central Spanish Pyrenees. *Arctic Antarctic and Alpine Research*, 37(2), 253–260. [https://doi.org/10.1657/1523-0430\(2005\)037\[0253:RVOSDI\]2.0.CO;2](https://doi.org/10.1657/1523-0430(2005)037[0253:RVOSDI]2.0.CO;2)
- Lu, Q., Zhao, D., & Wu, S. (2017). Simulated responses of permafrost distribution to climate change on the Qinghai–Tibet Plateau. *Scientific Reports*, 7(1), 3845. <https://doi.org/10.1038/s41598-017-04140-7>
- Luce, C., Staab, B., Kramer, M., Wenger, S., Isaak, D., & McConnell, C. (2014). Sensitivity of summer stream temperatures to climate variability in the Pacific Northwest. *Water Resources Research*, 50(4), 3428–3443. <https://doi.org/10.1002/2013WR014329>
- Luce, C. H., Abatzoglou, J. T., & Holden, Z. A. (2013). The missing mountain water: Slower westerlies decrease orographic enhancement in the Pacific Northwest USA. *Science*, 342(6164), 1360–1364. <https://doi.org/10.1126/science.1242335>
- Luce, C. H., Lopez-Burgos, V., & Holden, Z. (2014). Sensitivity of snowpack storage to precipitation and temperature using spatial and temporal analog models. *Water Resources Research*, 50(12), 9447–9462. <https://doi.org/10.1002/2013WR014844>
- Lugauer, M., & Winkler, P. (2005). Thermal circulation in South Bavaria climatology and synoptic aspects. *Meteorologische Zeitschrift*, 14(1), 15–30. <https://doi.org/10.1127/0941-2948/2005/0014-0015>
- Lundquist, J., Hughes, M., Gutmann, E., & Kapnick, S. (2019). Our skill in modeling mountain rain and snow is bypassing the skill of our observational networks. *Bulletin of the American Meteorological Society*, 100(12), 2473–2490. <https://doi.org/10.1175/BAMS-D-19-0001.1>
- Lundquist, J. D., & Cayan, D. R. (2007). Surface temperature patterns in complex terrain: Daily variations and long-term change in the central Sierra Nevada, California. *Journal of Geophysical Research*, 112(D11), D11124. <https://doi.org/10.1029/2006JD007561>
- Lundquist, J. D., Minder, J. R., Neiman, P. J., & Sukovich, E. (2010). Relationships between barrier jet heights, orographic precipitation gradients, and streamflow in the Northern Sierra Nevada. *Journal of Hydrometeorology*, 11(5), 1141–1156. <https://doi.org/10.1175/2010JHM1264.1>
- Lundquist, J. D., Pepin, N., & Rochford, C. (2008). Automated algorithm for mapping regions of cold-air pooling in complex terrain. *Journal of Geophysical Research*, 113(D22), D22107. <https://doi.org/10.1029/2008JD009879>
- Lute, A. C., & Luce, C. H. (2017). Are model transferability and complexity antithetical? Insights from validation of a variable-complexity empirical snow model in space and time. *Water Resources Research*, 53(11), 8825–8850. <https://doi.org/10.1002/2017WR020752>
- Magalhães, N. de, Evangelista, H., Condom, T., Rabatel, A., & Ginot, P. (2019). Amazonian biomass burning enhances tropical Andean glaciers melting. *Scientific Reports*, 9(1), 16914. <https://doi.org/10.1038/s41598-019-53284-1>
- Marzeion, B., Kaser, G., Maussion, F., & Champollion, N. (2018). Limited influence of climate change mitigation on short-term glacier mass loss. *Nature Climate Change*, 8(4), 305–308. <https://doi.org/10.1038/s41558-018-0093-1>
- Mass, C., Johnson, N., Warner, M., & Vargas, R. (2015). Synoptic control of cross-barrier precipitation ratios for the Cascade Mountains. *Journal of Hydrometeorology*, 16(3), 1014–1028. <https://doi.org/10.1175/JHM-D-14-0149.1>
- Mastrotheodoros, T., Pappas, C., Molnar, P., Burlando, P., Manoli, G., Parajka, J., et al. (2020). More green and less blue water in the Alps during warmer summers. *Nature Climate Change*, 10(2), 155–161. <https://doi.org/10.1038/s41558-019-0676-5>
- Matiu, M., Crespi, A., Bertoldi, G., Carmagnola, C. M., Marty, C., Morin, S., et al. (2021). Observed snow depth trends in the European Alps: 1971 to 2019. *The Cryosphere*, 15(3), 1343–1382. <https://doi.org/10.5194/TC-15-1343-2021>
- Mauritsen, T., Stevens, B., Roeckner, E., Crueger, T., Esch, M., Giorgetta, M., et al. (2012). Tuning the climate of a global model. *Journal of Advances in Modeling Earth Systems*, 4(3). <https://doi.org/10.1029/2012MS000154>
- Mayr, G. J., & Armi, L. (2010). The influence of downstream diurnal heating on the descent of flow across the Sierras. *Journal of Applied Meteorology and Climatology*, 49(9), 1906–1912. <https://doi.org/10.1175/2010JAMC2516.1>
- Mayr, G. J., Armi, L., Gohm, A., Zängl, G., Durran, D. R., Flamant, C., et al. (2007). Gap flows: Results from the mesoscale Alpine Programme. *Quarterly Journal of the Royal Meteorological Society*, 133(625), 881–896. <https://doi.org/10.1002/qj.66>
- McCabe, G. J., & Fountain, A. G. (1995). Relations between atmospheric circulation and mass balance of South Cascade Glacier, Washington, USA. *Arctic and Alpine Research*, 27(3), 226–233. <https://doi.org/10.2307/1551953>
- Menne, M. J., Williams, C. N., Gleason, B. E., Jared Rennie, J., & Lawrimore, J. H. (2018). The global historical climatology network monthly temperature dataset, version 4. *Journal of Climate*, 31(24), 9835–9854. <https://doi.org/10.1175/JCLI-D-18-0094.1>
- Mernild, S. H., Lipscomb, W. H., Bahr, D. B., Radić, V., & Zemp, M. (2013). Global glacier changes: A revised assessment of committed mass losses and sampling uncertainties. *The Cryosphere*, 7(5), 1565–1577. <https://doi.org/10.5194/TC-7-1565-2013>
- Meybeck, M., Green, P., & Vörösmarty, C. (2001). A new typology for mountains and other relief classes. *Mountain Research and Development*, 21(1), 34–45. [https://doi.org/10.1659/0276-4741\(2001\)021\[0034:antfma\]2.0.co;2](https://doi.org/10.1659/0276-4741(2001)021[0034:antfma]2.0.co;2)
- Molina, L. T., Gallardo, L., Andrade, M., Baumgardner, D., Borbor-Córdova, M., Bórquez, R., et al. (2015). Pollution and its impacts on the South American cryosphere. *Earth's Future*, 3(12), 345–369. <https://doi.org/10.1002/2015EF000311>
- Morice, C. P., Kennedy, J. J., Rayner, N. A., & Jones, P. D. (2012). Quantifying uncertainties in global and regional temperature change using an ensemble of observational estimates: The HadCRUT4 data set. *Journal of Geophysical Research*, 117(D8). <https://doi.org/10.1029/2011JD017187>
- Mote, P. W., Hamlet, A. F., Clark, M. P., & Lettenmaier, D. P. (2005). Declining mountain snowpack IN western North America. *Bulletin of the American Meteorological Society*, 86(1), 39–50. <https://doi.org/10.1175/BAMS-86-1-39>
- Mote, P. W., Li, S., Lettenmaier, D. P., Xiao, M., & Engel, R. (2018). Dramatic declines in snowpack in the western US. *Npj Climate and Atmospheric Science*, 1(1), 2. <https://doi.org/10.1038/s41612-018-0012-1>
- Musselman, K. N., Clark, M. P., Liu, C., Ikeda, K., & Rasmussen, R. (2017). Slower snowmelt in a warmer world. *Nature Climate Change*, 7(3), 214–219. <https://doi.org/10.1038/nclimate3225>
- Napoli, A., Crespi, A., Ragone, F., Maugeri, M., & Pasquero, C. (2019). Variability of orographic enhancement of precipitation in the Alpine region. *Scientific Reports*, 9(1), 13352. <https://doi.org/10.1038/s41598-019-49974-5>



- Narkhedkar, S. G., Morwal, S. B., Padmakumari, B., Deshpande, C. G., Kothawale, D. R., Mahes Kumar, R. S., & Kulkarni, J. R. (2015). Rainfall mechanism over the rain-shadow region of north peninsular India. *Climate Dynamics*, *45*(5–6), 1493–1512. <https://doi.org/10.1007/s00382-014-2403-2>
- Nickus, U., & Vergeiner, I. (1984). The thermal structure of the inn valley atmosphere. *Archives for Meteorology, Geophysics, and Bioclimatology Series A*, *33*(2–3), 199–215. <https://doi.org/10.1007/BF02257725>
- Nogues-Bravo, D., Araújo, M. B., Lasanta, T., & Moreno, J. I. L. (2008). Climate change in mediterranean Mountains during the 21st century. *AMBIO: A Journal of the Human Environment*, *37*(4), 280–285. [https://doi.org/10.1579/0044-7447\(2008\)37\[280:CCIMMD\]2.0.CO;2](https://doi.org/10.1579/0044-7447(2008)37[280:CCIMMD]2.0.CO;2)
- Norris, J., Carvalho, L. M. V., Jones, C., & Cannon, F. (2020). Warming and drying over the central Himalaya caused by an amplification of local mountain circulation. *Npj Climate and Atmospheric Science*, *3*(1), 1. <https://doi.org/10.1038/s41612-019-0105-5>
- Notarnicola, C. (2020). Hotspots of snow cover changes in global mountain regions over 2000–2018. *Remote Sensing of Environment*, *243*, 111781. <https://doi.org/10.1016/j.rse.2020.111781>
- Oerlemans, J. (1994). Quantifying global warming from the retreat of glaciers. *Science*, *264*(5156), 243–245. <https://doi.org/10.1126/science.264.5156.243>
- Ohmura, A. (2012). Enhanced temperature variability in high-altitude climate change. *Theoretical and Applied Climatology*, *110*(4), 499–508. <https://doi.org/10.1007/s00704-012-0687-x>
- Olefs, M., Koch, R., Schöner, W., & Marke, T. (2020). Changes in snow depth, snow cover duration, and potential snowmaking conditions in Austria, 1961–2020—A model based approach. *Atmosphere*, *11*(12), 1330. <https://doi.org/10.3390/atmos11121330>
- Olson, M., & Rupper, S. (2019). Impacts of topographic shading on direct solar radiation for valley glaciers in complex topography. *The Cryosphere*, *13*(1), 29–40. <https://doi.org/10.5194/tc-13-29-2019>
- Oyler, J. W., Dobrowski, S. Z., Ballantyne, A. P., Klene, A. E., & Running, S. W. (2015). Artificial amplification of warming trends across the mountains of the western United States. *Geophysical Research Letters*, *42*(1), 153–161. <https://doi.org/10.1002/2014GL062803>
- Pagès, M., Pepin, N., & Miró, J. R. (2017). Measurement and modelling of temperature cold pools in the Cerdanya valley (Pyrenees), Spain. *Meteorological Applications*, *24*(2), 290–302. <https://doi.org/10.1002/met.1630>
- Palazzi, E., Filippi, L., & von Hardenberg, J. (2017). Insights into elevation-dependent warming in the Tibetan Plateau-Himalayas from CMIP5 model simulations. *Climate Dynamics*, *48*(11–12), 3991–4008. <https://doi.org/10.1007/s00382-016-3316-z>
- Palazzi, E., von Hardenberg, J., & Provenzale, A. (2013). Precipitation in the Hindu-Kush Karakoram Himalaya: Observations and future scenarios. *Journal of Geophysical Research: Atmospheres*, *118*(1), 85–100. <https://doi.org/10.1029/2012JD018697>
- Palazzi, E., von Hardenberg, J., Terzago, S., & Provenzale, A. (2015). Precipitation in the Karakoram-Himalaya: A CMIP5 view. *Climate Dynamics*, *45*(1–2), 21–45. <https://doi.org/10.1007/s00382-014-2341-z>
- Parajka, J., Blaschke, A. P., Blöschl, G., Haslinger, K., Hepp, G., Laaha, G., et al. (2016). Uncertainty contributions to low-flow projections in Austria. *Hydrology and Earth System Sciences*, *20*(5), 2085–2101. <https://doi.org/10.5194/hess-20-2085-2016>
- Parmesan, C. (2006). Ecological and evolutionary responses to recent climate change. *Annual Review of Ecology and Systematics*, *37*(1), 637–669. <https://doi.org/10.1146/annurev.ecolsys.37.091305.110100>
- Paul, F., Rastner, P., Azzoni, R. S., Diolaiuti, G., Fugazza, D., Le Bris, R., et al. (2020). Glacier shrinkage in the Alps continues unabated as revealed by a new glacier inventory from Sentinel-2. *Earth System Science Data*, *12*(3), 1805–1821. <https://doi.org/10.5194/essd-12-1805-2020>
- Pavelsky, T. M., Sobolowski, S., Kapnick, S. B., & Barnes, J. B. (2012). Changes in orographic precipitation patterns caused by a shift from snow to rain. *Geophysical Research Letters*, *39*(18). <https://doi.org/10.1029/2012GL052741>
- Pepin, N., Bradley, R. S., Diaz, H. F., Baraer, M., Caceres, E. B., Forsythe, et al. (2015). Elevation-dependent warming in mountain regions of the world. *Nature Climate Change*, *5*(5), 424–430. <https://doi.org/10.1038/nclimate2563>
- Pepin, N., Deng, H., Zhang, H., Zhang, F., Kang, S., & Yao, T. (2019). An examination of temperature trends at high elevations across the Tibetan Plateau: The use of MODIS LST to understand patterns of elevation-dependent warming. *Journal of Geophysical Research: Atmospheres*, *124*(11), 5738–5756. <https://doi.org/10.1029/2018JD029798>
- Pepin, N. C., & Lundquist, J. D. (2008). Temperature trends at high elevations: Patterns across the globe. *Geophysical Research Letters*, *35*(14), L14701. <https://doi.org/10.1029/2008GL034026>
- PERMOS. (2016). Permafrost in Switzerland 2010/2011 to 2013/2014. In J. Noetzi, R. Luethi, & B. Staub (Eds.), *Glaciological Report Permafrost No. 12–15 of the Cryospheric Commission of the Swiss Academy of Sciences* (p. 85). [https://scnat.ch/en/uuid/i/3f5b9b40-6099-5c0e-a408-eedb4dd647fe-Permafrost\\_in\\_Switzerland\\_20102011\\_to\\_20132014](https://scnat.ch/en/uuid/i/3f5b9b40-6099-5c0e-a408-eedb4dd647fe-Permafrost_in_Switzerland_20102011_to_20132014)
- Pierrehumbert, R. T., & Wyman, B. (1985). Upstream effects of mesoscale mountains. *Journal of the Atmospheric Sciences*, *42*(10), 977–1003. [https://doi.org/10.1175/1520-0469\(1985\)042<0977:UEOMM>2.0.CO;2](https://doi.org/10.1175/1520-0469(1985)042<0977:UEOMM>2.0.CO;2)
- Pike, G., Pepin, N. C., & Schaefer, M. (2013). High latitude local scale temperature complexity: The example of Kevo Valley, Finnish Lapland. *International Journal of Climatology*, *33*(8), 2050–2067. <https://doi.org/10.1002/joc.3573>
- Price, M. F., Arnesen, T., Gløersen, E., & Metzger, M. J. (2019). Mapping mountain areas: Learning from global, European and Norwegian perspectives. *Journal of Mountain Science*, *16*(1), 1–15. <https://doi.org/10.1007/s11629-018-4916-3>
- Price, M. F., Byers, A. C., Friend, D. A., Kohler, T., & Price, L. W. (2013). *Mountain geography: Physical and human dimensions*. University of California Press.
- Qian, Y., Flanner, M. G., Leung, L. R., & Wang, W. (2011). Sensitivity studies on the impacts of Tibetan Plateau snowpack pollution on the Asian hydrological cycle and monsoon climate. *Atmospheric Chemistry and Physics*, *11*(5), 1929–1948. <https://doi.org/10.5194/acp-11-1929-2011>
- Qin, D., Liu, S., & Li, P. (2006). Snow cover distribution, variability, and response to climate change in western China. *Journal of Climate*, *19*(9), 1820–1833. <https://doi.org/10.1175/jcli3694.1>
- Qin, J., Yang, K., Liang, S., & Guo, X. (2009). The altitudinal dependence of recent rapid warming over the Tibetan Plateau. *Climatic Change*, *97*(1–2), 321–327. <https://doi.org/10.1007/s10584-009-9733-9>
- Qixiang, W., Wang, M., & Fan, X. (2018). Seasonal patterns of warming amplification of high-elevation stations across the globe. *International Journal of Climatology*, *38*(8), 3466–3473. <https://doi.org/10.1002/joc.5509>
- Rangwala, I., & Miller, J. R. (2012). Climate change in mountains: A review of elevation-dependent warming and its possible causes. *Climatic Change*, *114*(3–4), 527–547. <https://doi.org/10.1007/s10584-012-0419-3>
- Rangwala, I., Sinsky, E., & Miller, J. R. (2016). Variability in projected elevation dependent warming in boreal midlatitude winter in CMIP5 climate models and its potential drivers. *Climate Dynamics*, *46*(7–8), 2115–2122. <https://doi.org/10.1007/s00382-015-2692-0>
- Richner, H., & Hächler, P. (2013). Understanding and forecasting alpine foehn. In F. K. Chow, S. F. J. De Wekker, & B. Snyder (Eds.), *Mountain weather research and forecasting* (pp. 219–260). Springer. [https://doi.org/10.1007/978-94-007-4098-3\\_4](https://doi.org/10.1007/978-94-007-4098-3_4)
- Roe, G. H. (2005). Orographic precipitation. *Annual Review of Earth and Planetary Sciences*, *33*(1), 645–671. <https://doi.org/10.1146/annurev.earth.33.092203.122541>
- Rotunno, R., & Ferretti, R. (2001). Mechanisms of intense Alpine rainfall. *Journal of the Atmospheric Sciences*, *58*(13), 1732–1749. [https://doi.org/10.1175/1520-0469\(2001\)058<1732:MOIAR>2.0.CO;2](https://doi.org/10.1175/1520-0469(2001)058<1732:MOIAR>2.0.CO;2)

- Rotunno, R., Grubišić, V., & Smolarkiewicz, P. K. (1999). Vorticity and potential vorticity in mountain wakes. *Journal of the Atmospheric Sciences*, 56(16), 2796–2810. [https://doi.org/10.1175/1520-0469\(1999\)056<2796:VAPVIM>2.0.CO;2](https://doi.org/10.1175/1520-0469(1999)056<2796:VAPVIM>2.0.CO;2)
- Rupp, D. E., Li, S., Mote, P. W., Shell, K. M., Massey, N., Sparrow, S. N., et al. (2017). Seasonal spatial patterns of projected anthropogenic warming in complex terrain: A modeling study of the western US. *Climate Dynamics*, 48(7–8), 2191–2213. <https://doi.org/10.1007/s00382-016-3200-x>
- Saavedra, F. A., Kampf, S. K., Fassnacht, S. R., & Sibold, J. S. (2018). Changes in Andes snow cover from MODIS data, 2000–2016. *The Cryosphere*, 12(3), 1027–1046. <https://doi.org/10.5194/tc-12-1027-2018>
- Salathé, E. P., Leung, L. R., Qian, Y., & Zhang, Y. (2010). Regional climate model projections for the State of Washington. *Climatic Change*, 102(1–2), 51–75. <https://doi.org/10.1007/s10584-010-9849-y>
- Sayre, R., Dangermond, J., Frye, C., Vaughan, R., Aniello, P., Breyer, S., et al. (2014). A new map of global ecological land units — An ecophysiological stratification approach. *Association of American Geographers*. <https://doi.org/10.13140/2.1.2167.8887>
- Sayre, R., Frye, C., Karagulle, D., Krauer, J., Breyer, S., Aniello, P., et al. (2018). A new high-resolution map of world mountains and an online tool for visualizing and comparing characterizations of global mountain distributions. *Mountain Research and Development*, 38(3), 240–249. <https://doi.org/10.1659/MRD-JOURNAL-D-17-00107.1>
- Scaff, L., Rutllant, J. A., Rahn, D., Gascoïn, S., & Rondanelli, R. (2017). Meteorological interpretation of orographic precipitation gradients along an Andes west slope basin at 30°S (Elqui Valley, Chile). *Journal of Hydrometeorology*, 18(3), 713–727. <https://doi.org/10.1175/JHM-D-16-0073.1>
- Schär, C., Fuhrer, O., Arteaga, A., Ban, N., Charpillot, C., Girolamo, S. D., et al. (2020). Kilometer-scale climate models: Prospects and challenges. *Bulletin of the American Meteorological Society*, 101(5), E567–E587. <https://doi.org/10.1175/bams-d-18-0167.1>
- Scherrer, S. C. (2020). Temperature monitoring in mountain regions using reanalyses: Lessons from the Alps. *Environmental Research Letters*, 15(4), 44005. <https://doi.org/10.1088/1748-9326/ab702d>
- Scherrer, S. C., Ceppi, P., Croci-Maspoli, M., & Appenzeller, C. (2012). Snow-albedo feedback and Swiss spring temperature trends. *Theoretical and Applied Climatology*, 110(4), 509–516. <https://doi.org/10.1007/s00704-012-0712-0>
- Schneider, U., Becker, A., Ziese, M., & Rudolf, B. (2018). Global Precipitation Analysis Products of the GPCC. *Global Precipitation Climatology Centre (GPCC)*, 1–14. Retrieved from [ftp://ftp-anon.dwd.de/pub/data/gpcc/PDF/GPCC\\_intro\\_products\\_2008.pdf](ftp://ftp-anon.dwd.de/pub/data/gpcc/PDF/GPCC_intro_products_2008.pdf)
- Schneider, U., Finger, P., Meyer-Christoffer, A., Rustemeier, E., Ziese, M., & Becker, A. (2017). Evaluating the hydrological cycle over land using the newly-corrected precipitation climatology from the global precipitation climatology Centre (GPCC). *Atmosphere*, 8(12), 52. <https://doi.org/10.3390/atmos8030052>
- Schnorbus, M., Werner, A., & Bennett, K. (2014). Impacts of climate change in three hydrologic regimes in British Columbia, Canada. *Hydrological Processes*, 28(3), 1170–1189. <https://doi.org/10.1002/hyp.9661>
- Scorer, R. S. (1949). Theory of waves in the lee of mountains. *Quarterly Journal of the Royal Meteorological Society*, 75(323), 41–56. <https://doi.org/10.1002/qj.49707532308>
- Seibert, P. (2012). The riddles of foehn – Introduction to the historic articles by Hann and Ficker. *Meteorologische Zeitschrift*, 21(6), 607–614. <https://doi.org/10.1127/0941-2948/2012/0398>
- Serafin, S., Adler, B., Cuxart, J., De Wekker, S., Gohm, A., Grisogono, B., et al. (2018). Exchange processes in the atmospheric boundary layer over mountainous terrain. *Atmosphere*, 9(3), 102. <https://doi.org/10.3390/atmos9030102>
- Shahgedanova, M., Adler, C., Gebrekirstos, A., Grau, H. R., Huguel, C., Marchant, R., et al. (2021). Mountain observatories: Status and prospects for enhancing and connecting a global community. *Mountain Research and Development*, 41(2). <https://doi.org/10.1659/MRD-JOURNAL-D-20-00054.1>
- Shen, S. S. P., Yao, R., Ngo, J., Basist, A. M., Thomas, N., & Yao, T. (2015). Characteristics of the Tibetan Plateau snow cover variations based on daily data during 1997–2011. *Theoretical and Applied Climatology*, 120(3–4), 445–453. <https://doi.org/10.1007/s00704-014-1185-0>
- Shepherd, T. G. (2014). Atmospheric circulation as a source of uncertainty in climate change projections. *Nature Geoscience*, 7(10), 703–708. <https://doi.org/10.1038/ngeo2253>
- Shi, X., & Durran, D. (2016). Sensitivities of extreme precipitation to global warming are lower over mountains than over oceans and plains. *Journal of Climate*, 29(13), 4779–4791. <https://doi.org/10.1175/JCLI-D-15-0576.1>
- Shi, X., & Durran, D. R. (2014). The response of orographic precipitation over idealized midlatitude mountains due to global increases in CO<sub>2</sub>. *Journal of Climate*, 27(11), 3938–3956. <https://doi.org/10.1175/JCLI-D-13-00460.1>
- Shi, X., & Durran, D. R. (2015). Estimating the response of extreme precipitation over midlatitude mountains to global warming. *Journal of Climate*, 28(10), 4246–4262. <https://doi.org/10.1175/JCLI-D-14-00750.1>
- Smith, C. D., Ross, A., Kochendorfer, J., Earle, M. E., Wolff, M., Buisán, S., et al. (2020). Evaluation of the WMO Solid Precipitation Intercomparison Experiment (SPICE) transfer functions for adjusting the wind bias in solid precipitation measurements. *Hydrology and Earth System Sciences*, 24(8), 4025–4043. <https://doi.org/10.5194/hess-24-4025-2020>
- Smith, R. B. (1979). The influence of mountains on the atmosphere. *Advances in Geophysics*, 21, 87–230. [https://doi.org/10.1016/S0065-2687\(08\)60262-9](https://doi.org/10.1016/S0065-2687(08)60262-9)
- Smith, R. B., & Barstad, I. (2004). A linear theory of orographic precipitation. *Journal of the Atmospheric Sciences*, 61(12), 1377–1391. [https://doi.org/10.1175/1520-0469\(2004\)061<1377:ALTOOP>2.0.CO;2](https://doi.org/10.1175/1520-0469(2004)061<1377:ALTOOP>2.0.CO;2)
- Smith, T., & Bookhagen, B. (2018). Changes in seasonal snow water equivalent distribution in High Mountain Asia (1987 to 2009). *Science Advances*, 4(1), e1701550. <https://doi.org/10.1126/sciadv.1701550>
- Stocker, T. F., Qin, D., Plattner, G.-K., Tignor, M., Allen, S. K., Boschung, J., et al. (2013). In Intergovernmental Panel on Climate Change (Ed.), *Climate change 2013: The physical science basis. Contribution of working group I to the fifth assessment report of the intergovernmental panel on climate change*. Cambridge University Press. <https://doi.org/10.1017/CBO9781107415324>
- Stone, P. H., & Carlson, J. H. (1979). Atmospheric lapse rate regimes and their parameterization. *Journal of the Atmospheric Sciences*, 36(3), 415–423. [https://doi.org/10.1175/1520-0469\(1979\)036<0415:ALRRAT>2.0.CO;2](https://doi.org/10.1175/1520-0469(1979)036<0415:ALRRAT>2.0.CO;2)
- Strauss, L., Serafin, S., & Grubišić, V. (2016). Atmospheric rotors and severe turbulence in a long deep valley. *Journal of the Atmospheric Sciences*, 73(4), 1481–1506. <https://doi.org/10.1175/JAS-D-15-0192.1>
- Sturm, M., Goldstein, M. A., & Parr, C. (2017). Water and life from snow: A trillion dollar science question. *Water Resources Research*, 53(5), 3534–3544. <https://doi.org/10.1002/2017WR020840>
- Taylor, K. E., Stouffer, R. J., & Meehl, G. A. (2012). An overview of CMIP5 and the experiment design. *Bulletin of the American Meteorological Society*, 93(4), 485–498. <https://doi.org/10.1175/BAMS-D-11-00094.1>
- Thornton, J. M., Brauchli, T., Mariethoz, G., & Brunner, P. (2021). Efficient multi-objective calibration and uncertainty analysis of distributed snow simulations in rugged alpine terrain. *Journal of Hydrology*, 598, 126241. <https://doi.org/10.1016/j.jhydrol.2021.126241>



- Thornton, J. M., Palazzi, E., Pepin, N. C., Cristofanelli, P., Essery, R., Kotlarski, S., et al. (2021). Toward a definition of essential mountain climate variables. *One Earth*, 4(6), 805–827. <https://doi.org/10.1016/j.oneear.2021.05.005>
- Troll, C. (1973). The upper timberline in different climatic zones. *Arctic Antarctic and Alpine Research*, 5, A13–A18.
- van Huijgevoort, M. H. J., van Lanen, H. A. J., Teuling, A. J., & Uijlenhoet, R. (2014). Identification of changes in hydrological drought characteristics from a multi-GCM driven ensemble constrained by observed discharge. *Journal of Hydrology*, 512, 421–434. <https://doi.org/10.1016/j.jhydrol.2014.02.060>
- Vergeiner, I., & Dreiseitl, E. (1987). Valley winds and slope winds – Observations and elementary thoughts. *Meteorology and Atmospheric Physics*, 36(1–4), 264–286. <https://doi.org/10.1007/BF01045154>
- Viviroli, D., Archer, D. R., Buytaert, W., Fowler, H. J., Greenwood, G. B., Hamlet, A. F., et al. (2011). Climate change and mountain water resources: Overview and recommendations for research, management and policy. *Hydrology and Earth System Sciences*, 15(2), 471–504. <https://doi.org/10.5194/hess-15-471-2011>
- Viviroli, D., Kummu, M., Meybeck, M., Kallio, M., & Wada, Y. (2020). Increasing dependence of lowland populations on mountain water resources. *Nature Sustainability*, 3(11), 917–928. <https://doi.org/10.1038/s41893-020-0559-9>
- Vose, R. S., Applequist, S., Squires, M., Durre, I., Menne, M. J., Williams, C. N., et al. (2014). Improved historical temperature and precipitation time series for U.S. Climate divisions. *Journal of Applied Meteorology and Climatology*, 53(5), 1232–1251. <https://doi.org/10.1175/JAMC-D-13-0248.1>
- Vuille, M., & Bradley, R. S. (2000). Mean annual temperature trends and their vertical structure in the tropical Andes. *Geophysical Research Letters*, 27, 3885–3888. <https://doi.org/10.1029/2000GL011871>
- Vuille, M., Bradley, R. S., Werner, M., & Keimig, F. (2003). 20th century climate change in the Tropical Andes: Observations and model results. *Climatic Change*, 59, 75–99. <https://doi.org/10.1023/A:1024406427519>
- Vuille, M., Carey, M., Huggel, C., Buytaert, W., Rabatel, A., Jacobsen, D., et al. (2018). Rapid decline of snow and ice in the tropical Andes – Impacts, uncertainties and challenges ahead. *Earth-Science Reviews*, 176, 195–213. <https://doi.org/10.1016/j.earscirev.2017.09.019>
- Vuille, M., Franquist, E., Garreaud, R., Lavado Casimiro, W. S., & Cáceres, B. (2015). Impact of the global warming hiatus on Andean temperature. *Journal of Geophysical Research: Atmospheres*, 120(9), 3745–3757. <https://doi.org/10.1002/2015JD023126>
- Wang, Q., Fan, X., & Wang, M. (2016). Evidence of high-elevation amplification versus Arctic amplification. *Scientific Reports*, 6(1), 19219. <https://doi.org/10.1038/srep19219>
- Wang, X., Wu, C., Wang, H., Gonsamo, A., & Liu, Z. (2017). No evidence of widespread decline of snow cover on the Tibetan Plateau over 2000–2015. *Scientific Reports*, 7(1), 14645. <https://doi.org/10.1038/s41598-017-15208-9>
- Whiteman, C. D. (2000). *Mountain meteorology: Fundamentals and applications* (1st ed.). Oxford University Press.
- Whiteman, C. D., & Hoch, S. W. (2014). *Bingham mine cold-air pool structure and evolution*. Retrieved from [https://www.inssc.utah.edu/\\$~\\$Shoch/kennecott/documents/UU\\_Final\\_Report.pdf](https://www.inssc.utah.edu/$~$Shoch/kennecott/documents/UU_Final_Report.pdf)
- Wrzesien, M. L., Pavelsky, T. M., Durand, M. T., Dozier, J., & Lundquist, J. D. (2019). Characterizing biases in mountain snow accumulation from global data sets. *Water Resources Research*, 55(11), 9873–9891. <https://doi.org/10.1029/2019WR025350>
- Yaqub, A., Seibert, P., & Formayer, H. (2011). Diurnal precipitation cycle in Austria. *Theoretical and Applied Climatology*, 103(1–2), 109–118. <https://doi.org/10.1007/s00704-010-0281-z>
- You, Q., Fraedrich, K., Min, J., Kang, S., Zhu, X., Pepin, N., & Zhang, L. (2014). Observed surface wind speed in the Tibetan Plateau since 1980 and its physical causes. *International Journal of Climatology*, 34(6), 1873–1882. <https://doi.org/10.1002/joc.3807>
- You, Q., Kang, S., Pepin, N., & Yan, Y. (2008). Relationship between trends in temperature extremes and elevation in the eastern and central Tibetan Plateau, 1961–2005. *Geophysical Research Letters*, 35(4), L04704. <https://doi.org/10.1029/2007GL032669>
- Zängl, G., Aulehner, D., Wastl, C., & Pfeiffer, A. (2008). Small-scale precipitation variability in the Alps: Climatology in comparison with semi-idealized numerical simulations. *Quarterly Journal of the Royal Meteorological Society*, 134(636), 1865–1880. <https://doi.org/10.1002/qj.311>
- Zardi, D., & Whiteman, C. D. (2013). Diurnal mountain wind systems. In F. K. Chow, S. F. J. De Wekker, & B. Snyder (Eds.), *Mountain weather research and forecasting* (pp. 35–119). Springer.
- Zemp, M., Frey, H., Gärtner-Roer, I., Nussbaumer, S. U., Hoelzle, M., Paul, F., et al. (2015). Historically unprecedented global glacier decline in the early 21st century. *Journal of Glaciology*, 61(228), 745–762. <https://doi.org/10.3189/2015JG15J017>
- Zemp, M., Haeblerli, W., Hoelzle, M., & Paul, F. (2006). Alpine glaciers to disappear within decades? *Geophysical Research Letters*, 33(13), L13504. <https://doi.org/10.1029/2006GL026319>
- Zemp, M., Huss, M., Thibert, E., Eckert, N., McNabb, R., Huber, J., et al. (2019). Global glacier mass changes and their contributions to sea-level rise from 1961 to 2016. *Nature*, 568(7752), 382–386. <https://doi.org/10.1038/s41586-019-1071-0>
- Zeng, Z., Chen, A., Ciais, P., Li, Y., Li, L. Z. X., Vautard, R., et al. (2015). Regional air pollution brightening reverses the greenhouse gases induced warming-elevation relationship. *Geophysical Research Letters*, 42(11), 4563–4572. <https://doi.org/10.1002/2015GL064410>
- Zhang, Y., Kang, S., Sprenger, M., Cong, Z., Gao, T., Li, C., et al. (2018). Black carbon and mineral dust in snow cover on the Tibetan Plateau. *The Cryosphere*, 12(2), 413–431. <https://doi.org/10.5194/tc-12-413-2018>

## References From the Supporting Information

- Archer, D. R., & Fowler, H. J. (2004). Spatial and temporal variations in precipitation in the Upper Indus Basin, global teleconnections and hydrological implications. *Hydrology and Earth System Sciences*, 8(1), 47–61. <https://doi.org/10.5194/hess-8-47-2004>
- Begert, M., & Frei, C. (2018). Long-term area-mean temperature series for Switzerland combining homogenized station data and high resolution grid data. *International Journal of Climatology*, 38(6), 2792–2807. <https://doi.org/10.1002/joc.5460>
- Bhutiyan, M. R., Kale, V. S., & Pawar, N. J. (2007). Long-term trends in maximum, minimum and mean annual air temperatures across the Northwestern Himalaya during the twentieth century. *Climatic Change*, 85(1–2), 159–177. <https://doi.org/10.1007/s10584-006-9196-1>
- Bhutiyan, M. R., Kale, V. S., & Pawar, N. J. (2010). Climate change and the precipitation variations in the northwestern Himalaya: 1866–2006. *International Journal of Climatology*, 30(4), 535–548. <https://doi.org/10.1002/joc.1920>
- Caloiero, T. (2015). Analysis of rainfall trend in New Zealand. *Environmental Earth Sciences*, 73(10), 6297–6310. <https://doi.org/10.1007/s12665-014-3852-y>
- Ceppi, P., Scherrer, S. C., Fischer, A. M., & Appenzeller, C. (2012). Revisiting Swiss temperature trends 1959–2008. *International Journal of Climatology*, 32(2), 203–213. <https://doi.org/10.1002/joc.2260>
- Chen, Y., Li, W., Deng, H., Fang, G., & Li, Z. (2016). Changes in central Asia's Water Tower: Past, Present and future. *Scientific Reports*, 6(1), 35458. <https://doi.org/10.1038/srep35458>

- Crochet, P. (2007). A study of regional precipitation trends in Iceland using a high-quality gauge network and ERA-40. *Journal of Climate*, 20(18), 4659–4677. <https://doi.org/10.1175/JCLI4255.1>
- Deng, H., Pepin, N. C., & Chen, Y. (2017). Changes of snowfall under warming in the Tibetan Plateau. *Journal of Geophysical Research: Atmospheres*, 122(14), 7323–7341. <https://doi.org/10.1002/2017JD026524>
- Dimri, A. P., & Dash, S. K. (2012). Wintertime climatic trends in the western Himalayas. *Climatic Change*, 111(3–4), 775–800. <https://doi.org/10.1007/s10584-011-0201-y>
- Elizbarashvili, M., Elizbarashvili, E., Tatishvili, M., Elizbarashvili, S., Meskhia, R., Kutaladze, N., et al. (2017). Georgian climate change under global warming conditions. *Annals of Agrarian Science*, 15(1), 17–25. <https://doi.org/10.1016/j.aasci.2017.02.001>
- Fujibe, F., Yamazaki, N., Katsuyama, M., & Kobayashi, K. (2005). The increasing trend of intense precipitation in Japan based on four-hourly data for a Hundred years. *SOLA*, 1, 41–44. <https://doi.org/10.2151/sola.2005-012>
- Gao, Y., Xu, J., & Chen, D. (2015). Evaluation of WRF mesoscale climate simulations over the Tibetan Plateau during 1979–2011. *Journal of Climate*, 28(7), 2823–2841. <https://doi.org/10.1175/JCLI-D-14-00300.1>
- Gilbert, A., & Vincent, C. (2013). Atmospheric temperature changes over the 20th century at very high elevations in the European Alps from englacial temperatures. *Geophysical Research Letters*, 40(10), 2102–2108. <https://doi.org/10.1002/grl.50401>
- Grose, M., Abbs, D., Bhend, J., Chiew, F. H. S., Church, J., Ekstrom, M., et al. (2015). *Southern Slopes Cluster Report, Climate Change in Australia Projections for Australia's Natural Resource Management Regions: Cluster Reports* (M. Ekström, P. Whetton, C. Gerbing, M. Grose, L. Webb, & J. Risbey, Eds.). CSIRO and Bureau of Meteorology.
- Hammad, A. A., & Salameh, A. M. (2019). Temperature analysis as an indicator of climate change in the Central Palestinian Mountains. *Theoretical and Applied Climatology*, 136(3–4), 1453–1464. <https://doi.org/10.1007/s00704-018-2561-y>
- Irannezhad, M., Ronkanen, A.-K., Kiani, S., Chen, D., & Kløve, B. (2017). Long-term variability and trends in annual snowfall/total precipitation ratio in Finland and the role of atmospheric circulation patterns. *Cold Regions Science and Technology*, 143, 23–31. <https://doi.org/10.1016/j.coldregions.2017.08.008>
- Kormann, C., Francke, T., Renner, M., & Bronstert, A. (2015). Attribution of high resolution streamflow trends in Western Austria – An approach based on climate and discharge station data. *Hydrology and Earth System Sciences*, 19(3), 1225–1245. <https://doi.org/10.5194/hess-19-1225-2015>
- Krishnan, R., Shrestha, A. B., Ren, G., Rajbhandari, R., Saeed, S., Sanjay, J., et al. (2019). Unravelling climate change in the Hindu Kush Himalaya: Rapid warming in the mountains and increasing extremes. In *The Hindu Kush Himalaya assessment* (pp. 57–97). Springer International Publishing. [https://doi.org/10.1007/978-3-319-92288-1\\_3](https://doi.org/10.1007/978-3-319-92288-1_3)
- Krishnaswamy, J., John, R., & Joseph, S. (2014). Consistent response of vegetation dynamics to recent climate change in tropical mountain regions. *Global Change Biology*, 20(1), 203–215. <https://doi.org/10.1111/gcb.12362>
- Lejeune, Y., Dumont, M., Panel, J.-M., Lafaysse, M., Lapalus, P., Le Gac, E., et al. (2019). 57 years (1960–2017) of snow and meteorological observations from a mid-altitude mountain site (Col de Porte, France, 1325 m of altitude). *Earth System Science Data*, 11(1), 71–88. <https://doi.org/10.5194/essd-11-71-2019>
- Liu, X., & Chen, B. (2000). Climatic warming in the Tibetan Plateau during recent decades. *International Journal of Climatology*, 20(14), 1729–1742. [https://doi.org/10.1002/1097-0088\(20001130\)20:14<1729::aid-joc556>3.0.co;2-y.CO;2-Y](https://doi.org/10.1002/1097-0088(20001130)20:14<1729::aid-joc556>3.0.co;2-y.CO;2-Y)
- Liu, X., Cheng, Z., Yan, L., & Yin, Z. Y. (2009). Elevation dependency of recent and future minimum surface air temperature trends in the Tibetan Plateau and its surroundings. *Global and Planetary Change*, 68(3), 164–174. <https://doi.org/10.1016/j.gloplacha.2009.03.017>
- Mao, Y., Nijssen, B., & Lettenmaier, D. P. (2015). Is climate change implicated in the 2013–2014 California drought? A hydrologic perspective. *Geophysical Research Letters*, 42(8), 2805–2813. <https://doi.org/10.1002/2015GL063456>
- Masson, D., & Frei, C. (2016). Long-term variations and trends of mesoscale precipitation in the Alps: Recalculation and update for 1901–2008. *International Journal of Climatology*, 36(1), 492–500. <https://doi.org/10.1002/joc.4343>
- Nepal, S. (2016). Impacts of climate change on the hydrological regime of the Koshi river basin in the Himalayan region. *Journal of Hydro-Environment Research*, 10, 76–89. <https://doi.org/10.1016/j.jher.2015.12.001>
- Panday, P. K., Thibeault, J., & Frey, K. E. (2015). Changing temperature and precipitation extremes in the Hindu Kush-Himalayan region: An analysis of CMIP3 and CMIP5 simulations and projections. *International Journal of Climatology*, 35(10), 3058–3077. <https://doi.org/10.1002/joc.4192>
- Pepin, N. C., & Seidel, D. J. (2005). A global comparison of surface and free-air temperatures at high elevations. *Journal of Geophysical Research*, 110(3), 1–15. <https://doi.org/10.1029/2004JD005047>
- Pérez-Zanón, N., Sigró, J., & Ashcroft, L. (2017). Temperature and precipitation regional climate series over the central Pyrenees during 1910–2013. *International Journal of Climatology*, 37(4), 1922–1937. <https://doi.org/10.1002/joc.4823>
- Rottler, E., Kormann, C., Francke, T., & Bronstert, A. (2019). Elevation-dependent warming in the Swiss Alps 1981–2017: Features, forcings and feedbacks. *International Journal of Climatology*, 39(5), 2556–2568. <https://doi.org/10.1002/joc.5970>
- Ruiz, D., Moreno, H. A., Gutiérrez, M. E., & Zapata, P. A. (2008). Changing climate and endangered high mountain ecosystems in Colombia. *The Science of the Total Environment*, 398(1–3), 122–132. <https://doi.org/10.1016/j.scitotenv.2008.02.038>
- Rusticucci, M., Zazulie, N., & Raga, G. B. (2014). Regional winter climate of the southern central Andes: Assessing the performance of ERA-Interim for climate studies. *Journal of Geophysical Research: Atmospheres*, 119(14), 8568–8582. <https://doi.org/10.1002/2013JD021167>
- Salerno, F., Guyennon, N., Thakuri, S., Viviano, G., Romano, E., Vuillemoz, E., et al. (2015). Weak precipitation, warm winters and springs impact glaciers of south slopes of Mt. Everest (central Himalaya) in the last 2 decades (1994–2013). *The Cryosphere*, 9(3), 1229–1247. <https://doi.org/10.5194/tc-9-1229-2015>
- Schmocker, J., Liniger, H. P., Ngeru, J. N., Brugnara, Y., Auchmann, R., & Brönnimann, S. (2016). Trends in mean and extreme precipitation in the Mount Kenya region from observations and reanalyses. *International Journal of Climatology*, 36(3), 1500–1514. <https://doi.org/10.1002/joc.4438>
- Scorzini, A. R., & Leopardi, M. (2019). Precipitation and temperature trends over central Italy (Abruzzo region): 1951–2012. *Theoretical and Applied Climatology*, 135(3–4), 959–977. <https://doi.org/10.1007/s00704-018-2427-3>
- Spinoni, J., Szalai, S., Szentimrey, T., Lakatos, M., Bihari, Z., Nagy, A., et al. (2015). Climate of the Carpathian region in the period 1961–2010: Climatologies and trends of 10 variables. *International Journal of Climatology*, 35(7), 1322–1341. <https://doi.org/10.1002/joc.4059>
- Tudoroiu, M., Eccel, E., Gioli, B., Gianelle, D., Schume, H., Genesio, L., & Miglietta, F. (2016). Negative elevation-dependent warming trend in the Eastern Alps. *Environmental Research Letters*, 11(4), 044021. <https://doi.org/10.1088/1748-9326/11/4/044021>
- Vincent, L. A., Zhang, X., Brown, R. D., Feng, Y., Mekis, E., Milewska, E. J., et al. (2015). Observed trends in Canada's climate and influence of low-frequency variability modes. *Journal of Climate*, 28(11), 4545–4560. <https://doi.org/10.1175/jcli-d-14-00697.1>
- Wendler, G., Gordon, T., & Stuefer, M. (2017). On the precipitation and precipitation change in Alaska. *Atmosphere*, 8(12), 253. <https://doi.org/10.3390/atmos8120253>

- Xu, F., Jia, Y., Peng, H., Niu, C., & Liu, J. (2018). Temperature and precipitation trends and their links with elevation in the Hengduan Mountain region, China. *Climate Research*, 75(2), 163–180. <https://doi.org/10.3354/cr01516>
- Yan, L., & Liu, X. (2014). Has climatic warming over the Tibetan Plateau Paused or continued in recent years. *Journal of Earth, Ocean and Atmospheric Sciences*, 1(1), 13–28.
- You, Q., Kang, S., Pepin, N., Flügel, W. A., Yan, Y., Behrawan, H., & Huang, J. (2010). Relationship between temperature trend magnitude, elevation and mean temperature in the Tibetan Plateau from homogenized surface stations and reanalysis data. *Global and Planetary Change*, 71(1–2), 124–133. <https://doi.org/10.1016/j.gloplacha.2010.01.020>
- Zazulie, N., Rusticucci, M., & Raga, G. B. (2017). Regional climate of the subtropical central Andes using high-resolution CMIP5 models—Part I: Past performance (1980–2005). *Climate Dynamics*, 49(11–12), 3937–3957. <https://doi.org/10.1007/s00382-017-3560-x>
- Zhang, D., Yang, Y., & Lan, B. (2018b). Climate variability in the northern and southern Altai Mountains during the past 50 years. *Scientific Reports*, 8(1), 3238. <https://doi.org/10.1038/s41598-018-21637-x>